SIZE EFFECTS IN COPPER WHISKERS

by

ZELMA ESTHER MOORE

A THESIS SUBMITTED IN PARTIAL FULFILMENT

OF THE REQUIREMENTS FOR THE DEGREE OF

MASTER OF APPLIED SCIENCE

IN THE DEPARTMENT

OF

MINING AND METALLURGY

We accept this thesis as conforming to the

standard required from candidates for

the degree of MASTER OF APPLIED SCIENCE

Members of the Department of

Mining and Metallurgy

THE UNIVERSITY OF BRITISH COLUMBIA

December 1961

In presenting this thesis in partial fulfilment of the requirements for an advanced degree at the University of British Columbia, I agree that the Library shall make it freely available for reference and study. I further agree that permission for extensive copying of this thesis for scholarly purposes may be granted by the Head of my Department or by his representatives. It is understood that copying or publication of this thesis for financial gain shall not be allowed without my written permission.

Department of MINING & METALLURGY

The University of British Columbia,
Vancouver 8, Canada.

Date JAN. 17/62

ABSTRACT

Whiskers were grown by the hydrogen reduction of cupric chloride. Tensile tests were performed on the whiskers, some of which were long enough to divide into two or three parts. After the whisker yielded ("primary tests") they were retested ("secondary tests") after removal of the deformed region.

In order to see if length had any effect on yield stress, a normalizing proceedure was established to convert the yield stress measured at any diameter d to an equivalent whisker with d = 10 μ. No observable length dependence of yield stress was found for either primary tests or secondary tests.

The diameter dependence of yield stress was found to depend on the type of tests. For primary tests, the yield stress was inversely proportional to $d^{1.6}$, while for secondary tests, inversely proportional to $d^{2.5}$. A dislocation mechanism to explain this was proposed in terms of only a part of the cross-sectional area (a small annular ring at the periphery of the whisker) taking part in the deformation. This mechanism was suitable only if the whiskers were assumed to be initially free of dislocations.

A decrease in the value of Young's Modulus of about 30% from the normal values was observed for whiskers subjected to a secondary test.

ACKNOWLEDGEMENT

The author wishes to thank her research director, Dr. E. Teghtsoonian, for his advice and encouragement given during this investigation. Thanks are extended to fellow graduate students, especially Dr. K. G. Davis, for many helpful discussions. Indebtedness is also acknowledged to Mr. W. J. Allday for his technical assistance.

This project was financed by Defence Research Board Grant Number 7510-33.

TABLE OF CONTENTS

TABLE OF CONTENTS CONTINUED

FIGURES

FIGURES CONTINUED

FIGURES CONTINUED

TABLES

INTRODUCTION

1. General

One of the scientific problems that has puzzled investigators for almost half a century is the discrepancy between the actual and the theoretical strengths of solids. As yet, because of the nature of the binding forces in metals, the theoretical strength of metal crystals has not been accurately calculated. However, various estimates of the theoretical shear stress τ_{th}, required to nucleate slip in the absence of dislocations have been made[1]. Mackenzie[2] arrived at a value of τ_{th} as G/30 where G is the elastic shear modulus in the shear direction. Also, by means of bubble raft studies, Bragg and Lomer[3] tended to confirm that the theoretical shear strength of perfect metal crystals is about G/30. In practice, bulk single crystals exhibit only a fraction of their ideal strengths deforming at stresses of less than 10^{-4}G. This large gap between the real and the ideal seemed to suggest that the theoretical strengths were too high.

It was not until 1952 that Herring and Galt[4] finally resolved this problem. They found that tiny filamentary growths or "whiskers" of tin had strengths of that predicted by theory. These whiskers were about 2 microns (μ) in diameter and a few millimeters (mm) in length. From simple bend tests they found that these whiskers could withstand an elastic strain as high as 2%, while in bulk tin, flow began at strains lower than 0.01%.

Since then, many people have entered the field of whisker research. Many important contributions have been made in the field of crystal growth and in the study of the solid state as certain measurements can be made that are otherwise impossible with bulk crystals.

2. Previous Work

a. Strength of Whiskers

In determining the strength of whiskers, tensile tests are more suitable than bending tests. The disadvantage of a bending test is that the stress is nonuniform both across and along the whisker. Special techniques for the tensile testing of whiskers have been devised by Gyulai[5], and Eisner[6], and Brenner[7]. Gyulai tested sodium chloride whiskers and he reported a maximum strength of 110Kg/mm^2. Eisner found a maximum strength of 390 Kg/mm^2 for silicon whiskers. This strength is about 2% of the Young's Modulus for the $\langle 111 \rangle$ direction.

Tensile tests were performed by Brenner on whiskers of iron, copper and silver. The maximum strengths of the whiskers and their sizes are given in Table I where σ_{max} equals the maximum stress the whisker sustained before fracture or yield occured and τ_{max} equals the calculated resolved shear stress.

TABLE I

Tensile Strength of Whiskers

				Bulk crystals	
1	2	3	4	5	6
Material	d (u)	σ_{max} (kg/mm^2)	τ_{max} (kg/mm^2)	$\tau_{critical}$ (kg/mm^2)	Ultimate tensile strength (kg/mm^2)
Fe	1.60	1340	364	4.5[a]	16–23[b]
Cu	1.25	300	82	0.10[b]	12.9–35.0[b]
Ag	3.80	176	72	0.06[b]	

Reproduced from Reference 7.

Compared with the reported strengths of bulk crystals [8,9] (columns 5 and 6), the yield point shear strengths of the whiskers are 80 to 1200 times greater than those of the large crystals. The ratios between the tensile strengths (columns 3 and 6) were lower. Brenner also found, as Table II shows, that the highest shear strengths of the whiskers were either close to or above

TABLE II

Shear Strength of Whiskers

1 Whiskers	2 Whisker axes	3 Slip system	4 G(kg/mm²)	5 $\frac{\tau_{max}}{G}$	6 $\frac{\tau_{th}}{G}$ (estimated)
Fe	[111]	(110) [111]	6100	0.060	0.033–0.19
Cu	[111]	(111) [101]	3700	0.022	0.033–0.13
Ag	[100]	(111) [101]	2300	0.031	0.033–0.13

Reproduced from Reference 7.

the estimate of the theoretical strength of perfect crystals. To account for this high strength of whiskers, Galt and Herring[4] have formulated two theories. One is that whiskers are free of dislocations. The other theory postulates that whiskers contain only a few dislocations and these are insufficient to cause multiplication.

b. Elastic Behaviour of Whiskers

The most outstanding characteristic of whiskers is their elastic behaviour. The tensile stress-strain curves of a variety of whiskers have been determined. Brenner[7] investigated the stress-strain behaviour of copper, iron and silver whiskers while Coleman, Price and Cabrera[10] performed stress-strain tests on cadmium and zinc whiskers. Evans, Marsh and Gordon[11] found stress-

strain curves for sodium and potassium chloride whiskers. The stress-strain curves for silicon whiskers were obtained from bending tests conducted by Pearson, Read and Feldman[12]. The whiskers listed in Table III, except for some of the whiskers grown by precipitation, exhibit a maximum elastic strain

TABLE III

Maximum Elastic Strains of Whiskers

Material	Max. elastic strain (%)	Method of testing	Method of growth
Fe	4.9	Tension	Halide reduction
Cu	2.8	Tension	Halide reduction
Ag	4.0	Tension	Halide reduction
Ni	1.8	Tension	Halide reduction
Si	2.0	Tension	Halide reduction
Zn	2.0	Tension	Vapor condensation
NaCl	2.6	Tension	Precipitation
SiO_2	5.2	Tension	Vapor condensation
Al_2O_3	3.0	Tension	Vapor condensation
MoO_3	1.0	Tension	Vapor condensation
C	2.0	Tension	Vapor condensation
Sn	2 to 3	Bending	Growth from solid
Ge	1.8	Bending	Halide reduction
ZnO	1.5	Bending	
ZnS	1.5	Bending	Vapor condensation
LiF	3	Bending	Cleavage
$MgSO_4 \cdot 7H_2O$, hydroquinone, etc.	> 2		Precipitation

Reproduced from Reference 29.

of at least 0.01, which is 100 to 1000 times greater than that of annealed bulk crystals. The elastic part of the stress-strain curves are reversible for fast strain rates, but for slow strain rates Cabrera[10,13] reported that for some zinc whiskers the strain was not reversible.

Brenner[7] observed large deviations from Hooke's Law for iron whiskers but not for copper whiskers. The true stress-strain curves of two iron whiskers are shown in Fig. 1. Hooke's Law was obeyed up to about 2% but beyond that, Young's Modulus, E, was no longer a constant. E was calculted from the initial slopes of the stress-strain curves. For one whisker this was close to

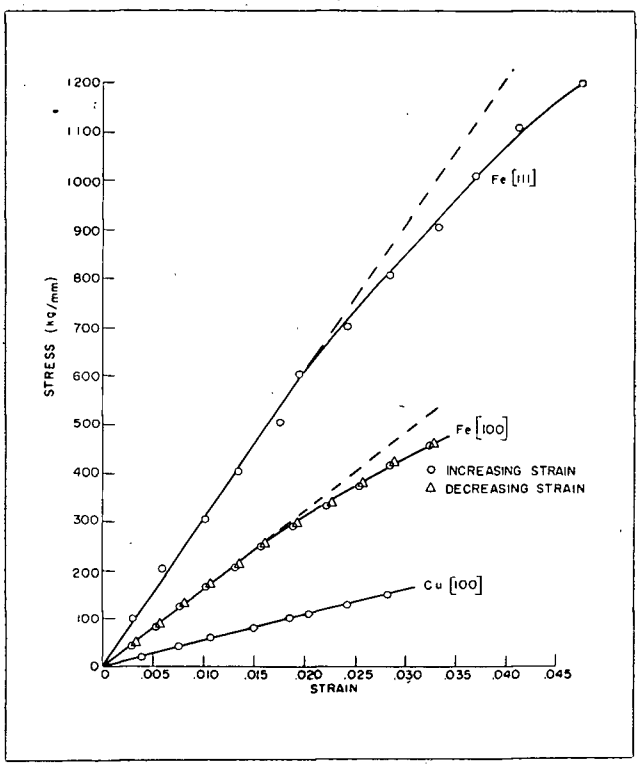

Figure 1. Stress-strain Curves of Iron and Copper Whiskers Pulled in Tension. Reproduced from Reference 14.

the value for a <100> direction. E was close to the value for a <111> direction for the other whisker. The orientation of the whisker appears to have little effect on the elastic behaviour.

Coleman et al[10] tested zinc and cadmium whiskers in the diameter range of 1-10μ. In all cases the initial elastic strain was always linear and reached values of 1-2%. The critical shear stress was several hundred times that observed in macroscopic crystals. They also found that the calculated moduli were consistently lower than the accepted values by a factor of about 0.7.

In a later paper, Cabrera and Price [13] observed that the elastic curve exhibited a deviation from linearity which was detectable at about 0.4% strain. The amount of this deviation at 1% strain varied between 0.02% and 0.12% strain. This implied the presence and motion of dislocations.

These whiskers also exhibited creep when subjected to a high stress for several hours. They found that after creep at a constant stress, the deviation from linearity was considerably reduced and that there was no change in the initial slope (Fig. 2).

To explain these results, they postulated a dislocation network containing Frank-Read sources. Under a suitable stress, dislocation loops will be generated. This will result in large elastic strains provided the surface is a strong enough obstacle to hold the dislocations inside. Upon removal of this applied stress, most of the loops will collapse into the source. In the case of a large crystal, the Frank-Read source could be far from the surface. Then the surface could not prevent slip at low stresses since a large enough pile-up of dislocations could be formed to multiply the applied stress at the head of the pile-up to an amount necessary to break through the barrier. However, in order to produce slip in a small crystal, the applied stress would have to be increased considerably. If it is assumed that during creep the high stress destroys the sources leaving only a certain number of loops already created, then the elastic stress-strain curve should show a smaller deviation from linearity, but the same slope. This is what was observed by Cabrera and Price.

c. Plastic Behaviour of Whiskers

When the elastic limit of a whisker is exceeded, either fracture or plastic deformation occurs. Brenner[14] has found that in the case of thin copper and iron whiskers, fracture will occur with very little plastic deformation if their elastic limit is very high. One reason is that, following a large elastic strain, the plastic strain rate is extremely high. In the case of ductile whiskers, Brenner[15] observed that their stress-strain curves,

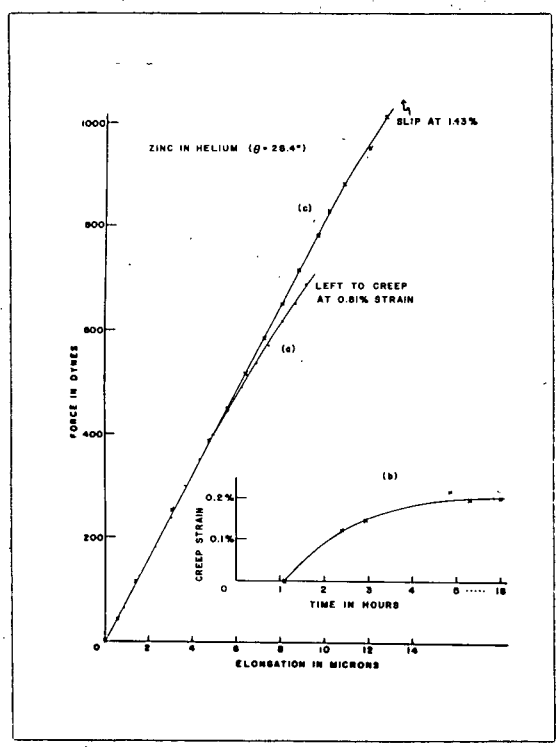

Figure 2. Effect of Creep on the Force-Elongation Curve (before yield).
Reproduced from Reference 13.

(a) Elastic behaviour of a typical whisker up to 0.81% strain before creep.

(b) Creep strain as a function of time at a constant stress of about 4.5×10 dyne/cm^2.

(c) Elastic behaviour after creep. The deviation from linearity begins at strains much higher than it did before creep. The yield point is increased at least 50%.

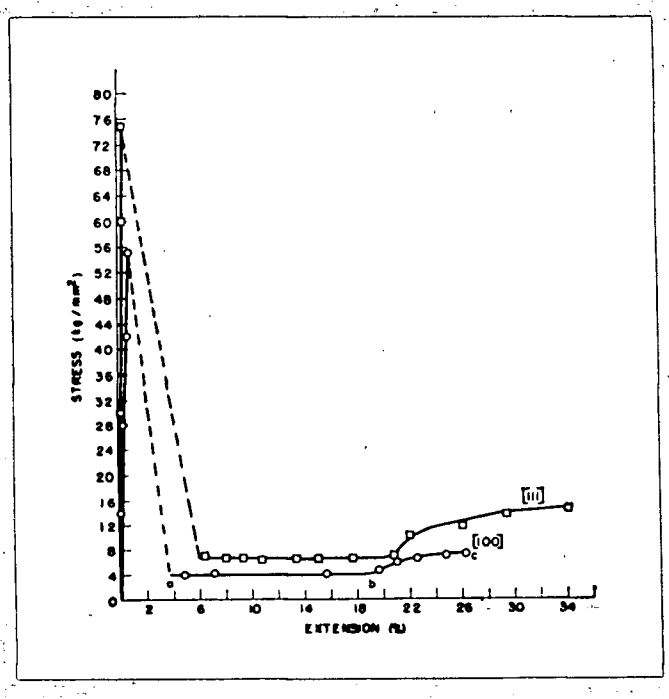

Figure 3. Stress-Strain Curves of Copper Whiskers Reproduced from Reference 29.

as shown in Fig. 3, are characterized by an extremely sharp yield point and an extensive "easy glide" region (a - b). The "easy glide" region was followed by a work-hardening region (b - c).

Deformation in the "easy glide" region occurred by the propagation of Lüders bands shown in Fig. 4. After yielding, one or more small deformation zones were observed. Upon reloading, the slipped region travelled along the whisker until the ends of the whisker were reached. The small, constant stress necessary to propagate this slipped region is called the flow stress σ_{fl}. Ratios between the yield stress σ_y and the flow stress σ_{fl} as high as 80 to 1 were measured by Brenner. Upon further reloading, work hardening occurred. In explaining these results, Brenner showed that the sharp yield point cannot be due to dislocation pinning by impurities as postulated by Cottrell[1]. He concluded that slip in whiskers was initiated either by the activation of very small dislocation sources already present in the system or by means of some other unknown mechanism. In a later revaluation, Brenner[14] explains that

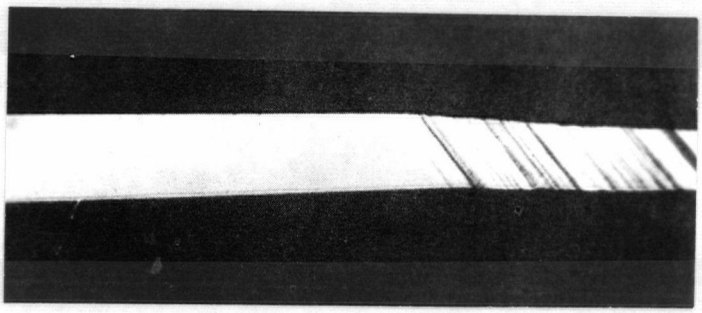

Figure 4. Propagation of a Lüders Band in a Copper Whisker, Mag. 80 X.
Reproduced from Reference 14.

the flat part of the stress-strain curve is not primarily to "easy glide" but rather is due to the fact that a certain stress is necessary to propagate the front of the Lüders band. Brenner compared the flow stress to the shear stresses that produce equivalent amounts of deformation, as in the Lüders bands, rather than to the critical shear stress of bulk crystals.

Coleman et al[10] found that for zinc and cadmium whiskers, yielding occurred at a particular region of the whisker. The propagation of Lüders bands at a flow stress 30 times smaller than the yield stress was observed. They felt that this formation of slip bands eliminated any possibility of the whisker being a nearly perfect crystal.

Price[16] deformed zinc whiskers in tension inside an electron microscope and studied the motion of individual dislocations. The whiskers were found to be initially free of dislocations and possessed sharp yield points whose values were determined by stress concentrations at large surface steps

or at the grips. After a very small amount of plastic strain, Price found dislocations in a narrow zone a few microns wide. The zone extended all the way across the crystal. These dislocations were essentially of two types: (i) long dislocations which were easily immobilized by obstacles, and (ii) short screw dislocations some of which broke up into long narrow loops which then split up into circular loops. With further strain the density of dislocations in this narrow zone increased and a large number of loops was produced. These loops blocked the motion of the long dislocations which in turn acted as obstacles to the glide of the screw dislocations. When the density of the loops was very high, all the dislocations became entangled. This resulted in further glide occurring at the edges of this deformed region where only a few loops were present. Thus the width of the deformed region was increased. The propagation of a deformation front which was optically observed as a Lüders band was the result of this process.

d. Size Effects in Whiskers

In 1924, Taylor[17] reported that the tensile strengths of very fine wires of antimony were between 18.0 to 22.0 Kg/mm^2. This compared to a tensile strength of 1.10 Kg/mm^2 for bulk antimony[18]. This was the first report of variations in the properties of crystals with diameter. These variations have been termed "size effects".

The strengths of whiskers as a function of size have been determined for sodium chloride whiskers by Gyulai[5] and by Brenner[7] for copper and iron whiskers (Fig. 5). Brenner found, despite a high scatter, that the strength of a copper or iron whisker was inversely proportional to the diameter.

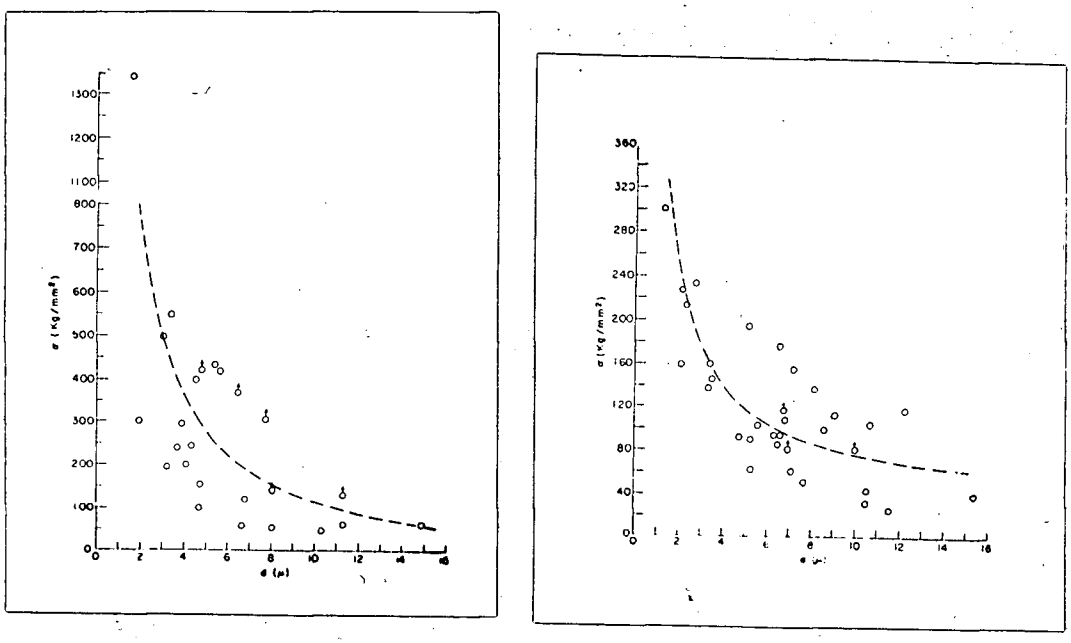

(a) (b)

Figure 5. Strength Versus Diameter for (a) Iron and (b) Copper Whiskers
Dashed Curves are for σ proportional to d^{-1}.
Reproduced from Reference 7.

In contradiction to Brenner, Eder and Meyer[19] found a relationship between yield stress τ_o and diameter as shown in Fig. 6. These measured values of τ_o lay within a scattered region whose boundaries showed a $1/d^2$ relation. It is interesting to note that all Brenners measurements lie completely outside the scattered region of their measurements. Eder and Meyer offered no explanation for these discrepancies.

No dependence of strength on diameter was observed by Coleman et al[10] in cadmium and zinc or by Pearson et al[12] in silicon whiskers. However, in a later paper, Evans and Marsh[20] report a size-strength relationship for silicon whiskers of diameters smaller than those of Pearson. They suggested that the reason for this was that the strength depends more on surface conditions rather than dimensions since for various reasons a rough surface is more probable in large whiskers than in small ones.

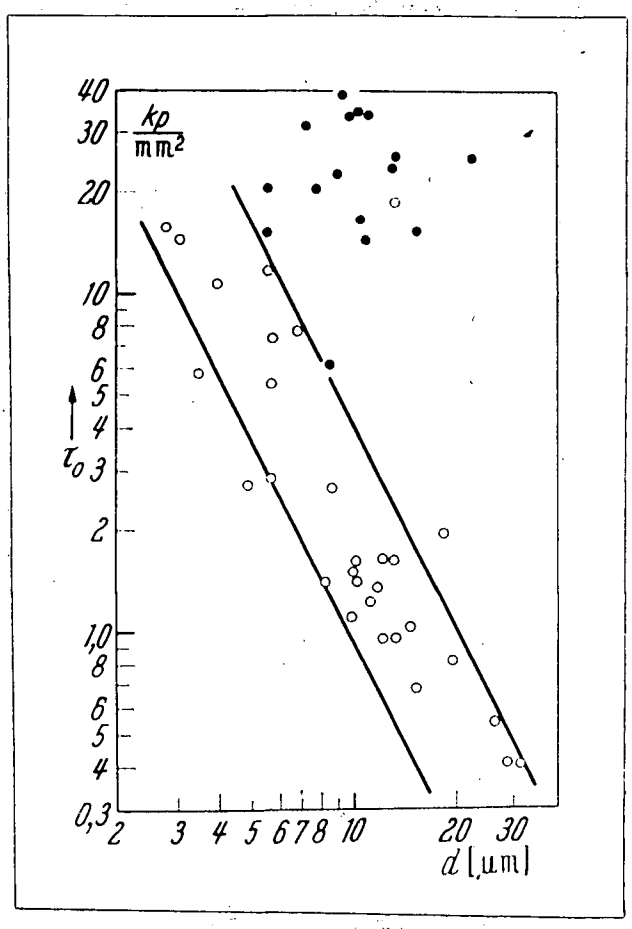

Figure 6. Dependence of Critical Shear Stress τ_o on Whisker Diameter.
Reproduced from Reference 19.

Brenner[7] also found that if, after the whisker yielded, the unyielded portion was remounted, the strength of the whisker increased as the length decreased (Fig. 7) Eisner[21] reported that for silicon whiskers which were remounted after fracture, their fracture stress was somewhat larger than before. This might be the result of nonumiformity of cross-section along the length of the whisker, the thinnest section fracturing first.

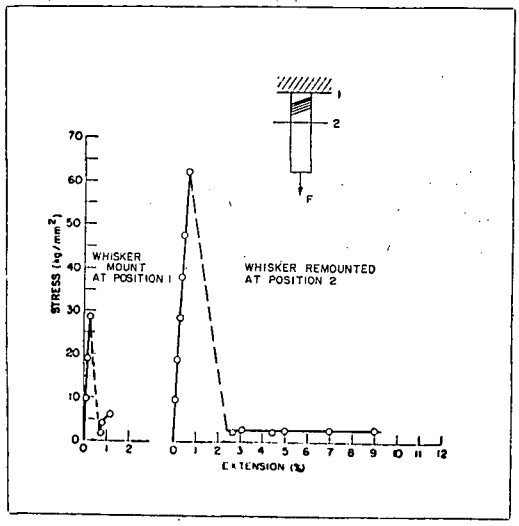

Figure 7. Recovery of Yield Point of a Copper Whisker After Removal of a Slipped Portion. Reproduced from Reference 15.

To account for these size effects, various explanations have been proposed.

i. Crystal Perfection

Although whiskers have exhibited the potential strength of perfect crystals, it has not been established whether they are structurally perfect. Structural perfection implies here only the absence of extended defects, in particular, dislocations. This does not include point defects such as vacancies, impurities etc. Brenner[7] concluded from his results on strength versus diameter that the whiskers contained a small number of defects which were distributed statistically in a rather complex manner both on the surface

and in the interior of the whiskers. He thought that the internal defects were probably dislocation sources of the type postulated by Frank and Read. The resolved shear stress necessary to operature this type of source is given by

$$\tau_y = \frac{Gb}{L}$$

where G is the shear modulus, b the Burger's vector of the dislocation segment and L the length of the pinned dislocation segment. In the copper and iron whiskers tested by Brenner, the length of the dislocation sources must be of the order of 0.1 microns. However, in a later paper, Brenner [15] stated that it was uncertain if a dislocation source of such short length could operate. Also, it was not clear why the dislocation sources were only a small fraction of the whisker diameter.

Tests on silicon whiskers and silicon rods cut from bulk silicon were performed over a range of temperatures by Pearson, Read and Feldmann[12]. According to Cottrell[1], the yield stress of a perfect crystal would vary insignificantly over the temperature range 600°C to 800°C. Pearson et al found that the yield stress of silicon whiskers at 800°C was less than half the yield stress at 650°C (Fig. 8). Thus, Pearson et al concluded, these high-temperature tests on the whiskers showed that room-temperature fracture strength was not an adequate criterion of crystal perfection. It was also found (Fig. 9) that for small enough diameters of silicon, their room-temperature fracture stress was the same as for the whiskers, but the yield stress was the same as bulk silicon at 800°C. This was further evidence that the room-temperature fracture strength was not due to a low dislocation density.

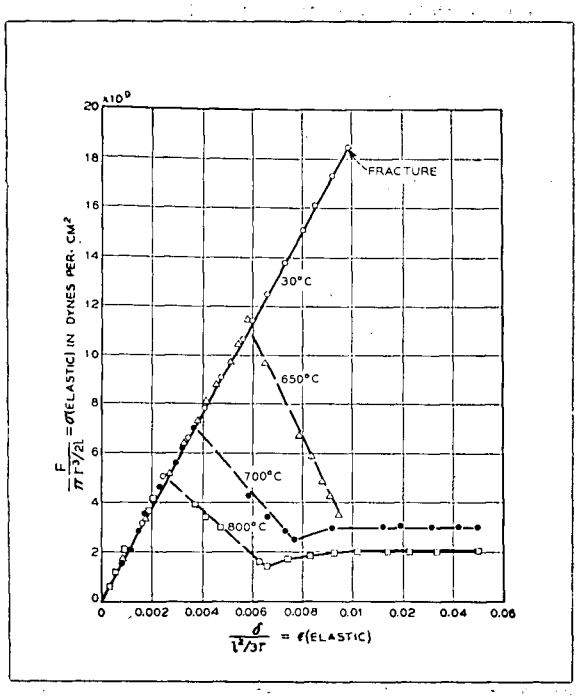

Figure 8. Dependence of the Strength of Silicon Whiskers on Temperature.
Reproduced from Reference 12.

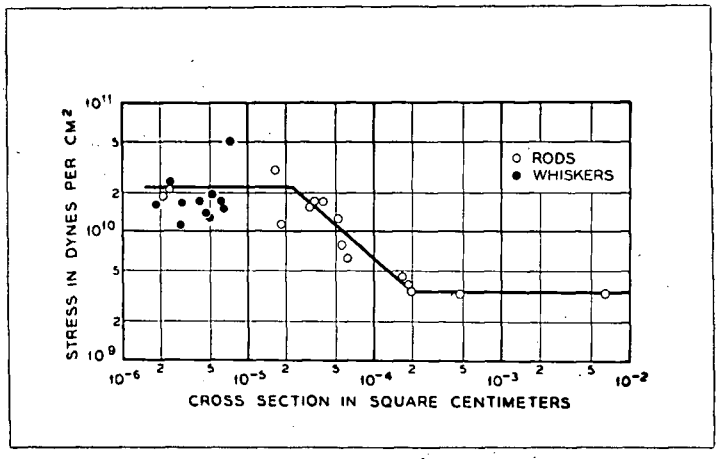

Figure 9. Tensile Strength of Silicon Rods and Whiskers
Reproduced from Reference 12.

On the other hand, Gorsuch[22], who measured the density and distribution of dislocations in iron whiskers by means of X-ray rocking curves, found that the more perfect whiskers have dislocation densities below 10^6 dislocations per cm^2. Therefore whiskers of less than 10μ in diameter would contain, at most, only a small number of dislocations and should behave as perfect crystals.

Various attempts have been made to resolve this question of whether whiskers are strong simply because they are small or whether high strength is peculiar to whiskers. Costanzo[23] attempted to determine if there was a size effect with fine polycrystalline copper wires. Wires down to 50μ in diameter were tested at room temperature and at -195°C. At room temperature, Costanzo found no definite size effect, but at -195°C he found that the yield stress decreased with diameter. Shlichta[24] also tried to compare metal whiskers with other types of filaments. He used Taylor-process wires[17] and electropolished drawn wires. These exhibited an increase in strength with decreasing diameter comparable to that observed for whiskers. However, in a later letter to Costanzo, he stated that these results were fortuitous. The tentative conclusion made by Shlichta was that the relation between size, strength, growth mechanism and crystalline perfection was more complex than originally thought.

ii. Effect of Surface Defects

It could be assumed that the yield stress is determined by some other type of imperfection rather than free dislocations or dislocation sources. Brenner[14] thought it more likely that dislocations are nucleated at submicroscopic imperfections on or near the surface. Experimentally, Brenner[15] found that yielding could not be induced in an elastically strained iron whisker by rubbing another iron whisker over it. This would indicate that if there are any defects, they must be of a specific nature. Pearson

et al[12] found that the fracture stress in bulk silicon could be raised by etching which suggested that surface irregularities were the important imperfections.

iii. Grip Effects

Fleischer and Chalmers[25] calculated the average shear stresses caused by the bending moment applied by the grips during a tensile test of a single crystal. It was shown that, in general, the resolved shear stress τ_j on the various crystal planes was the sum of the contributions from the applied stress, σ_a, and the grip stress τ_g:

$$\tau_j = m_j \sigma_a + \sum_i n_{ij} \tau_g^i$$

where $m_j = \cos\theta_j \cos\lambda_j$, the Schmid factor for the j th slip system,

λ_j = the angle between the speciment axis and the j^{th} slip direction,

θ_j = the angle between the speciment axis and the j^{th} slip plane normal,

τ_g^i = the grip stress resulting from slip on the i^{th} system,

n_{ij} = the fraction of the grip stresses arising from slip on system i that is resolved on system j.

In case of slip on the primary system, the resultant stress τ_p is:

$$\tau_p = m_p(\sigma_a - \epsilon E (a/L)^2 \tan^2\lambda_p)$$

where a = crystal diameter

L = crystal length

It can be seen that the effect on yield stress, since it is developed at small strains, is virtualy negligible.

e. Effect of Surface Films on Whiskers

It was thought that the presence of a thin oxide film on metal whiskers might contribute to their strengths. It was found by Roscoe[26], and Cottrell and Gibbons[27], that an oxide film increased the strength of a crystal and also that the thicker the oxide, the greater the strengthening

effect. This increased strength was explained as resulting from the hinderance of dislocations moving out of the crystal by the film.

Cabrera and Price[13] found that the yield points of zinc and cadmium whiskers were increased by a factor of about 2 by the presence of an oxide layer. They found an optimum thickness of the oxide the order of tens of angstroms. Beyond this optimum value, it is possible that nonuniform oxidation will weaken the whisker at several points.

Brenner[7] formed continuous oxide films on copper whiskers by heating in air at 100°C to 150°C, but found that their strengths were not significantly changed. Saimoto[28], tested copper whiskers in dilute sulphuric acid and also found that the oxide coating did not contribute appreciably to the strength of the whiskers.

f. Effect of Impurities in Whiskers

Most of the whiskers which have been tested are not exceptionally pure. Brenner[15] found that copper whiskers grown from CuI contained about 30 ppm of silver while iron whiskers grown from $FeBr_2$ contained about 100 ppm. Impurities could strengthen the whiskers by pinning the few dislocation sources that may be present in the whiskers. Brenner[7] stated that in the case of copper, dislocation pinning does not contribute to the strength of the whisker. If the reverse was true, a strong temperature and time dependence on strength would be expected. This was not found. By using purified CuI, Brenner[14] grew copper whiskers containing less than 1 ppm of silver, but no significant change in strength was observed. However, if a few percent of silver halide was added to the CuI from which the whiskers were grown, Brenner[14] reported that their strengths were about 1/3 that of pure whiskers. Hence, during whisker growth, impurities may weaken the whisker by forming dislocation sources.

3. Purpose of Present Investigation

The main purpose of this investigation was to extend the study of size effects in copper whiskers both for length and diameter.

EXPERIMENTAL PROCEDURE

1. Growth

The copper whiskers used in this investigation were grown by the method of halide reduction by hydrogen [29]. Standard reagent grade anhydrous cupric chloride was used. The maximum limits of impurities as stated by the Allied Chemical and Dye Corporation are:

Insoluble	0.01%
Nitrate (NO_3)	0.005%
Sulphate (SO_4)	0.005%
Iron (Fe)	0.01%
Substances not precipitated by H_2S (as sulphates)	0.20%

The whiskers were grown in a tube furnace as illustrated in Fig. 10 and 11. The procedure in making a growth run was as follows. The

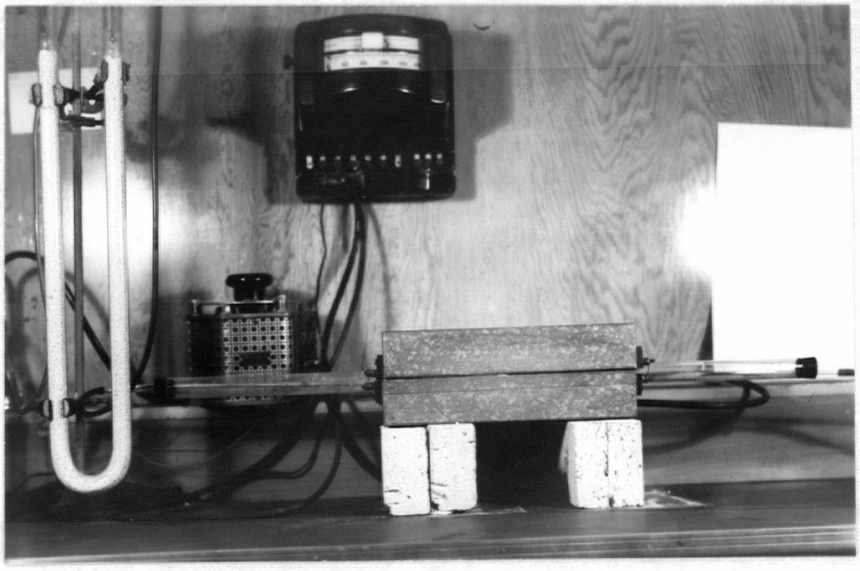

Figure 10. Whisker Growing Furnace

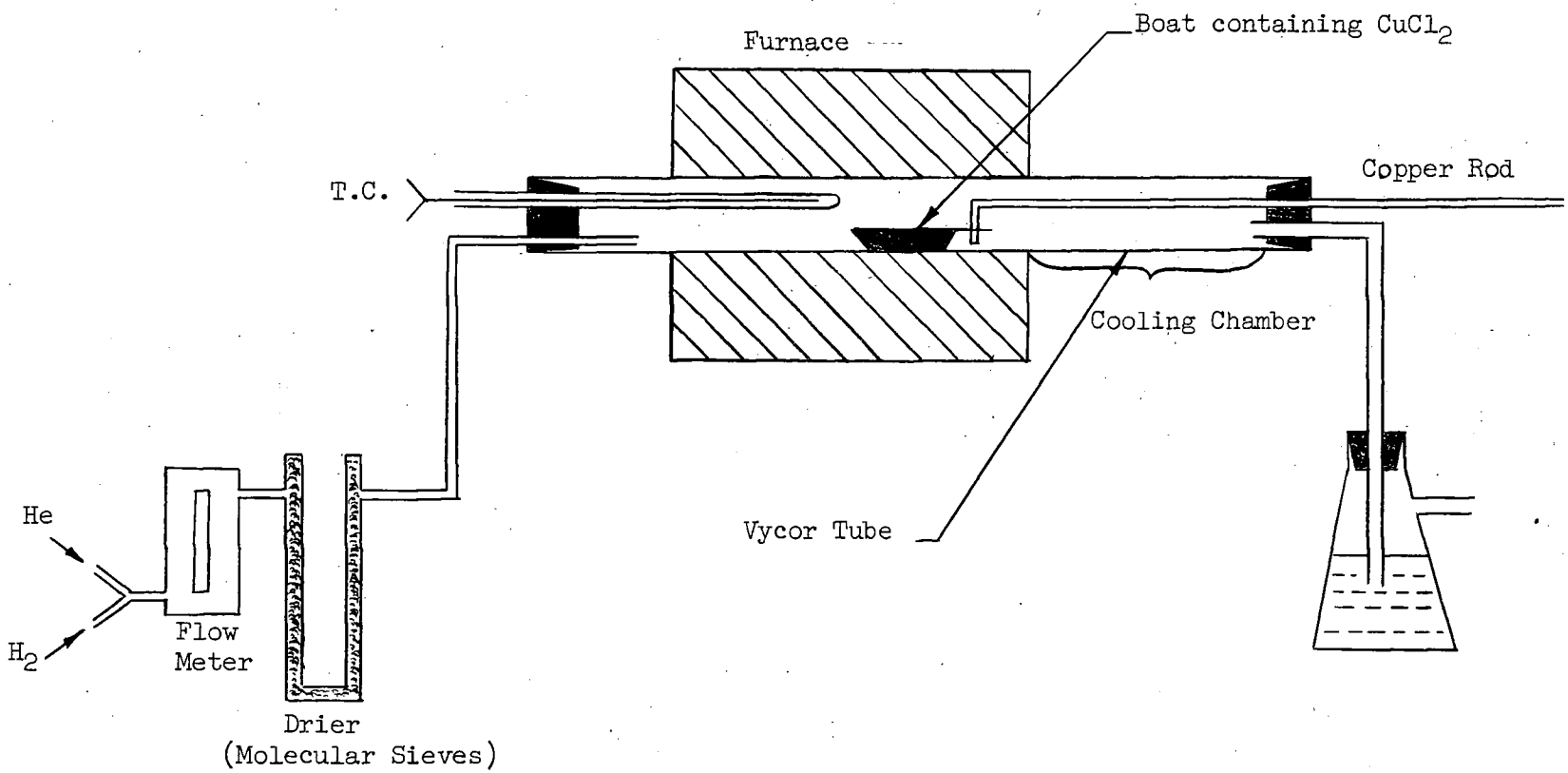

Figure 11. Schematic Diagram of Whisker Growing Furnace

Vycor tube was cleaned with nitric acid, then rinsed and dried with acetone. The hydrogen was first passed through a catalytic purifier and then through a drier of molecular sieves which removed any water that might be present. The helium was passed through a liquid nitrogen cold trap and then, for convenience, also through the molecular sieves. The flow of gas was opposite to the direction in which the boat was inserted in order to prevent air from entering and contaminating the hot furnace.

The helium was first turned on and then a fireclay boat, which had previously been dried to remove water, was filled with cupric chloride and pushed into the cooling chamber. The furnace was then flushed with helium for about 20 - 30 minutes after which the flow of helium was replaced by hydrogen. The boat was then pushed into the furnace. After the reduction, which lasted anywhere from 5 minutes to one hour depending on the temperature, the boat was drawn from the furnace to the cooling chamber. After the boat had cooled down, the flow of hydrogen was replaced by helium. The cool boat was then removed and placed in a dessicator.

2. Selection

When a suitable boat of whiskers was obtained, it was examined with a Reichert stereoscopic microscope at 12 and 36 magnification (Fig. 12). Upon location of a good whisker it was removed at the substrate by a pair of very fine straight tweezers. The insides of the claws of the tweezer were metallographically polished and degreased in order to prevent the whisker from sticking to the claws. The whisker was then placed on a white card and examined under a Reichert metallographic microscope at 110 and 390 magnification. The criteria for whisker selection were these:

(1) straight, untapered and at least 3 mm long;

(2) no surface defects such as pits or short branch growth;

Figure 12. Whisker Handling Apparatus

(3) the surface facets must not change along the length of the whisker.

If the whisker met the above requirements, it was stored in a dessicator for future use.

3. Specimen Mounting

A pyrex probe with a U-shaped tungsten filament, the current through which was controlled by a foot switch, was used to transfer the whisker from the card to the tensile machine. On the tip of the probe a blob of glue was melted. This mounting compound was diphenyl carbazide which melts at 173°C. The whisker was picked up with the tip of the probe by melting and then freezing the glue. The current to the two grips of the tensile machine was adjusted until the temperature was well above the melting point of the glue. The glue was prevented from boiling off by subjecting it to a stream of cold dry helium. This produced a thin, tacky skin of glue on each filament. The whisker was mounted by touching the free end to the movable filament, A. The probe was then lowered until the whisker came into contact with the glue on the fixed filament, B. At this point the probe was removed by heating the tip and carefully withdrawing it from the surrounding glue. The whisker was then ready for its initial tensile test. These initial tests will be referred to as "primary tests".

With this method it was possible to mount successfully about two out of every five whiskers without contaminating the whisker with glue, yielding the whisker or forming a thick oxide coat of the whisker.

For a test, in which the unyielded portion of a whisker was re-mounted, the following procedure was used. After the whisker yielded, it was examined under the Reichert stereoscopic microscope to see where the formation of Lüders bands had occurred. If yielding had started at one point near one

of the grips, then it was possible to remount the whisker. The filament nearest the Lüders bands was heated until the glue began to sag away from the whisker The whisker was then removed by quickly screwing away filament B. This left the whisker attached to one filament. The whisker was then remounted by either slightly raising or lowering filament B and then screwing it back until the yielded portion of the whisker rested on the glue. A blob of glue was then carefully dropped over the yielded portion. Tensile tests now performed were called "secondary tests".

This remounting method combined with the initial mounting technique and also taking into account where the whisker yielded, gave about one successful test out of every ten attempts.

4. Measurement of Specimen Length

The length of the whisker was measured by a graticule in one of the 6X eyepieces of the Reichert stereoscopic microscope. The hairline in the graticule was divided into ten main divisions each one of which was itself divided into ten small divisions. The length of a small division was 80μ with the 2X objective, 26.7μ with the 6X objective and 16μ with the 10X objective. In a given measurement, the error in length was $\pm$ 1.0 division for each end of the whisker. Hence, for the lengths tested the maximum error in measuring the length was 6%.

5. Determination of Cross Sectional Area

An initial cross sectional area of a whisker was determined by measuring the diameter of the whisker with a microscope equipped with a travelling eyepiece. A circular cross section was assumed since for the cross sections observed this approximation is satisfactory. This initial value was then used in computing the stress on the whisker, and a stress-

strain curve for the whisker was plotted. From this curve, a correction to the initial value of cross sectional area was made in the following manner. The slope from the stress-strain curve gave E_m, Young's Modulus, and this value was compared to the values of Young's Modulus E_c for the three main directions of growth, the [111], [110] and [100] directions[7]. These values of E_c were computed from the formula

$$\frac{1}{E} = S_{11} - 2(S_{11}-S_{12}-S_{44}/2)(\gamma_1^2\gamma_2^2 + \gamma_2^2\gamma_3^2 + \gamma_1^2\gamma_3^2)$$

where S_{ij} are the elastic compliance constants which were computed from Overton and Gaffney's[30] values of C_{11}, C_{12}, and C_{44}. $\gamma_{1,2,3}$ are the cosines of the angles formed by the axis of the specimen with the three edges of the unit cube. In almost all cases E_m was close to one value of E_c. Using this value of E_c, a new stress-strain curve was plotted. From any point on this new plot, a new value of stress for that point could be calculated since stress = E_c(strain). In turn, from this new stress, a more correct value of cross sectional area was calculated.

6. Tensile Testing Apparatus

a. Construction

The whisker tensometer used in this investigation was the same one used by Saimoto, and hence only a brief description of the tensometer will be given here.

This tensometer was constructed following a design similar to that of Brenner[15] and is illustrated schematically in Fig. 13 and is shown in Fig. 14. Basically it consists of a fixed mount to which one end of the whisker is attached. The other end of the whisker is attached to a suspended rod in which an Alnico permanent magent is imbedded at a suitable position. When the solenoid surrounding the magnet is activated, the magnet and rod are pulled towards the solenoid centre thus imparting a force on the whisker. The

extension of the whisker is measured by means of an impedance transducer. An important feature of this apparatus is a micrometer-stop which is used as a brake to interrupt plastic flow after yielding. If the loading force is not reduced immediately after yielding, flow occurs so rapidly that the deformation cannot be followed. It is also used to calibrate the impedance transducer.

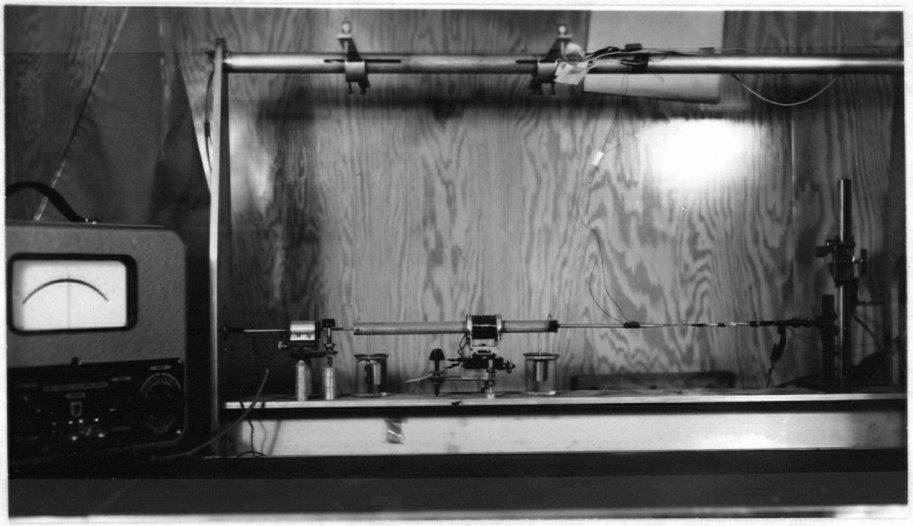

Figure 14. Whisker Tensometer

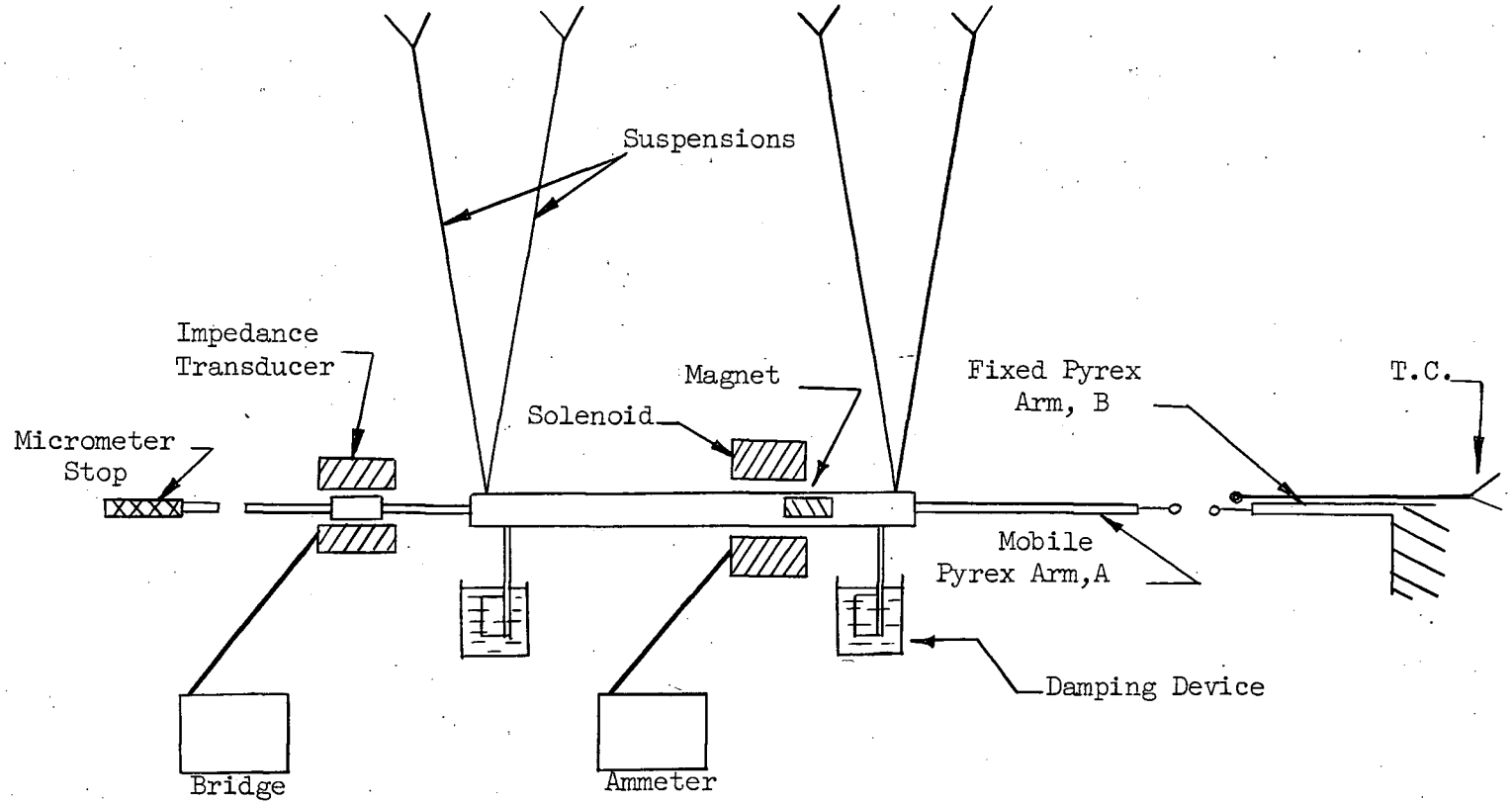

Figure 13. Schematic Diagram of the Whisker Tensometer

b. Calibration

The tensometer was recalibrated using the same method as described by Saimoto. The results of this recalibration agreed very well with the results of Saimoto, the difference being 2%. All the calibration curves are found in Appendix I.

7. Annealing Furnace

An annealing furnace was constructed out of a glass T-junction. The top of the T was wound with Chromel A, 1/8" ribbon. The range of temperatures in which this furnace could be used was limited by the low melting point of the glue, ie. 173°C. The temperature was controlled by a thermocouple which was embedded in the glue on the fixed grip. The furnace rested on a strip of insulating material on an aluminium block and was positioned over the fixed grip clearing the end of the grip by about 2 inches. It was then positioned over the whisker which was annealed in an atmosphere of helium that entered the furnace through the bottom of the T.

8. Experimental Procedure

a. Tensile Tests

After a suitable whisker had been obtained and placed on a white card, a small drop of glue was placed on one end of the whisker which secured it to the card. This was found to be necessary as otherwise the whisker could easily by blown away by a small gust of air. The diameter was then measured. A portion of the whisker was then removed by cutting it with a razor blade which had been degreased with acetone. It was then mounted on the tensometer and pulled. Most whiskers were cut into two pieces, but a few were long enough to divide into three or four pieces.

b. Annealing Tests

Annealing tests were performed in two ways:

(i) A whisker was mounted and pulled until it yielded and flowed. The whisker was then detached from grip A in the manner described in the section on specimen mounting, and the annealing furnace was slipped over the whisker. It was annealed in a helium atmosphere for 12 - 14 hours at 100°C. After annealing the whisker was remounted and pulled.

(ii) After the whisker was detached from grip A as above, it was removed from grip B with a pair of tweezers. It was then placed in a porcelain boat and the glue was dissolved from the end of the whisker with acetone. The boat was then wrapped in aluminium foil which was perforated with a needle. The boat was then placed in the whisker growing furnace and annealed under an atmosphere of hydrogen for 1 - 2 hours at 400°C. Afterwards the whisker was remounted and pulled.

EXPERIMENTAL OBSERVATIONS AND RESULTS

1. Growth Observations

Cupric chloride reacts with water in the following manner:

$$CuCl_2 + H_2O \rightleftharpoons CU(OH)_2 + 2HCl$$

The presence of this $Cu(OH)_2$ in the $Cucl_2$ has a very disastrous effect on the growth of whiskers. If as received anhydrous cupric chloride was used, in almost all instances, no whiskers were produced. It was thus found necessary to purify the $CuCl_2$ by passing dry HCl gas through it. The quality and quantity of the whiskers grown from the purified $CuCl_2$ decreased rapidly with increasing exposure to the air as $CuCl_2$ is very hygroscopic.

Whiskers were grown in the temperature range of 550°C to 800°C. The reproducibility of whisker growth for apparently the same conditions is not very good and hence only general tendencies are listed below.

(i) At temperatures between 550°C and 700°C the whisker growth was heavy with most of the whiskers being less than 15 μ in diameter. Some boats of whiskers contained very long (1 - 4 cm) whiskers, but these usually were tapered or contained surface irregularities such as very short branch growths.

(ii) At temperatures above 700°C the whiskers were usually coarse (up to 100 μ in diameter) and the growth was not as profuse as in (i).

(iii) The hydrogen flow rate did not seem to effect the growth results provided it was above a minimum rate of about 100cc per minute. The flow rate was usually between 200-300cc/min.

(iv) Aside from the presence of any $Cu(OH)_2$ in the $CuCl_2$, a very important factor determining the quality of the whiskers was the cleanliness of the reducing atmosphere and surroundings. If the Vycor tube was cleaned before each growth run, much better whiskers were obtained than if several growth runs were done in the tube before cleaning it.

Most of the whiskers were straight, usually with either short branches or other types of surface defects. However, as also reported by Brenner[29] and Saimoto[28], a large variety of other shapes such as polygonal spirals, circular and polygonal helices, twists, kinks and many others such as the one shown in Fig. 15 were observed.

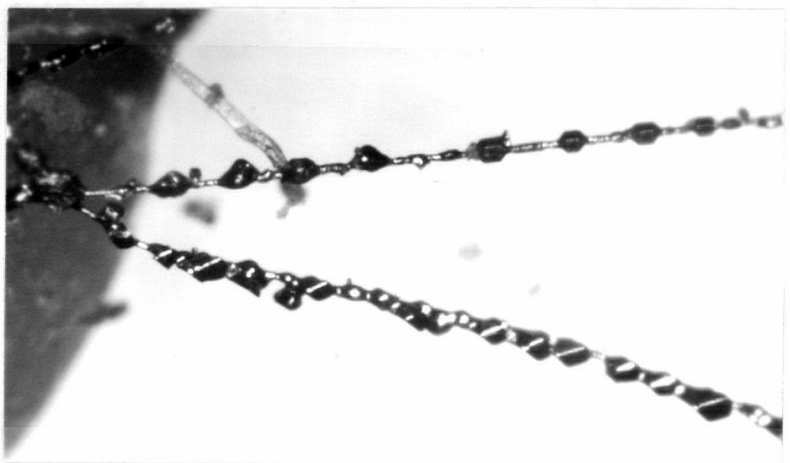

Figure 15. An Odd Shaped Whisker, Mag. 400X.

2. Cross Sectional Area

Table IV, Appendix II, compares the results in measuring the area optically and in calculating the area, by the method previously described, of the whiskers. This calculated value of area was used in all the stress calculations. In most cases, the agreement between the two values of area was good. In the optical measurements of diameters a minimum error of 2 divisions or 0.7 μ was possible.

3. Tensile Tests

a. Reliability of the Quantitative Measurements

In measuring the yield stress of the whiskers, the two major sources of error are the force calibration of the apparatus and the cross sectional area determination of the whiskers. The maximum error introduced due to the compensation for restoring force is about 10mg. This would give an error in the yield stress of, at the very most, 2%, since the smallest load measured at yield was about 500 mg. Hence the probable error for the load measurements, which includes calibrating (5%) and compensating errors, is about 7%.

The error in measuring the cross sectional area was discussed in some detail by Saimoto[28]. He showed that the assumption of Young's Modulus being the same for both whiskers and bulk crystals is reasonable. The error is due to the assumption that the whiskers have orientations of [111], [100], or [110]. Saimoto found in his investigations that the whiskers which possess axes off the low index ones do so by about 15°. This would introduce a maximum error in the Young's Modulus of 10% (Appendix III). Therefore the values of stress may have an error of as much as 16%. However, it should be noted that most whiskers do have low index axes and hence this error in stress is an extreme.

b. Statistical Treatment of the Data

Since a comparatively large number of results was obtained, a statistical treatment of these results was made. The methods used are discussed in Appendix IV. Also, the probable error of the calibrations in Appendix I was computed statistically and is shown on the graphs.

c. Primary Tests

The results of the primary tests are listed in Appendix II, Table V. From these results, the yield stress, σ_m, was plotted against the diameter, d (Fig. 16). In order to determine the best line to draw through these points, log σ_m was plotted against log d (Fig. 17) since σ_m was assumed to be a function of d^n. The slope, n, of the band containing the points was found to be -1.6. The method used in calculating this slope is found in Appendix IV. Thus σ_m was inversely proportional to $d^{1.6}$. In comparison, as was previously mentioned in the introduction, Brenner found the yield stress of his whiskers proportional to 1/d. Brenner determined his relationship by plotting the average value of yield stress of whiskers of approximately the same diameter against $1/d_{ave}$ (Fig. 18). This method was tried for the results obtained in this investigation, but it proved very unsatisfactory since approximate straight lines could be drawn both for σ_m versus 1/d and $1/d^2$.

A plot of σ_m against $1/d^{1.6}$ (Fig. 19) gave that

$$\sigma_c = \frac{1571}{d^{1.6}} + 2.8 \text{ Kg/mm}^2 \qquad \text{(d in microns)} \qquad (1)$$

In this equation, σ_m was replaced by σ_c for convenience in future calculations. The line drawn through the points on Fig. 16 was calculated using the above equations.

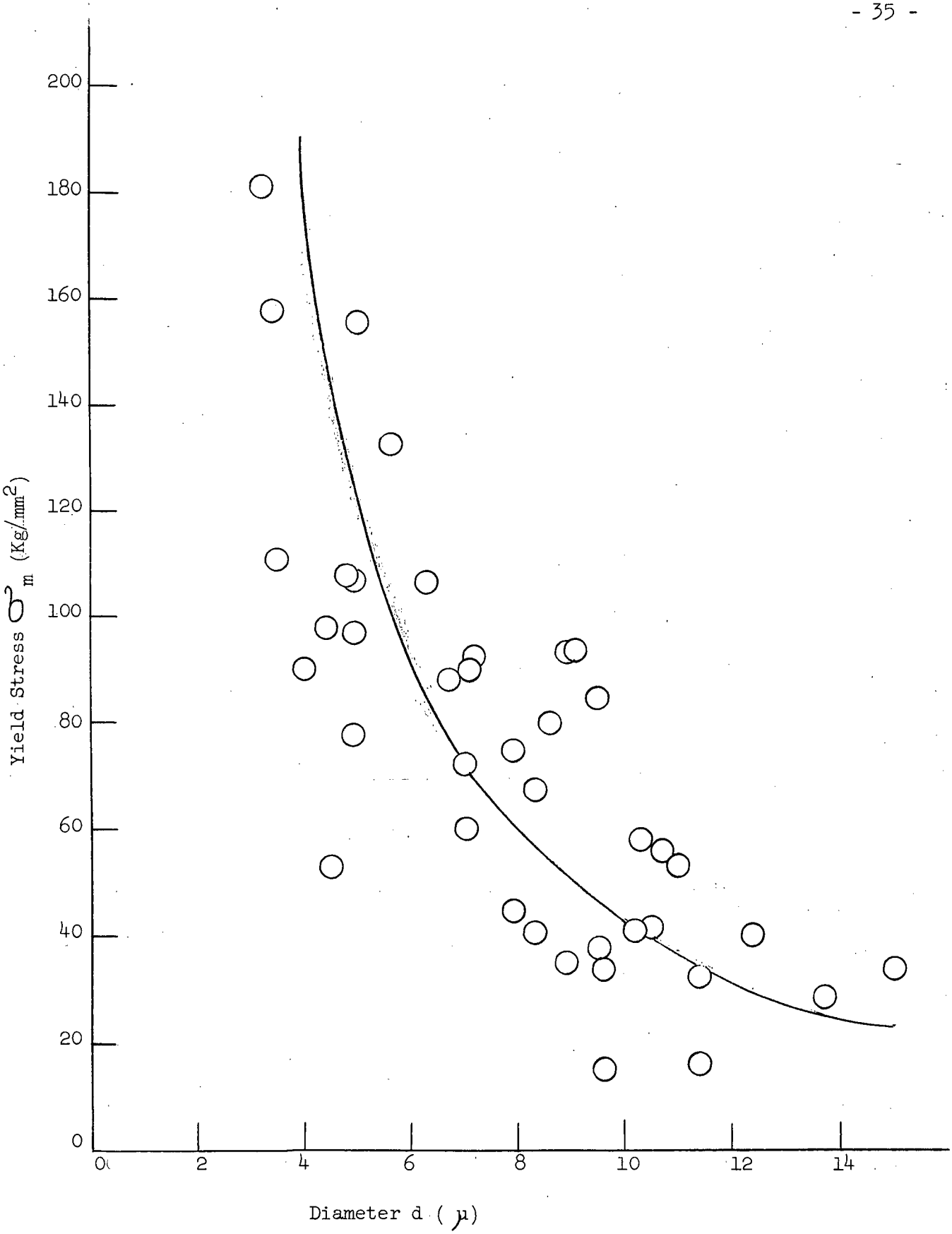

Figure 16. Primary Yield Stress as a Function of Diameter.

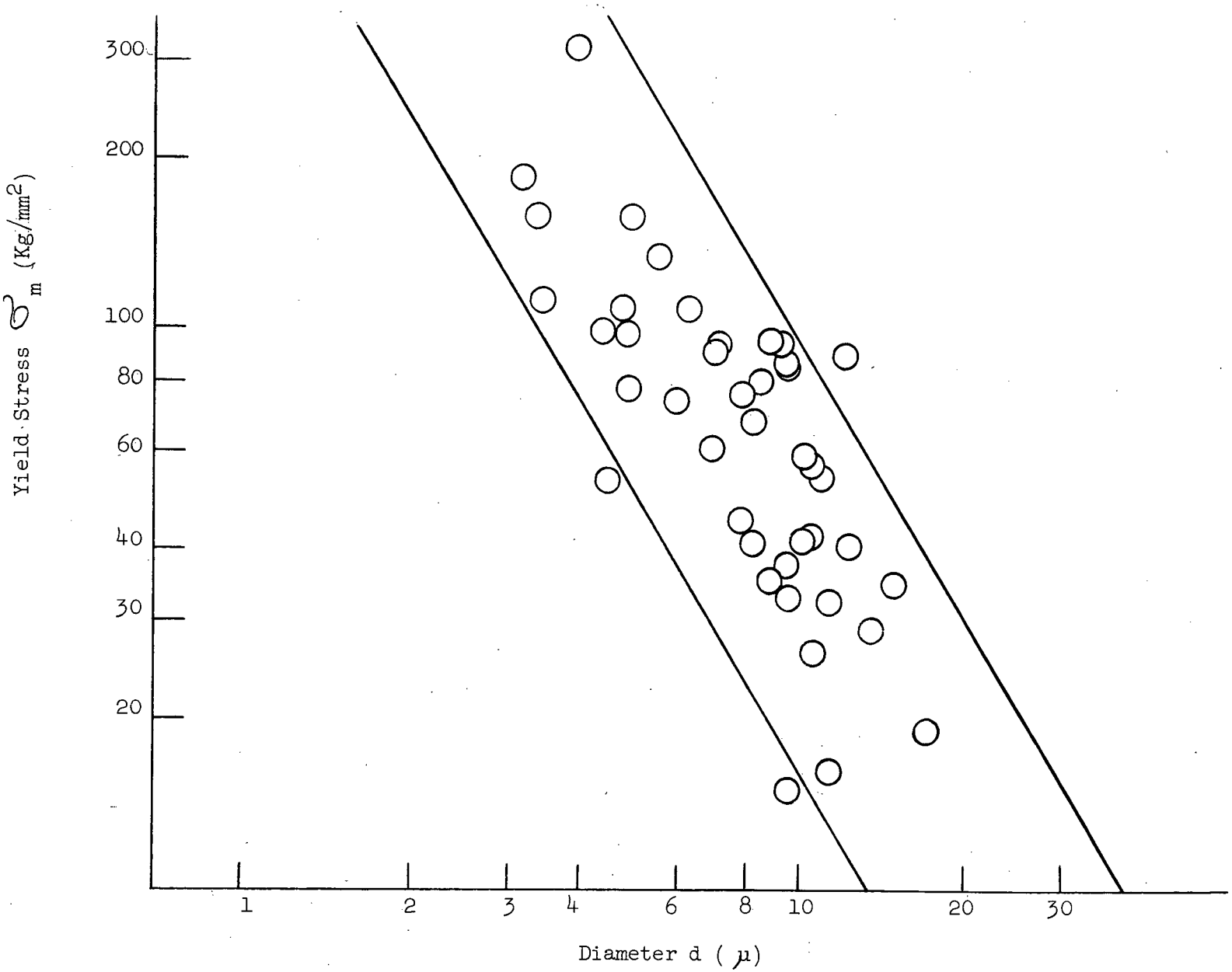

Figure 17. Log Plot of Primary Yield Stress Against Diameter.

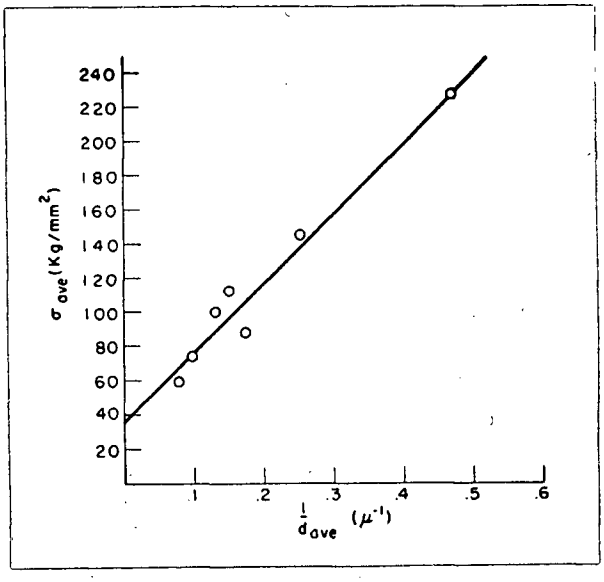

Figure 18. The Average Strength of Copper Whiskers as a Function of the Reciprocal of the Diameter. Reproduced from Reference 7.

The graph of σ_m against length, L, is shown in Fig. 20. The various symbols denoting primary tests, secondary tests and annealing tests were used to distinguish between whiskers which were later retested and those that were not. As can been seen for Fig. 20, no particular dependence of σ_m on L is apparent. However, since this plot was for whiskers of various diameters as well as lengths, any trend could well be hidden by the dependence of σ_m on d. Therefore it was decided to use a normalizing procedure to convert the strengths of whiskers of various diameters to comparable strengths for whiskers of one diameter. The normalizing procedure was as follows. Consider a plot of yield stress σ, against diameter d as shown in Fig. 21. Let a whisker of diameter d_s and of strength σ_a be chosen as a standard whisker. If a whisker of diameter d_c with strength σ_c was now considered to be a whisker of diameter d_s, its strength would then be σ_s. In the case of a whisker with the same diameter d_c, but now of strength σ_m (position A), a comparable strength of a whisker of diameter d_s (position A^1) is given by

$$\sigma_n = \sigma_s \frac{\sigma_m}{\sigma_c} \qquad (2)$$

A standard whisker of 10 μ in diameter was chosen since many of the whiskers had diameters around this value. Using equation (1) to calculate the value of σ_s for d = 10 μ, equation (2) becomes

$$\sigma_n = 42.3 \frac{\sigma_m}{\sigma_c} \qquad (3)$$

The values of σ_c for all the whiskers was calculated using equation (1) and then σ_n was calculated from equation (3). These results are listed in Appendix II, Table V. Fig. 22 shows the plot of σ_n against L and again these is no apparent trend. Since the scatter was quite high it was possible that any trend could be masked by this scatter and so

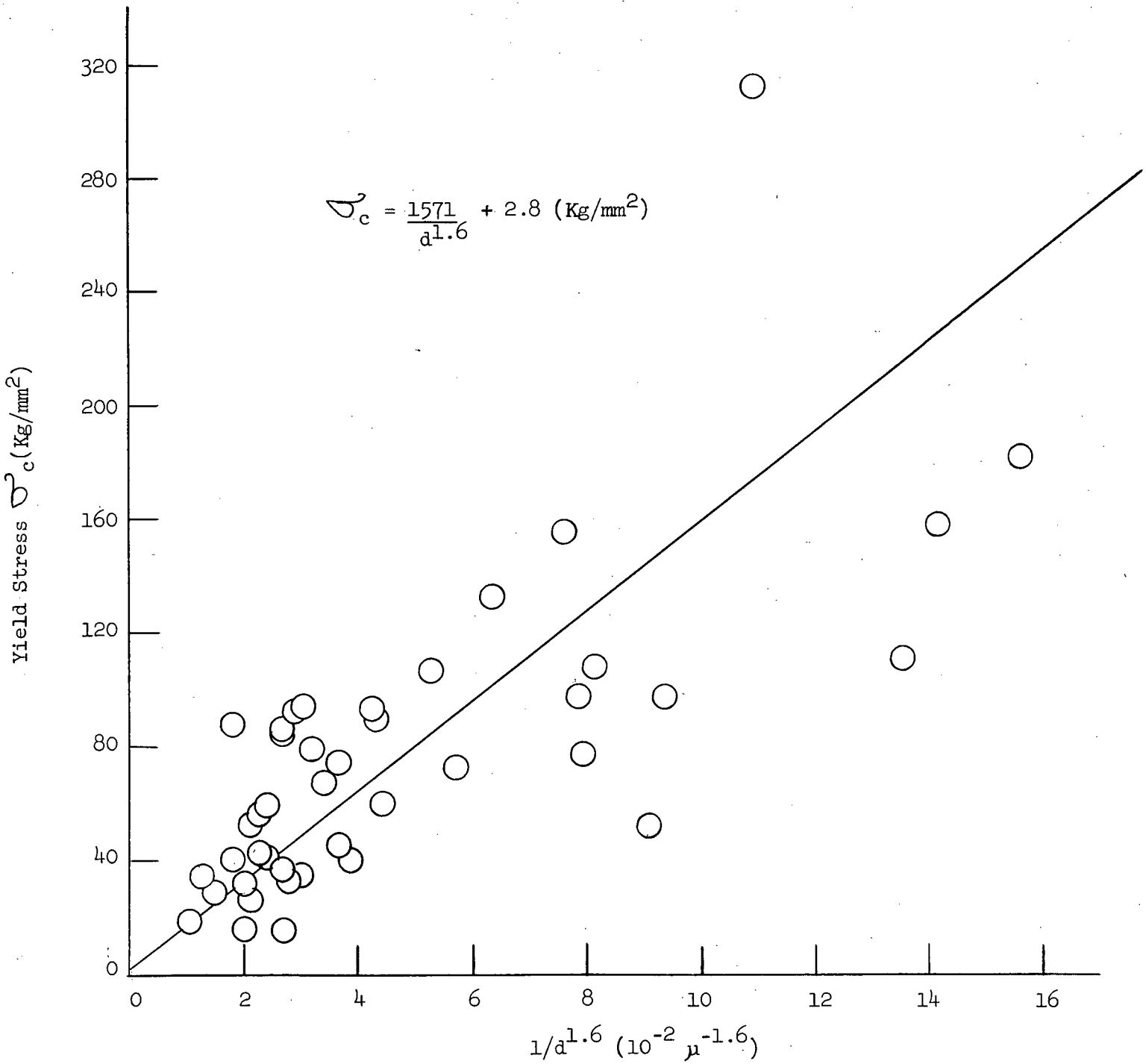

Figure 19. Primary Yield Stress Against Diameter.

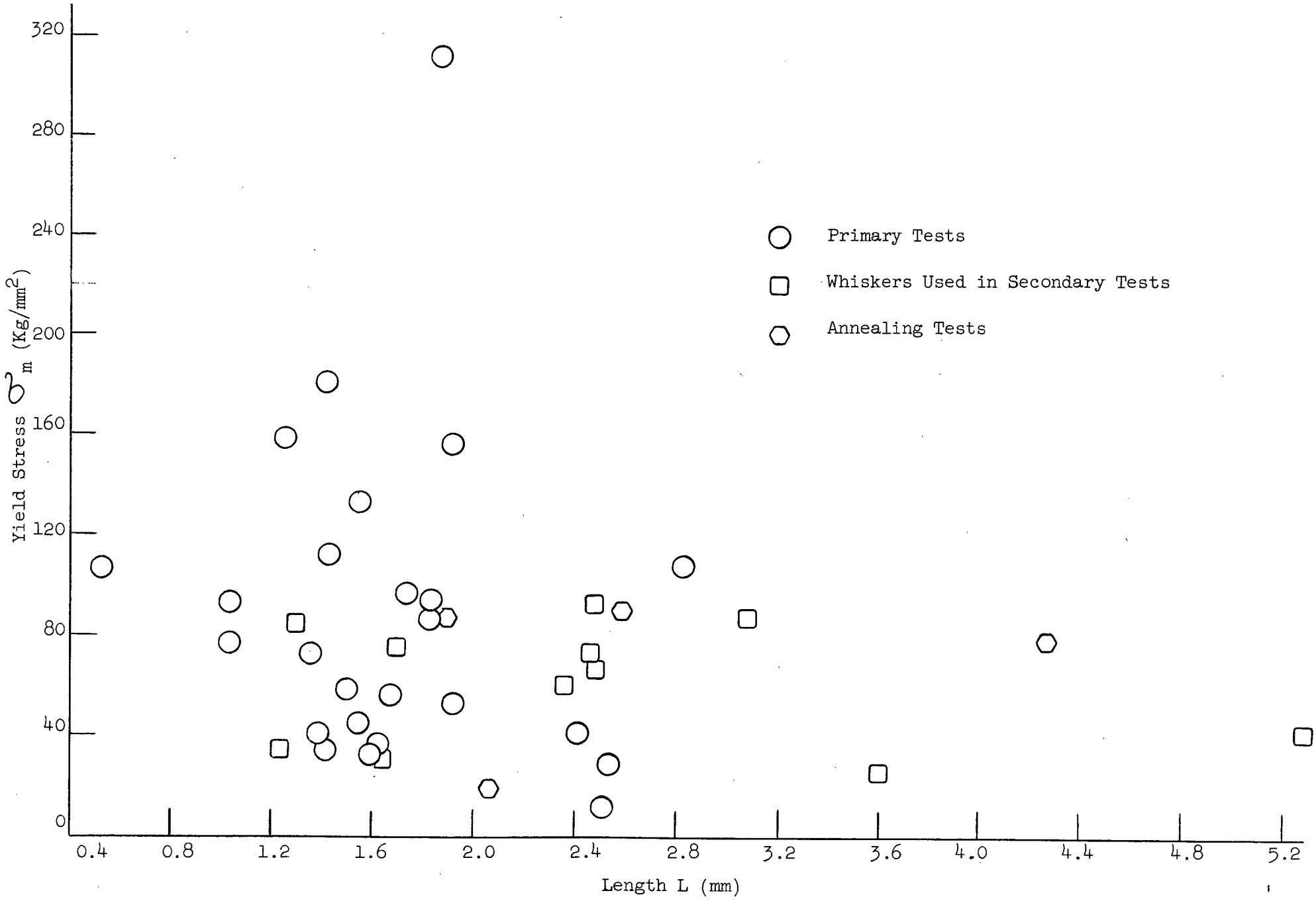

Figure 20. Primary Yield Stress as a Function of Length.

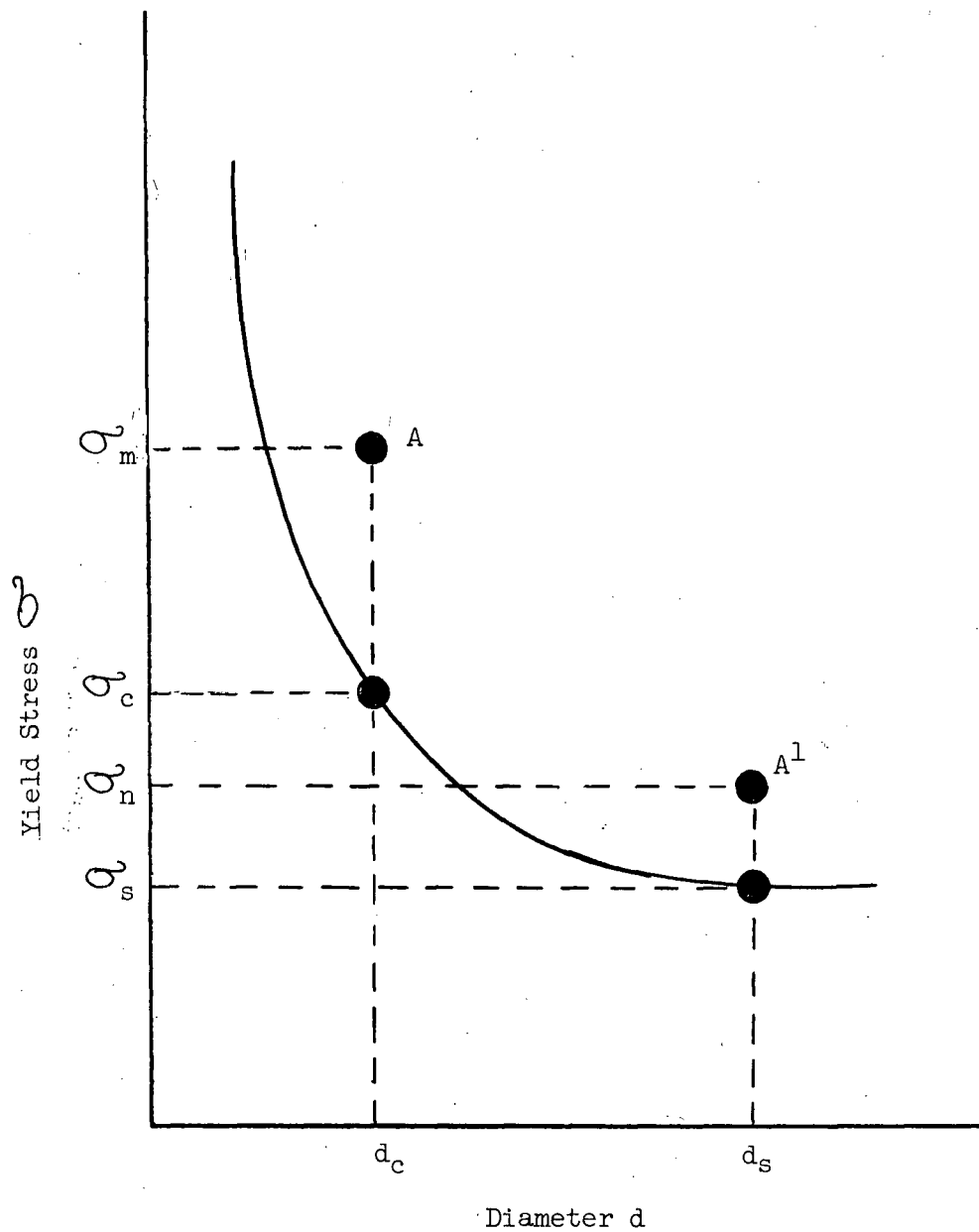

Figure 21. Diagram Illustrating Derivation of the Normalizing Procedure.

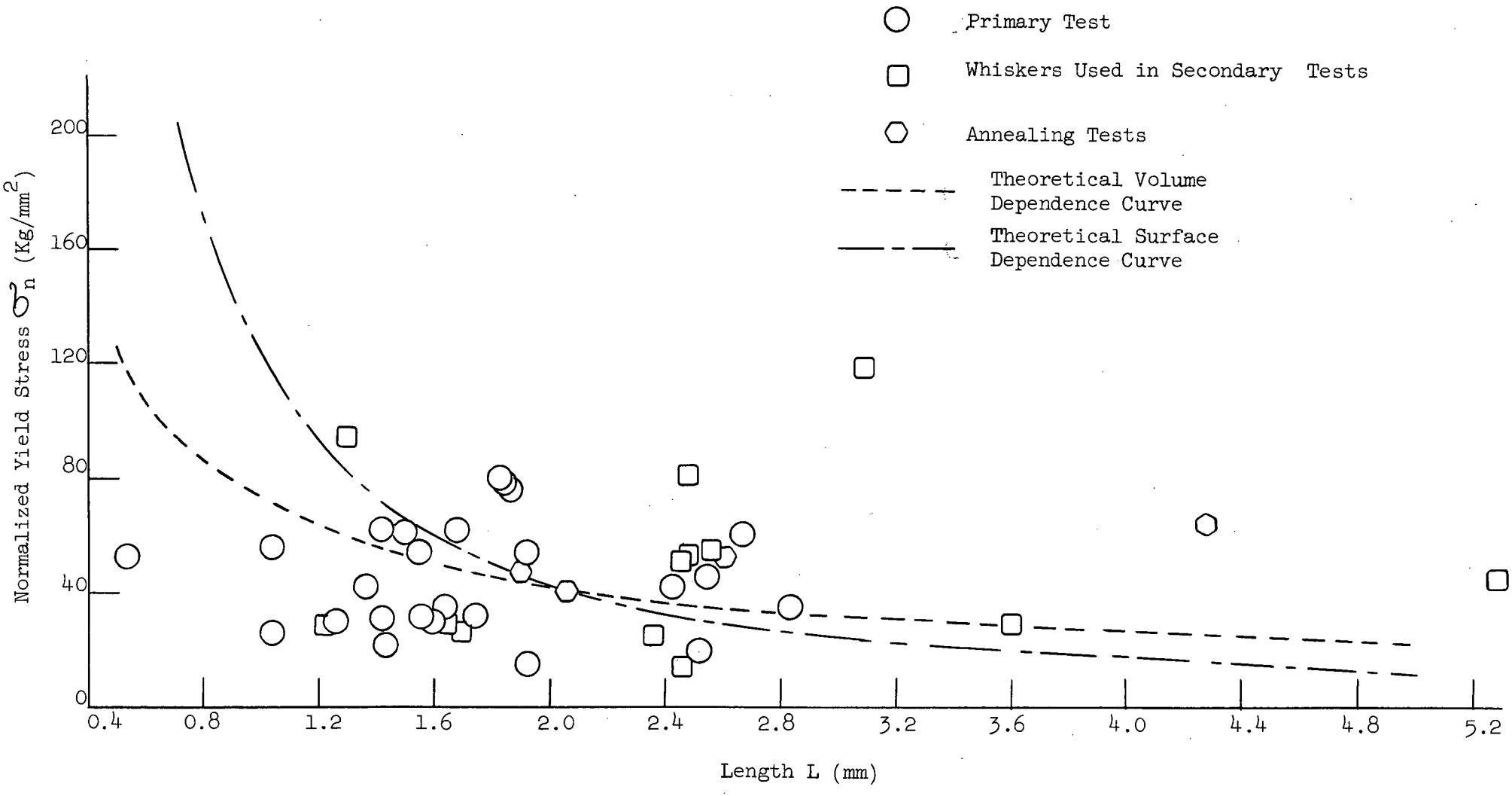

Figure 22. Normalized Primary Yield Stress as a Function of Length.

theoretical curves, assuming either a volume dependence or a surface dependence for yield stress, were calculated and plotted on Fig. 22. The method of calculating these curves is given in Appendix V, Part A. In the case of a volume dependence, for whiskers of diameter 10 μ and varying in length from 1000 μ to 5000 μ, a variation in σ_n of approximately 3 [Appendix V, Part B], would be expected between the two limiting values of L. However, since the scatter is of this order, any volume dependence would not be observed. Similarly, in the case of a surface dependence, a variation of about 10 would be expected. This was not observed. It would thus seem that if there is a length dependence for yield stress, it is so small as to be unobservable.

d. Annealing Tests

The annealing of whiskers mounted on the tensometer was very unsatisfactory. Only one test out of about twenty attempts was successful (whisker GG). The major problems were the low melting point of the mounting compound and the tendency of this compound to contaminate the whisker by forming a coat on its surface. Three other successful annealing tests were obtained by method (ii) as described on page 30.

Since the results of the tests on these annealed whiskers did not vary significantly from the results of secondary tests on ordinary whiskers, they will be included in the next section.

e. Secondary Tests

Appendix II, Table VI lists the results of the secondary tests. The primes refer to the number of times that each whisker was retested. As can be seen in Figs. 20 and 22, the initial values of yield stress for secondary tested whiskers show no particular patterns of their own.

These results were treated in a similar manner as the results in the previous section. However, the area used in calculating the yield stress was the same as the area calculated from the primary test and not from the secondary tests on the same whisker since the diameter of the whisker was assumed not to change. As before, yield stress σ_m, was plotted against diameter, d (Fig. 23) and log σ_m was plotted against log d (Fig. 24). The slope of the band containing the points was found to be -2.5, so that σ_m was now inversely proportional to $d^{2.5}$. The plot of σ_m against $1/d^{2.5}$ (Fig. 25) gave

$$\sigma_c = \frac{4425}{d^{2.5}} + 39.0 \text{ Kg/mm}^2 \quad (d \text{ in } \mu) \qquad (4)$$

with σ_c again replacing σ_m for convenience. The line drawn through the points on Fig. 23 was calculated by this equation.

The graph of σ_m against length L is shown in Fig. 26. In this case there seemed to be an increase of strength with a decrease in length. However, as this plot did not take into account the fact that the whiskers were of various diameters, these whiskers were normalized in the same manner, as in the previous section, to whiskers of 10 μ in diameter. The normalizing procedure gave that

$$\sigma_n = 53.0 \frac{\sigma_m}{\sigma_c} \qquad (5)$$

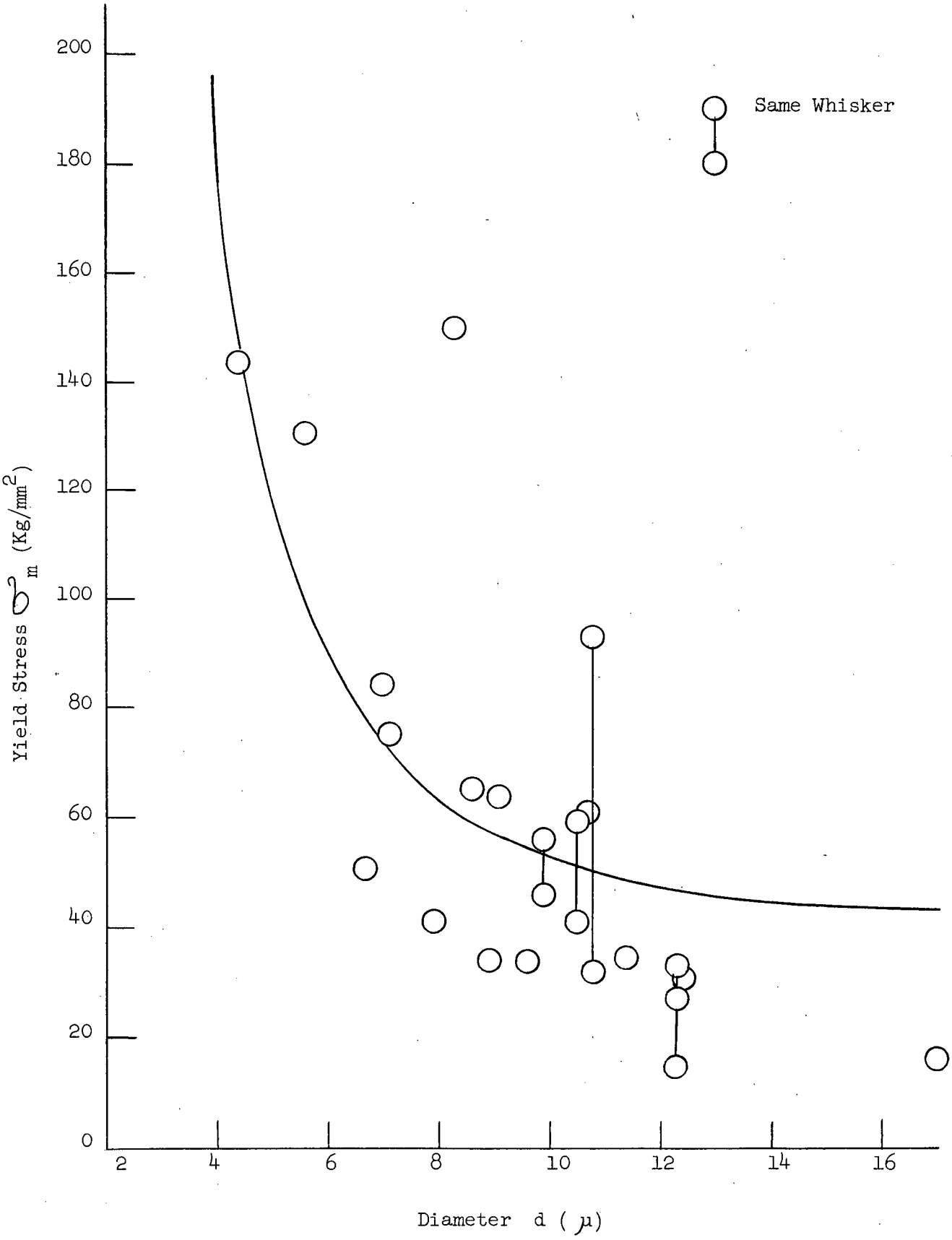

Figure 23. Secondary Yield Stress as a Function of Diameter.

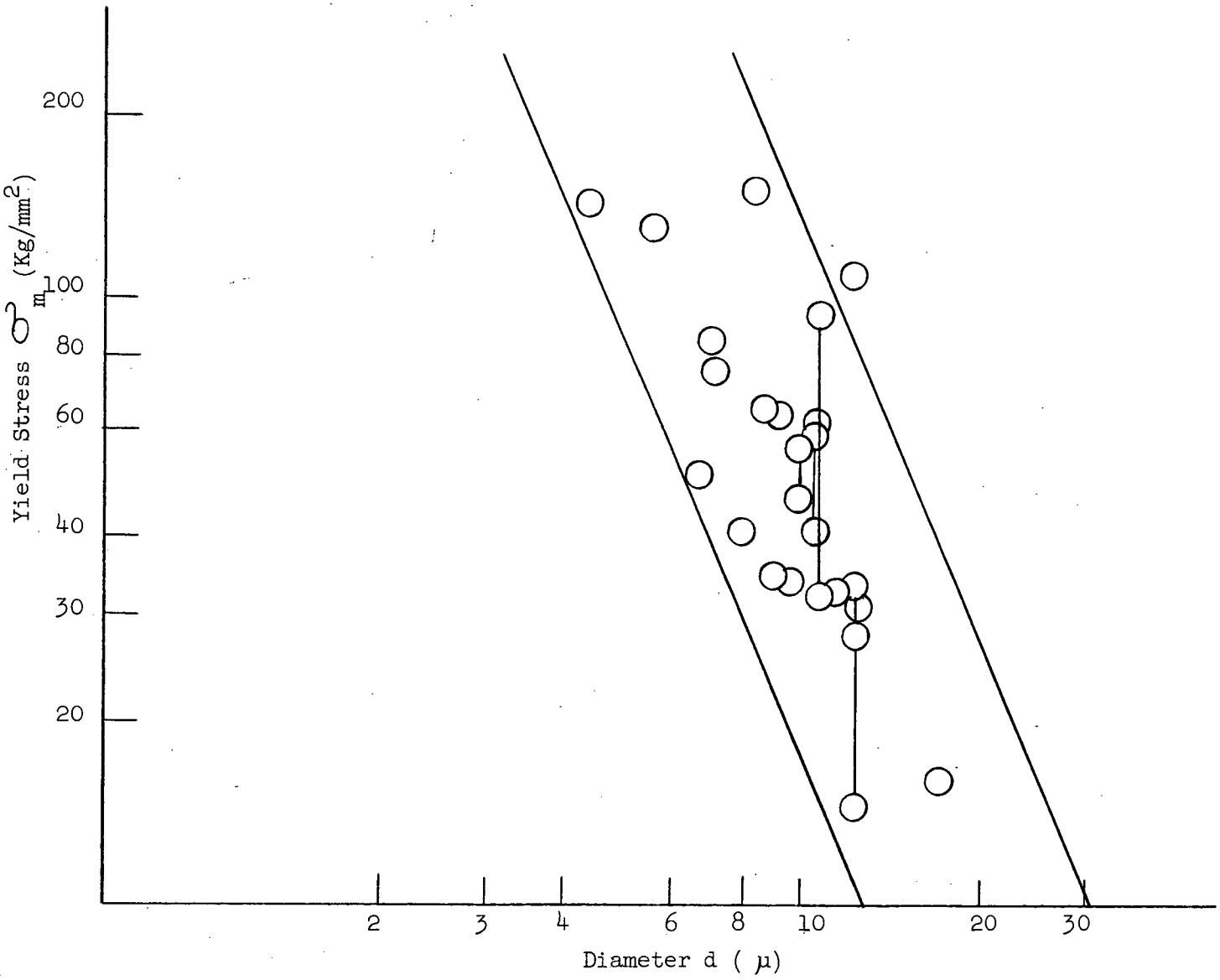

Figure 24. Log Plot of Secondary Yield Stress Against Diameter.

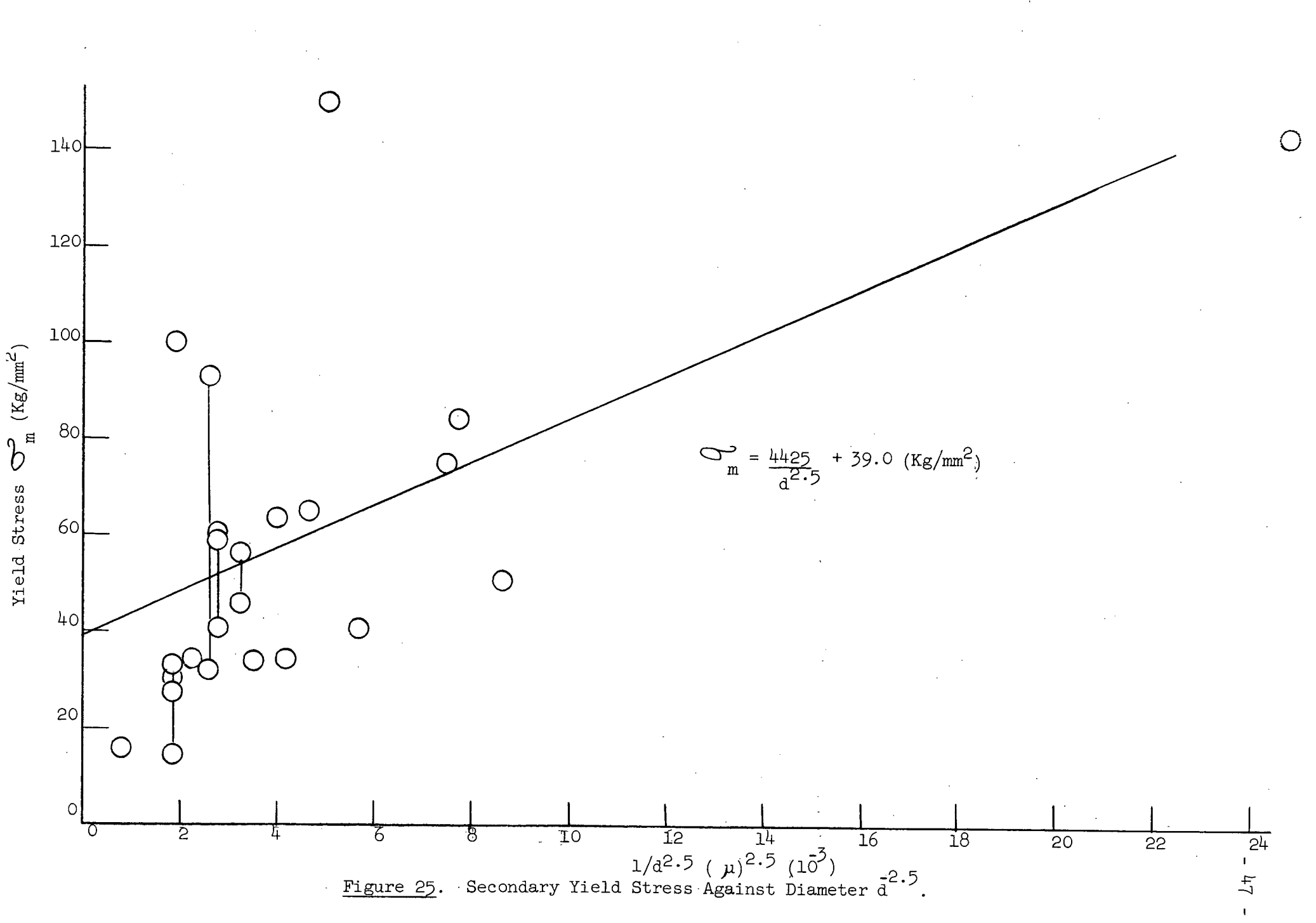

Figure 25. Secondary Yield Stress Against Diameter $d^{-2.5}$.

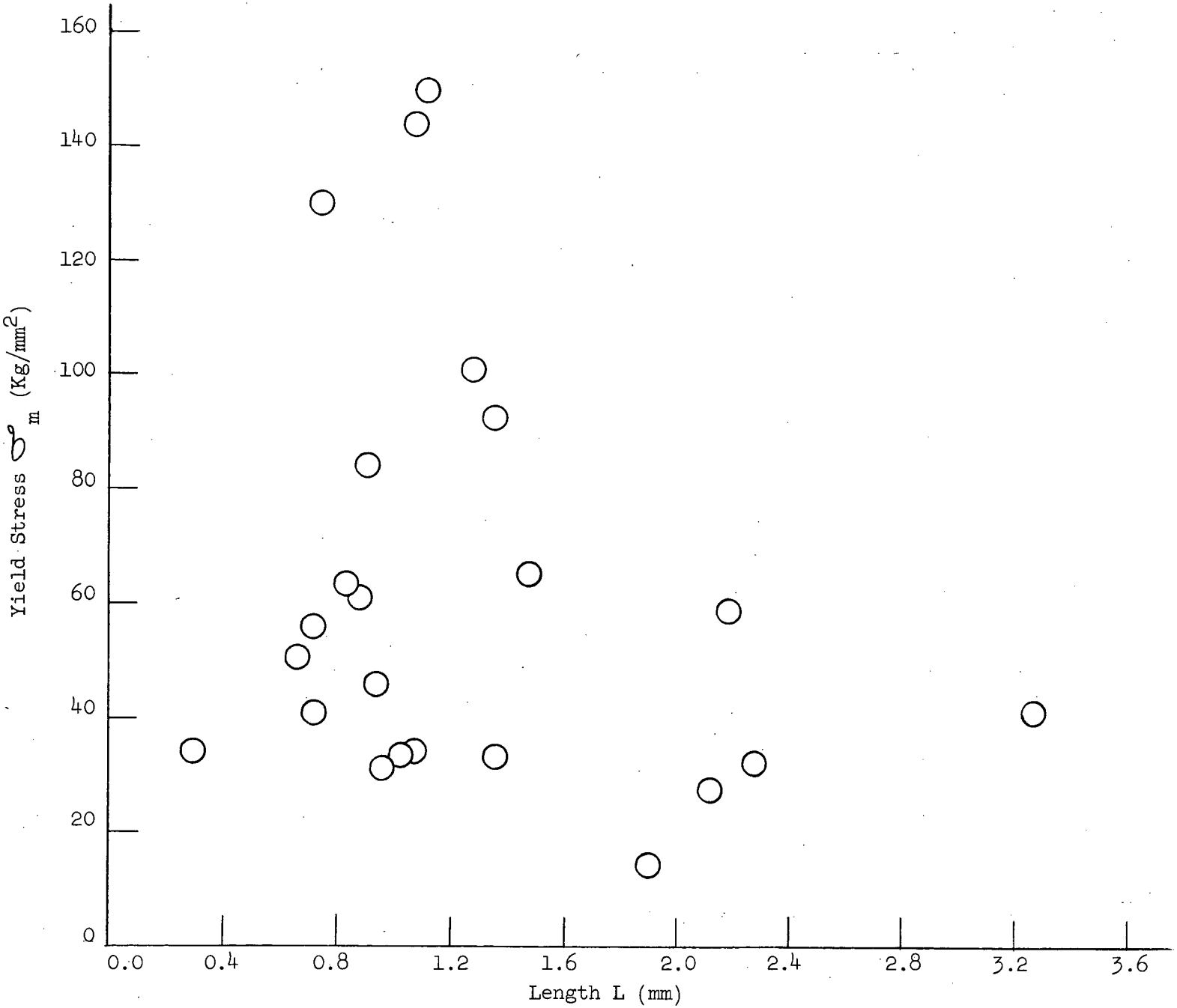

Figure 26. Secondary Yield Stress as a Function of Length.

and the results both for values of σ_c and σ_m are given in Appendix II, Table VI. The plot of σ_n against L is given in Fig. 27. The values of σ_n for most of the points lie between about 30 - 70 Kg/mm^2. This compares reasonably well with the results obtained for the primary tests (Fig. 22) where the points have values of σ_n between 20 - 80 Kg/mm^2. Again theoretical curves for the volume and surface dependence of yield stress were calculated (Appendix V, Part A). For the case of volume dependence for whiskers of 10 μ in diameter with the limiting values of L being 500 μ and 3500 μ, a variation of around 2 (Appendix V, PartB) would be expected. From Fig. 27 it can be seen that any volume dependence on stress would be masked by the scatter. In the case of a surface dependence, the variation expected is about 6. This is not observed. Thus the results for secondary tests are about the same as those of primary tests, ie. any length dependence of yield stress was so small as to be unobserved.

f. Variation of Young's Modulus

A rather surprising result obtained from the secondary tests is that there is an apparent change in the Young's Moduli of these whiskers. Appendix II, Table VI, lists the values of E/E_i where E_i is the value of the Young's Modulus obtained from the primary test on the whisker and E is the value obtained from the secondary test. Fig. 28 is a diagrammatical representation of the variation of E/E_i with E_i. Figs. 29 and 30 show stress-strain curves for two whiskers, both of which were retested. The stress-strain curves of both the primary and the secondary tests were reversible.

Initially, values of E and the ratio of E/E_i were plotted against such parameters as the initial elongation of the whisker (Fig. 31), diameter, initial length, etc, but no correlation was found. However, when the ratio E/E_i was plotted against the normalized value of primary yield stress,

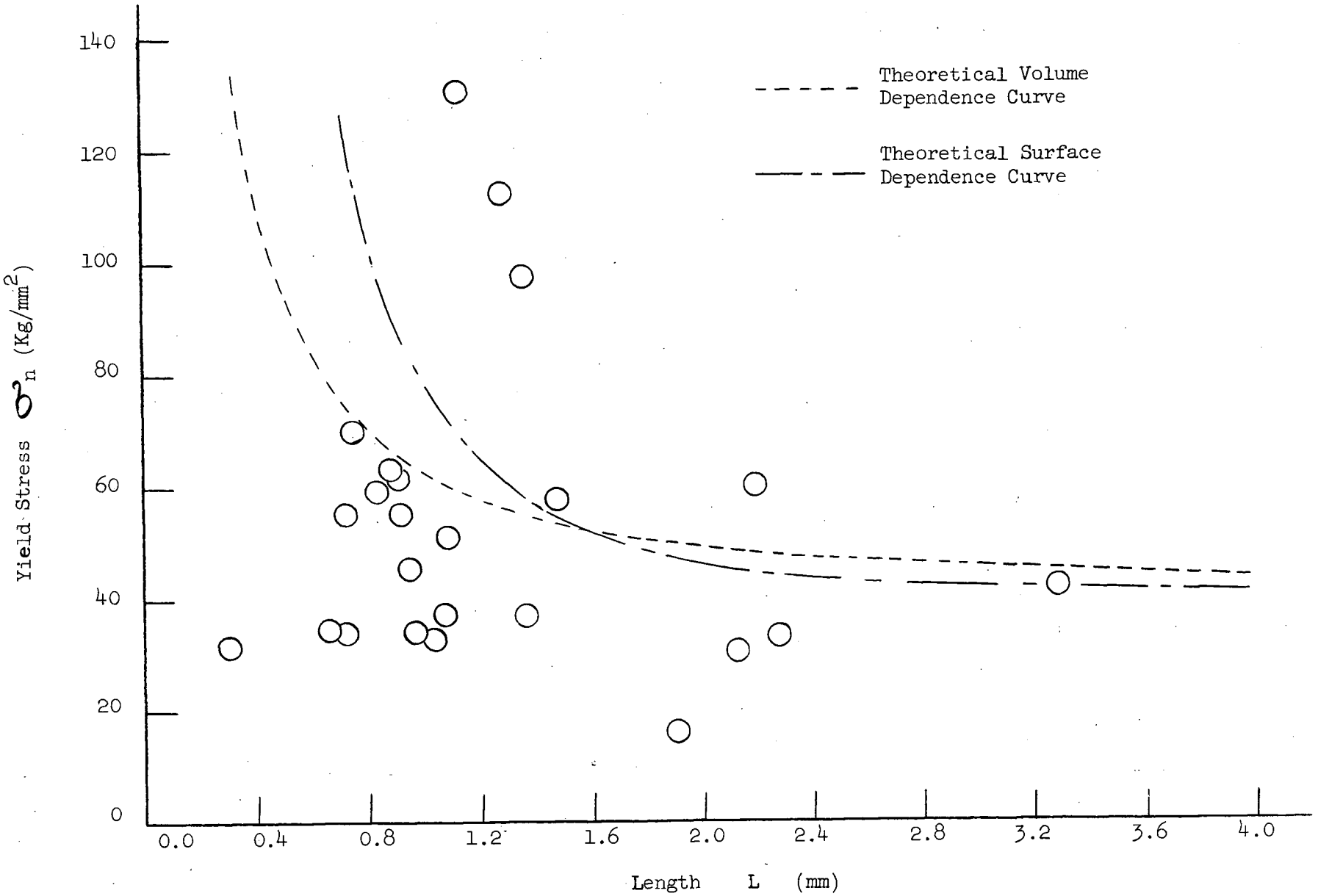

Figure 27. Normalized Secondary Yield Stress as a Function of Length.

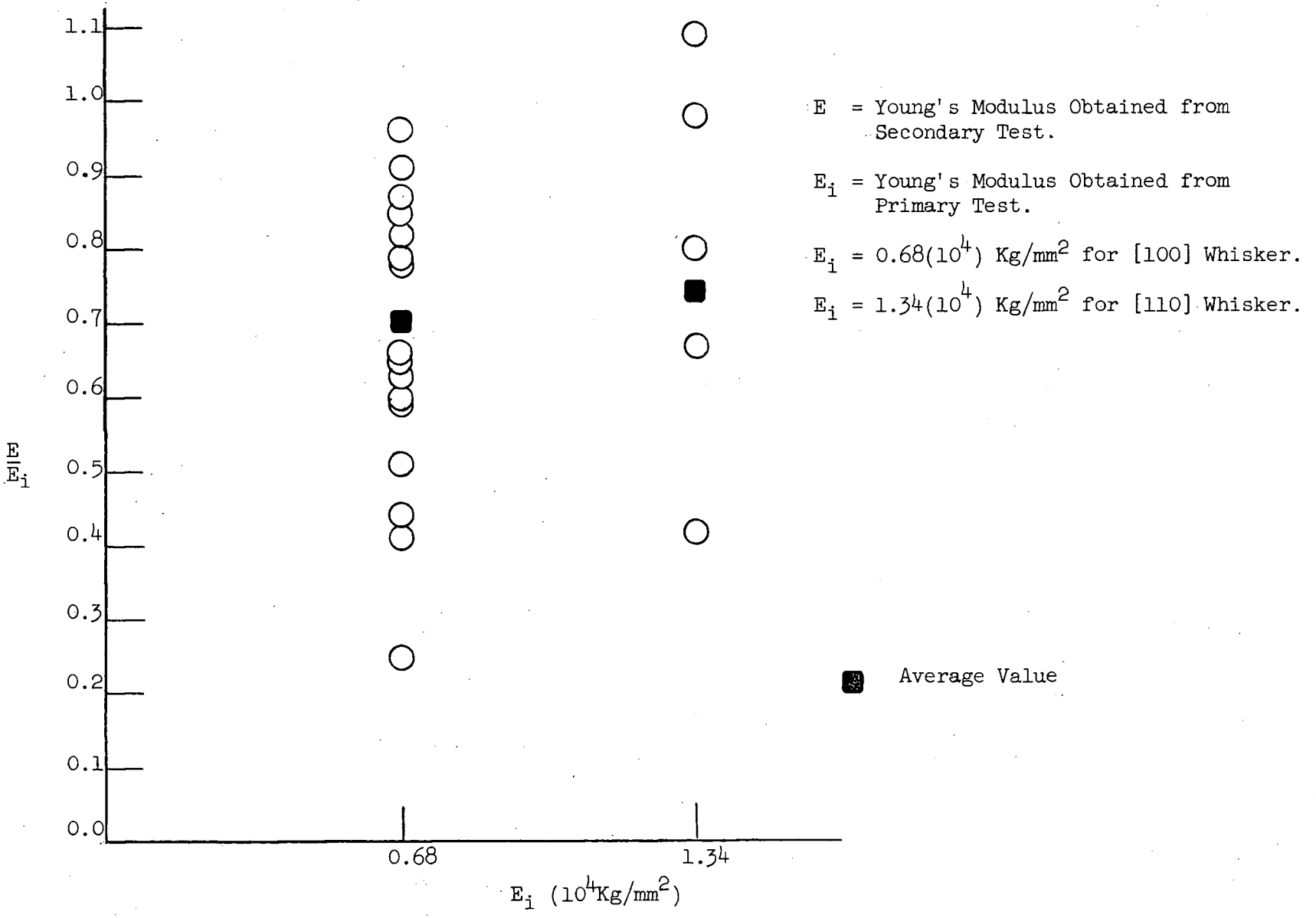

Figure 28. Plot of the Ratios E/E_i of Young's Moduli Against E_i.

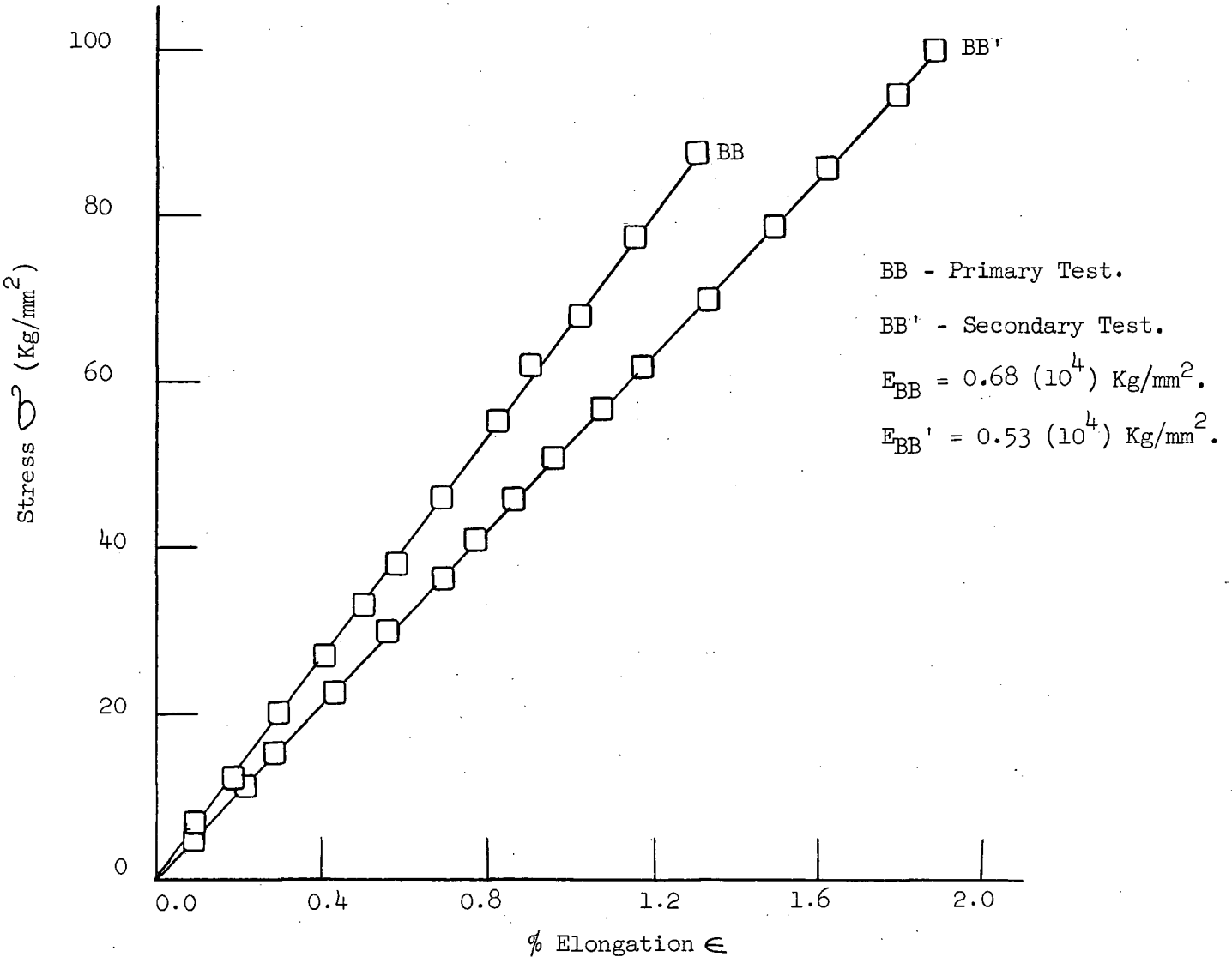

Figure 29. Stress-Strain Curve of Whisker BB.

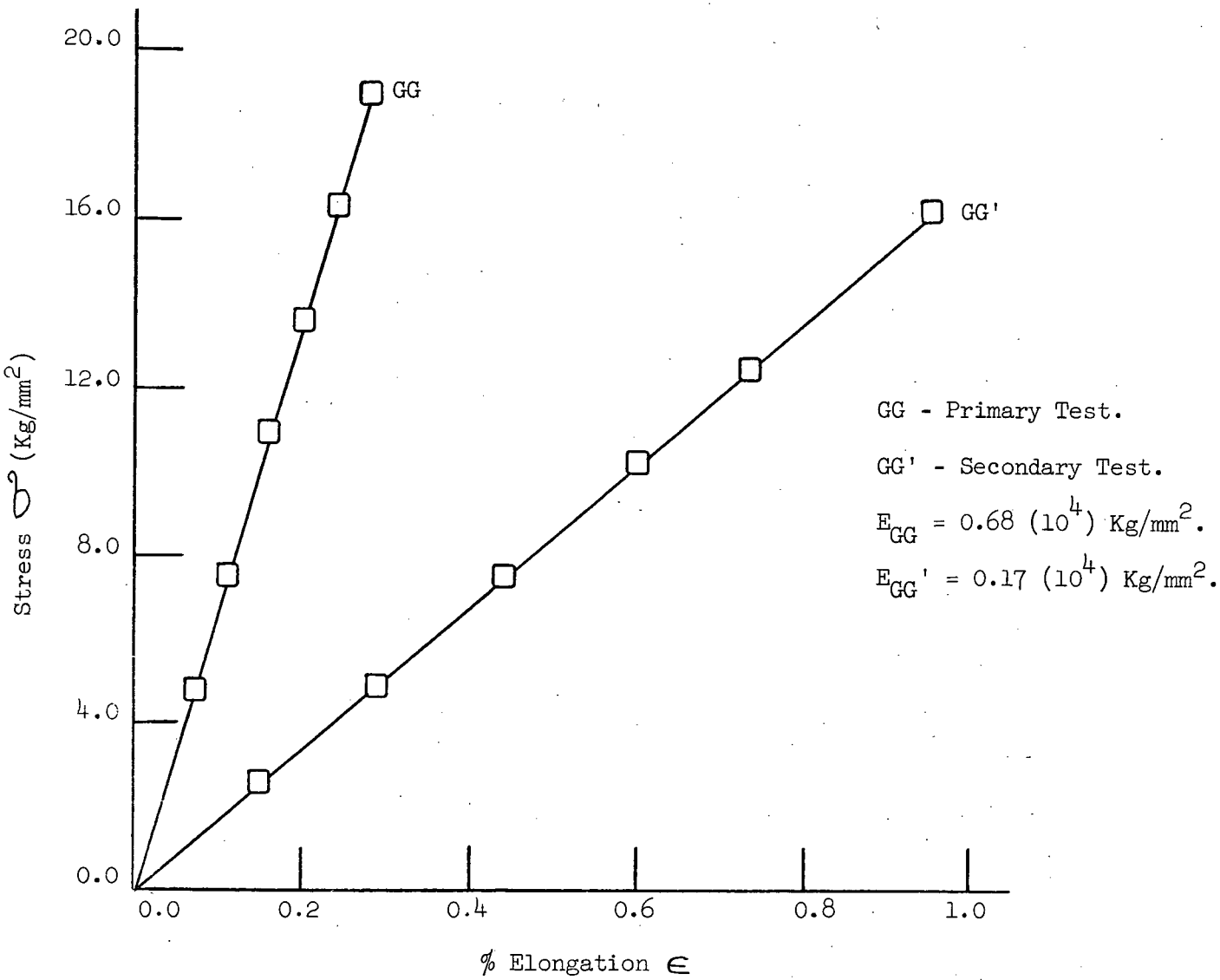

Figure 30. Stress-Strain Curve of Whisker GG.

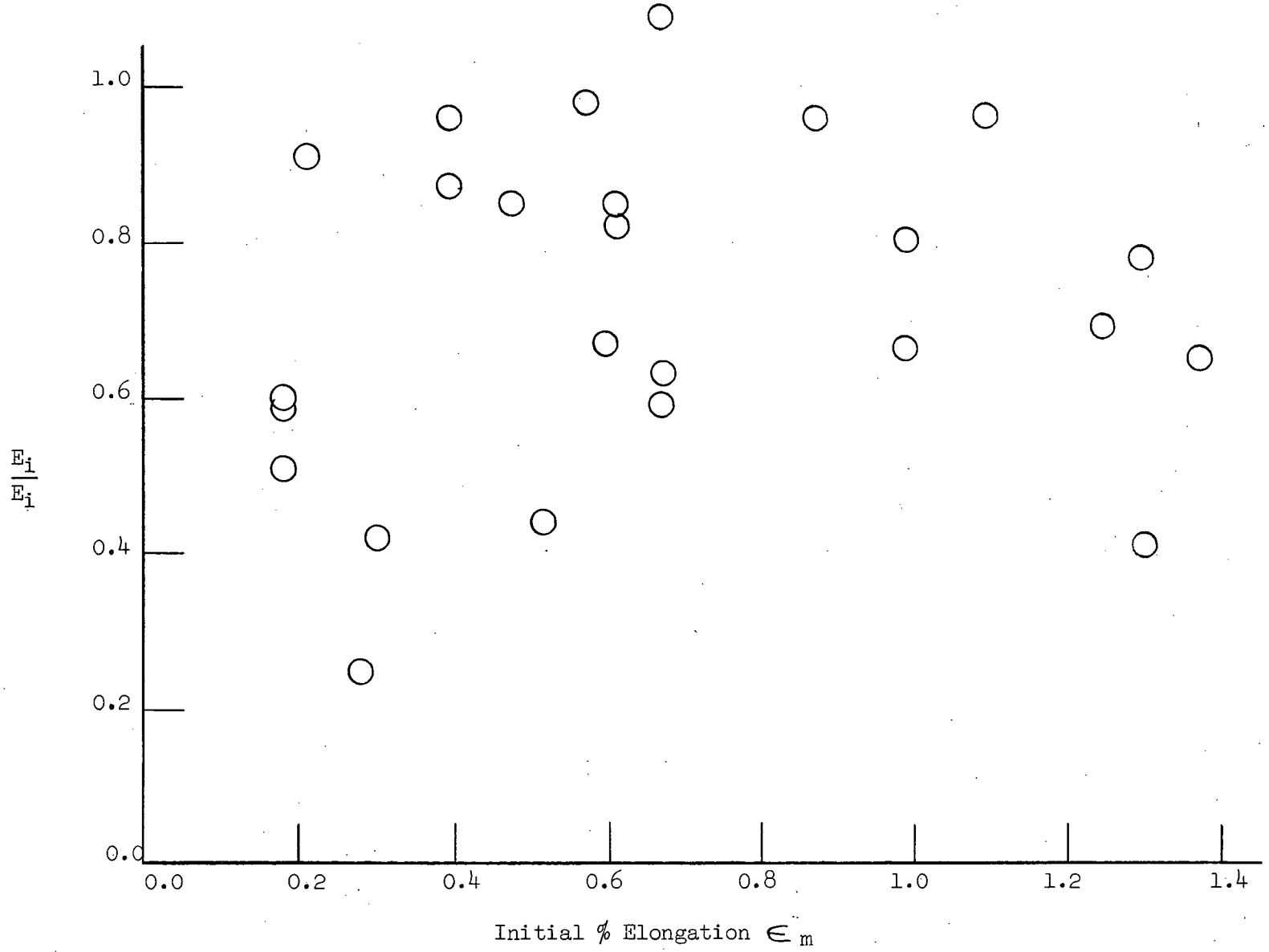

Figure 31. Ration E/E_i of the Young's Moduli Against Initial % Elongation.

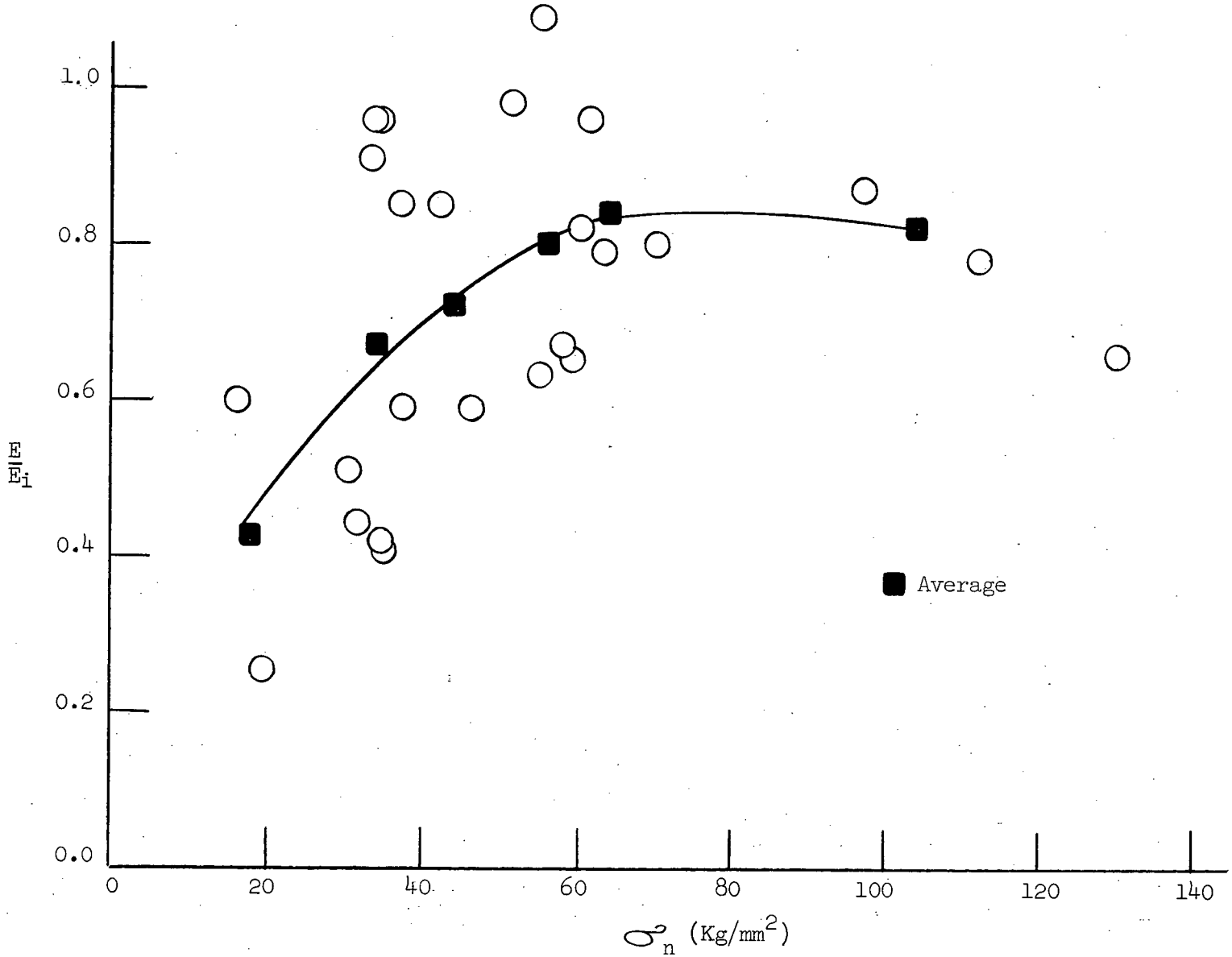

Figure 32. Ratio E/E_i of the Young's Moduli Against Primary Normalized Yield Stress.

σ_n (Fig. 32), it was found that E/E_i increased with an increase of σ_n up to a value of σ_n equal to about 80 Kg/mm^2 where the curve seemed to level off. The points in the squares were determined by averaging values of E/E_i over intervals of σ_n from 10 - 20, 30 - 40, 50 - 60, 60 - 70 and 95 - 115 Kg/mm^2.

g. Summary

The results of the primary test showed the following:

(i) the yield strengths of the whiskers were proportional to $d^{-1.6}$,

(ii) no observable dependence of length of yield strength.

The results of the secondary tests showed the following:

(i) the yield strengths of the whiskers were proportional to $d^{-2.5}$,

(ii) no observable dependence on length of yield strength,

(iii) an apparent decrease in the Young's Modulus of about 30%.

DISCUSSION

1. Growth

While the study of whisker growth was beyond the scope of this investigation, a brief discussion of the effect of the presence of water on whisker growth will be given for the sake of completeness.

The classical theory of crystal growth considered a crystal to be structurally perfect and assumed that each time a step on the crystal swept over the surface, a new one had to be nucleated on the freshly completed crystal layer. A critical supersaturation was required for continued growth because the creation of a step on the surface increased the surface energy of the crystal. However, since it was found that crystals grew at supersaturations which were immeasurably small, Frank[31] concluded that real crystals were not perfect, but contained screw dislocations which were developed during the early stages of their growth. It was these screws which provided the crystals with permanent growth steps.

For the case of whisker growth, it was proposed by Sears[32] that whiskers contained a single axial screw dislocation with the lateral crystal surfaces bounded by surfaces which are atomically smooth.

As has been previously mentioned, whiskers were grown by the hydrogen reduction of $CuCl_2$. Actually this will first be reduced to CuCl which then disproportionates[33] to give Cu and $CuCl_2$. Without going into the thermodynamics of it, the reduction potential of the hydrogen will be lowered by the presence of any H_2O. However, in this case, the potential is still sufficient enough that all the $CuCl_2$ is reduced to copper.

At present, because of experimental results and thermodynamic considerations[34,35], so far only one theory of the growth of whiskers by hydrogen reduction is acceptable. This theory states that the liquid halide is transported up the walls of the whisker. This transport is then followed by catalytic decomposition at the whisker tip. It has been observed by Shetty[36] that there is a growth step for each face at the tip of the whisker.

H_2O molecules are strong dipoles with a dipole moment of $1.7(10^{-18})$ esu. Sarakhov[37] studied the adsorption and desorption of water vapour on gold foil at 18°C. The desorption never proceeded to zero concentration of H_2O at 18°C even after ten days evacuation and required 30-40 hours evacuation at 450°C. Allan and Webb[38] observed that when a boat containing CuCl was pushed into the furnace, growth occurred only after the boat became coated with a film of copper. Hence, it is not unlikely that the whisker growth sites would be poisoned by the presence of any H_2O dipoles. This process would therefore prohibit the growth of the whiskers. Also, even when a whisker had started growing, these dipoles could inhibit the growth by adsorbing on one or more of the faces at the whisker tip. This would account for the decrease in the quality of the whiskers that are produced.

2. Comparison of Results With Previous Work

The results of tensile tests performed on copper by Brenner[15] and Saimoto[28] are listed in Appendix VI. Fig. 33 is a comparison of the resolved critical shear stress τ_{cr}, against diameter for whiskers of orientations $[100]$, $[110]$ and $[111]$ as found by the author, Brenner and Saimoto. The points obtained by the author and Saimoto show, despite a high scatter, that there is a dependence of the critical resolved shear stress on diameter. However, in the case of Brenner, no particular dependence is observed. This

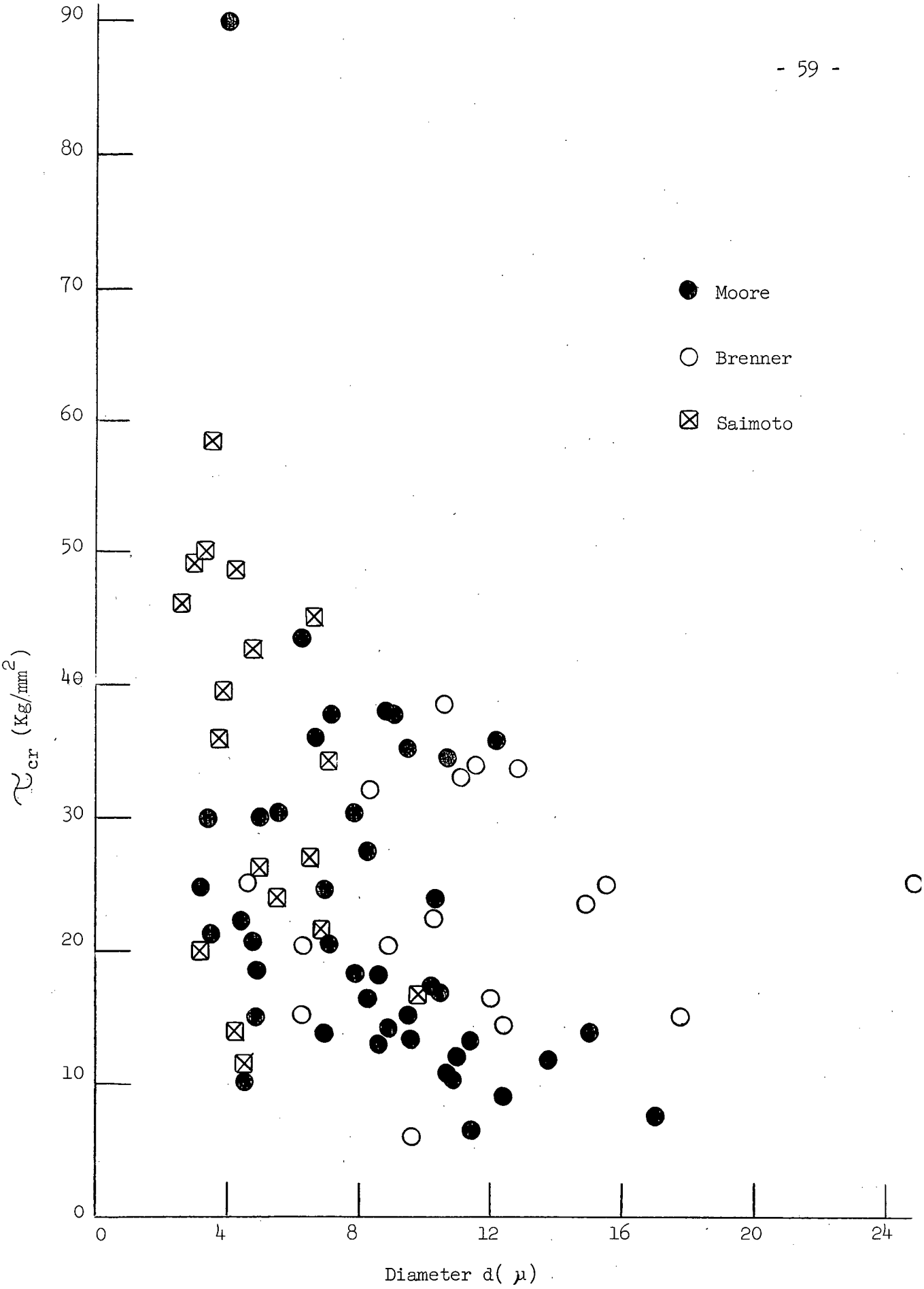

Figure 33. Critical Resolved Shear Stress Against Diameter.

is most likely a result of the relatively small number of points obtained, most of which were for whiskers with diameters greater than 8 μ for which the dependence of τ_{cr} on diameter is not so pronounced.

It has been found that the yield stress does depend on diameter. Now if, in fact, the critical shear stress did not depend on diameter this would lead to the rather startling conclusion that the yield stress of a whisker would no longer depend on the amount of stress necessary to cause shear on the slip plane. Therefore the yield stress would have to depend on some other factor.

Figs. 34, 35 and 36 are plots of the critical shear stress against diameter for whiskers of orientation [100], [110] and [111] respectively. The curves drawn through these points were obtained from the equation which relates yield stress against diameter as follows:

$$\sigma_c = \frac{1571}{d^{1.6}} + 2.8 \text{ Kg/mm}^2 \quad \text{(d in microns)}$$

This equation was then multiplied by the appropriate Schmid factor to give the correct curve for the various orientations. For the case of whiskers with a [100] orientation (Fig. 34), the points lie reasonably well along the curve. For whiskers with either a [110] (Fig. 35) or a [111] (Fig. 36) orientation, the few points lie more or less on the curve.

As was previously mentioned in the introduction, Eder and Meyer[19] found that the critical shear stress was proportional to d^{-2}. Fig. 37 compares the results obtained by Eder and Meyer with those obtained by the author, Brenner and Saimoto. As can be seen from this graph, the values of τ_{cr} observed by Eder and Meyer are, on the whole, much lower than those observed by the author, Brenner and Saimoto. In fact, Eder and Meyer's

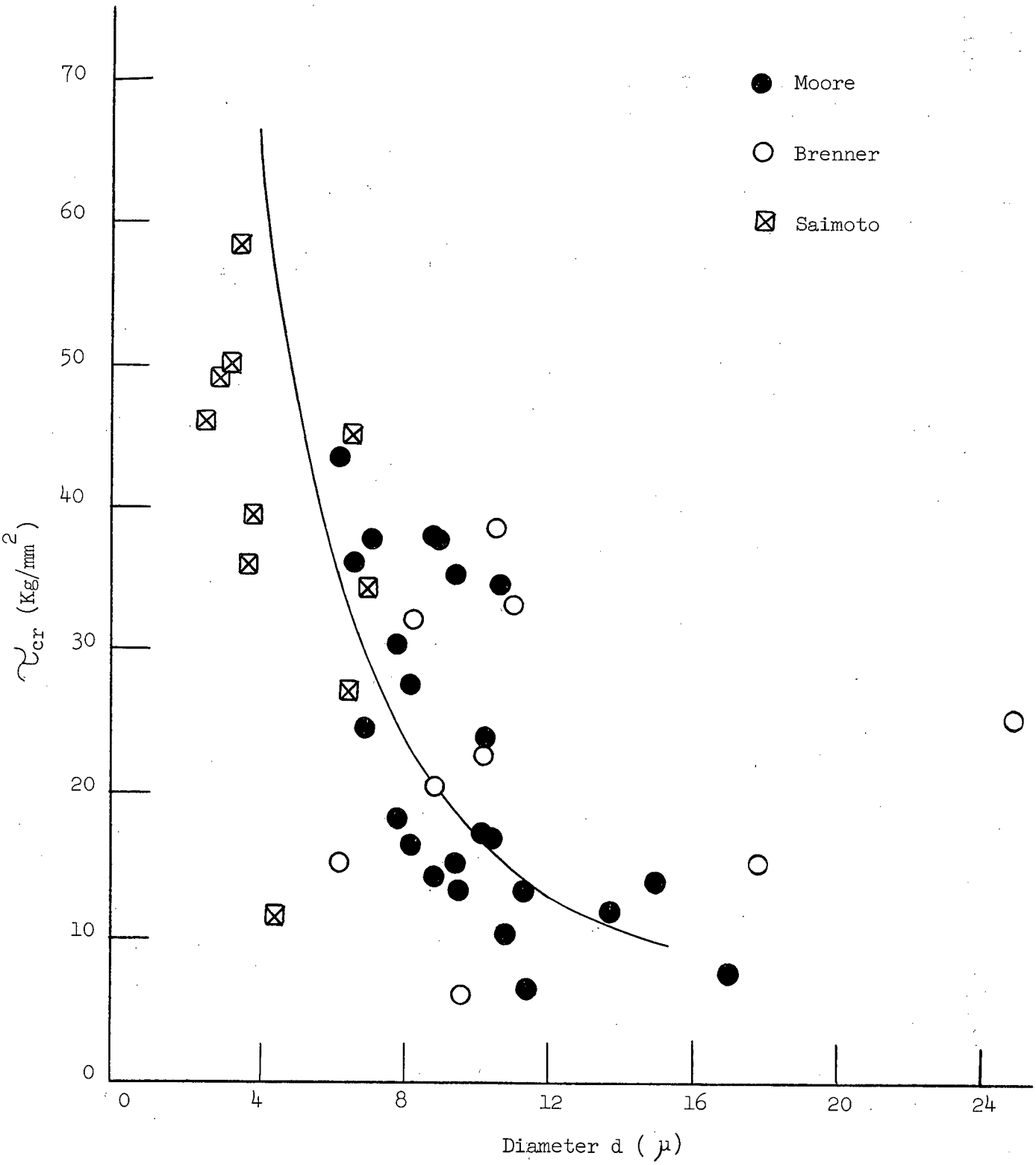

Figure 34. Critical Resolved Shear Stress for [100] Whiskers Against Diameter.

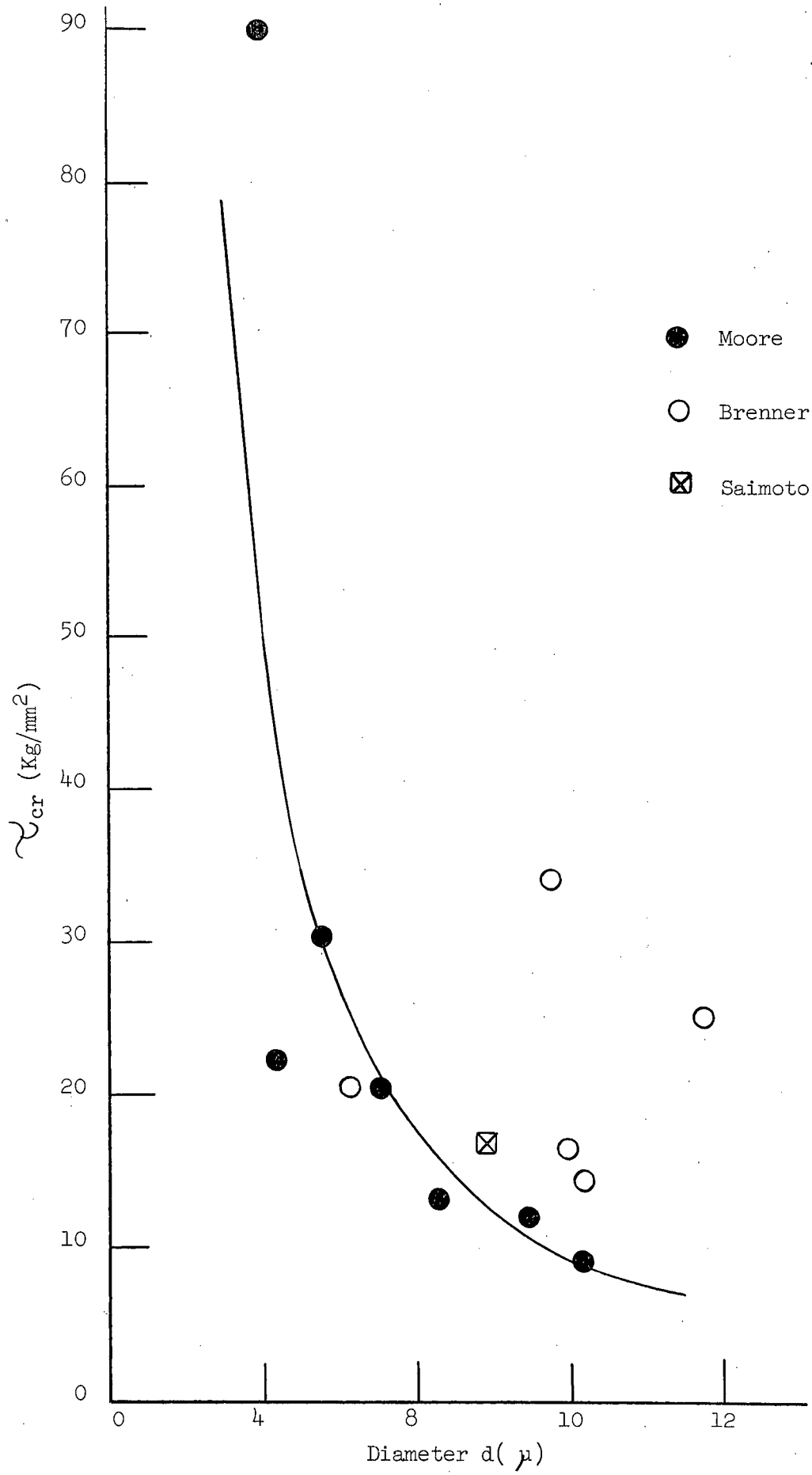

Figure 35. Critical Resolved Shear Stress for [110] Whiskers Against Diameter.

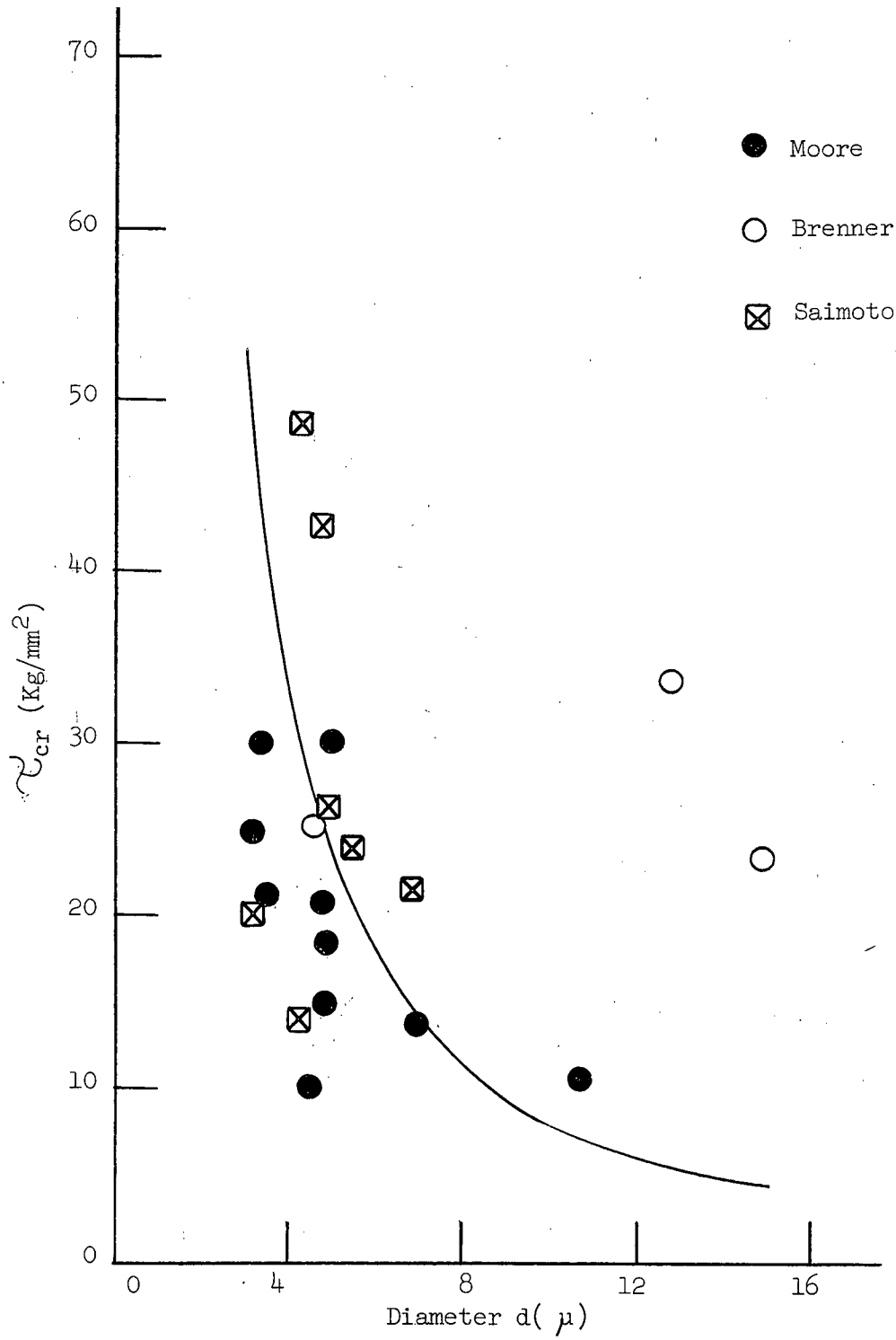

Figure 36. Critical Resolved Shear Stress for [111] Whiskers Against Diameter.

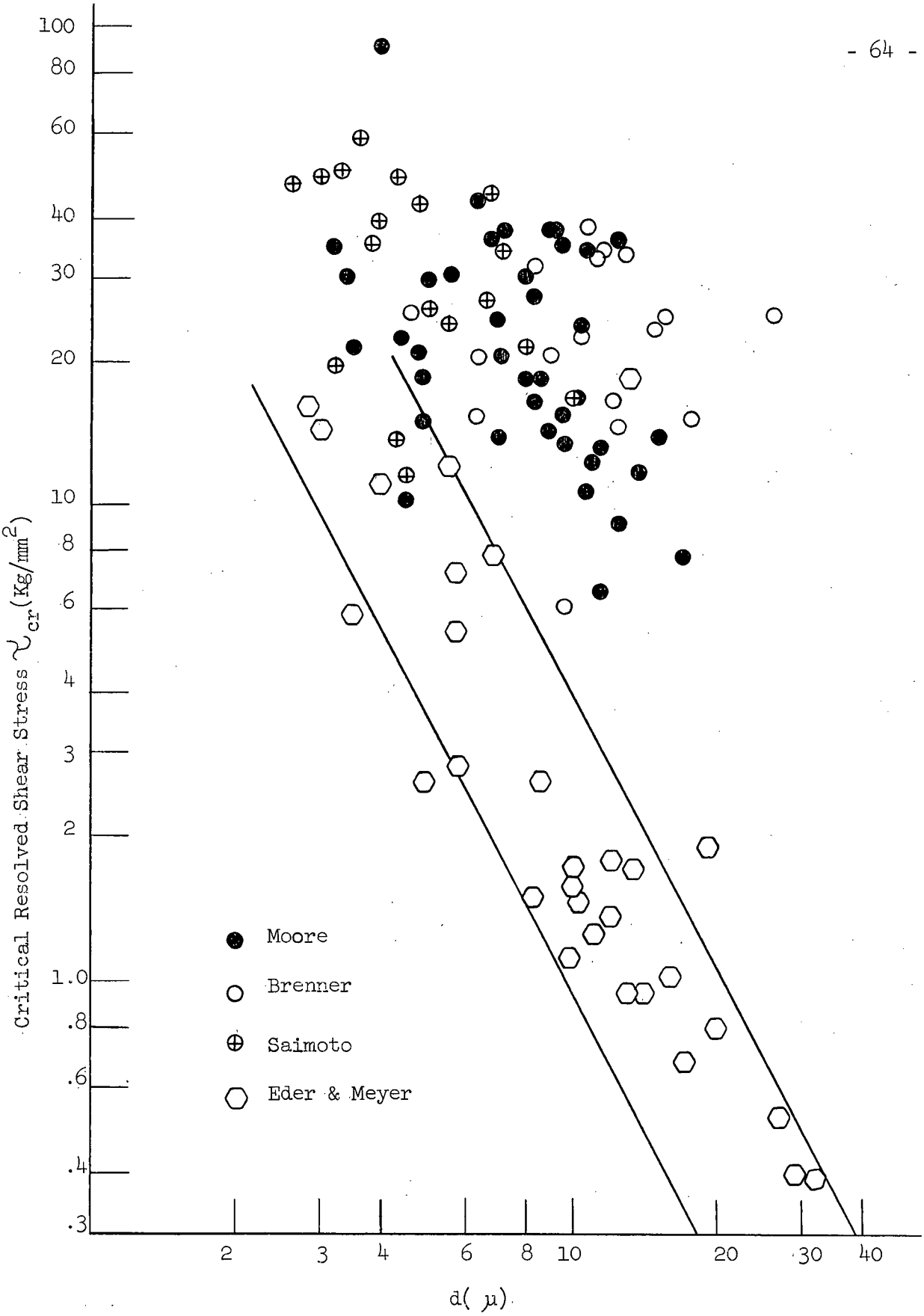

Figure 37. Log Plot of the Critical Resolved Shear Stress Against Diameter.

values of the critical shear stress are of the same order as the critical flow stresses τ_{fl} measured by Brenner and Saimoto. Fig. 38 is a log plot of τ_{fl} against diameter as observed by Eder and Meyer. These points are also of the same order as their values of τ_{cr}. However, the relationship between τ_{fl} and the diameter is different than in the case of τ_{cr}. The critical flow stress is proportional to d^{-1}.

The ratios of τ_{cr} to τ_{fl} as found by Brenner and Saimoto, vary anywhere from about 90:1 to about 4:1, with the average ratio being around 20:1. However, in the case of Eder and Meyer (Fig. 39), the ratios vary between about 5:1 to 1:1, with most of the ratios being between 2:1 and 1:1. It would thus seem to be the case that Eder and Meyer did not observe true whisker behaviour. Just why these whiskers of Eder and Meyer are so weak is not clear, particularly since no information was given with regard to the perfection of the whiskers tested, the method of growing, or the method of mounting. The only information given that might have a bearing on their results is their method of testing. Apparently the load was applied continuously to the whisker rather than in steps as in the case of tests performed by the author, Brenner and Saimoto. The force was recorded by the drive of a chart pen. If the strain rate was too high, it would be possible to miss the true yield point. The author tested a few whiskers of large ($> 20\,\mu$) diameter on the Instron Testing Machine. Because of gripping problems, only one successful test was obtained. In the case of this one whisker (Fig. 40), a whisker-type of stress-elongation curve was found, but it appeared that the true yield stress was missed because of the relatively fast strain rate ($>$ 0.01"/min.). The apparent yield stress was 12.8 Kg/mm^2 while the flow stress was 8.6 Kg/mm^2. The whisker failed at one grip. Since the orientation of the whisker was unknown, the critical resolved shear stress

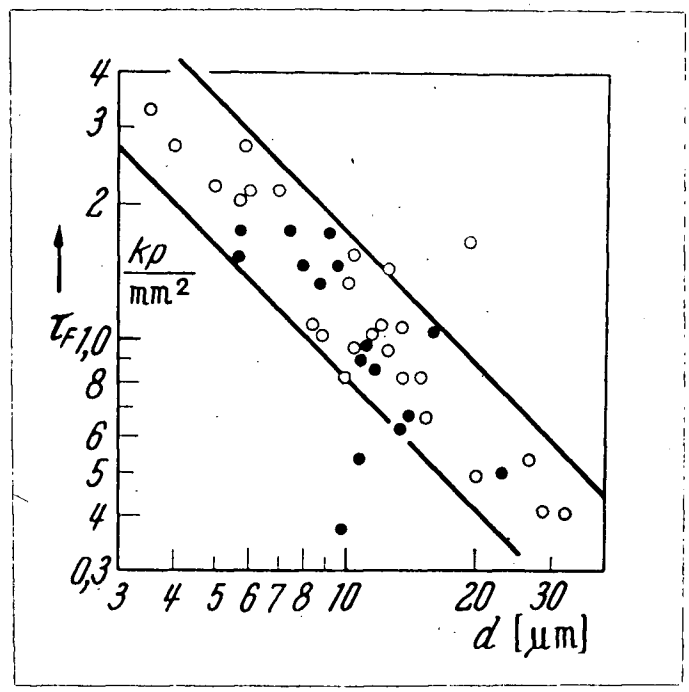

Figure 38. Dependence of Flow Stress on Diameter. Reproduced from Reference 19.

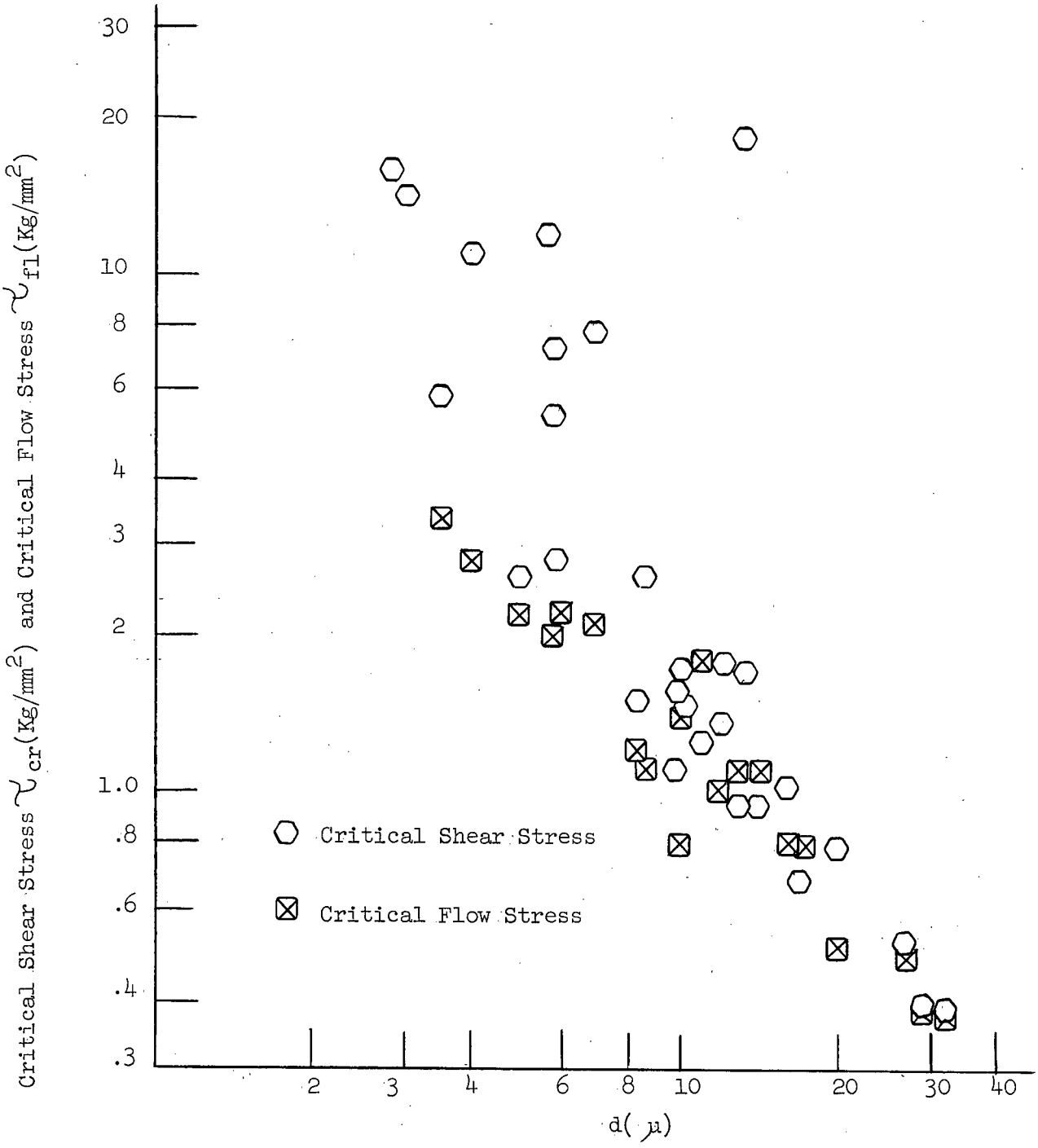

Figure 39. Comparison of Critical Resolved Shear Stress With Critical Resolved Flow Stress.

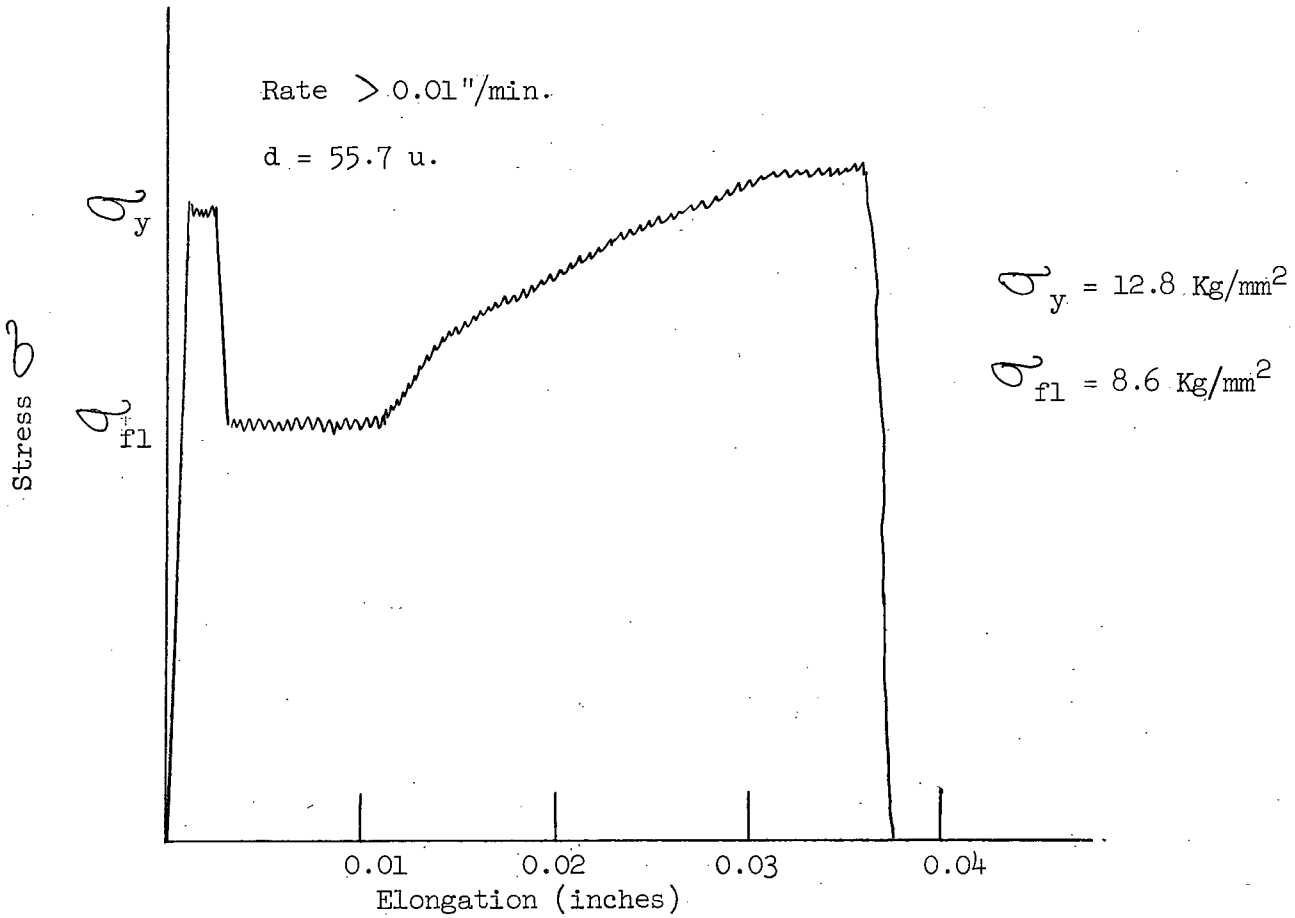

Figure 40. Stress-Elongation Curve of A Whisker Tested on the Instron.

and flow stress could not be calculated. However, the ratio between the two stresses is the same in both cases. This ratio is about 1.5:1 which is of the same order as the ratios observed by Eder and Meyer.

3. Diameter Dependence of Stress

One of the problems in explaining the diameter dependence of yield stress for copper whiskers, is that the dislocation content of the whiskers is unknown. As was previously mentioned in the introduction, Price[16] found that zinc whiskers could be initially free of dislocations. Gorsuch[22] also observed that the dislocation density of some iron whiskers was so small ($< 10^6$ dislocations/cm^2) that essentially the whiskers contained no dislocations. On the other hand, Pearson et al[12] felt that the dislocation content of their silicon whiskers was not very different from that of bulk silicon.

No experimental data is available concerning the dislocation density of copper whiskers. Therefore the two possibilities of either dislocation free whiskers or dislocation containing whiskers will have to be considered.

Assume, aside from the presence of axial screw dislocations which will contribute nothing to the deformation, that the whiskers are initially free of dislocations. The problem that must now be considered is one of the nucleation of slip in a perfect crystal.

Becker[39] was the first to consider the possibility that slip could take place at some applied stress less than the critical stress by the thermal fluctuations of the lattice helping the applied stress to form a nucleus of slip on the slip plane. Cottrell[1] defines a nucleus of slip as

> "the smallest region of slip that can be made to grow by the action of the applied stress alone. Any region smaller than this will slip back into its original and perfect configuration once the thermal fluctuation that caused the region to slip has passed."

The smallest nucleus will be a disk-shaped element in the slip plane bounded by a dislocation loop. Cottrell has shown that the radius of the loop has a critical value such that if the loop is of this size it can then grow by the action of the applied stress alone. If the radius of the loop is less than this critical value, it will collapse. This value of the critical radius r_c is given by

$$r_c = \frac{\mu b}{4\pi\sigma}\left[\log\left(\frac{r_c}{r_o}\right) + 1\right] \qquad (6)$$

where μ = shear modulus,
σ = applied stress,
r_o = equilibrium distance between atoms.

Further, Cottrell has shown that the activation energy for nucleating slip in a perfect lattice is of the order 1-2 eV. In effect, this means that slip cannot be nucleated unless the applied stress $\sigma = \frac{\mu}{100}$. This is of the same order as the theoretical shear stress which is about $\frac{\mu}{30}$. For copper, $\mu = 4\ (10^{11})$ dynes/cm^2 which gives a value of applied stress σ of around 40 Kg/mm^2. This is of the order of that observed experimentally in whiskers. In turn this means that the critical diameter d_c of a loop is about 10^{-6} cm.

The question now arises as to the maximum number of sites that could produce loops of this critical size in any given area on the slip plane. Since it is not possible to calculate the number of sites from any fundamental considerations, some model will have to be postulated in order to give an estimation of this number. Consider unit area of slip plane containing at

each possible site a square loop with the length of one side equal to the critical diameter d_c. Let each loop be a distance d from the next loop as shown in Fig. 41. The number of these sites will be given by $\left[\frac{1}{d + d_c}\right]^2$ where $d_c = 10^{-6}$cm. Although no exact value of d can be given, a reasonable

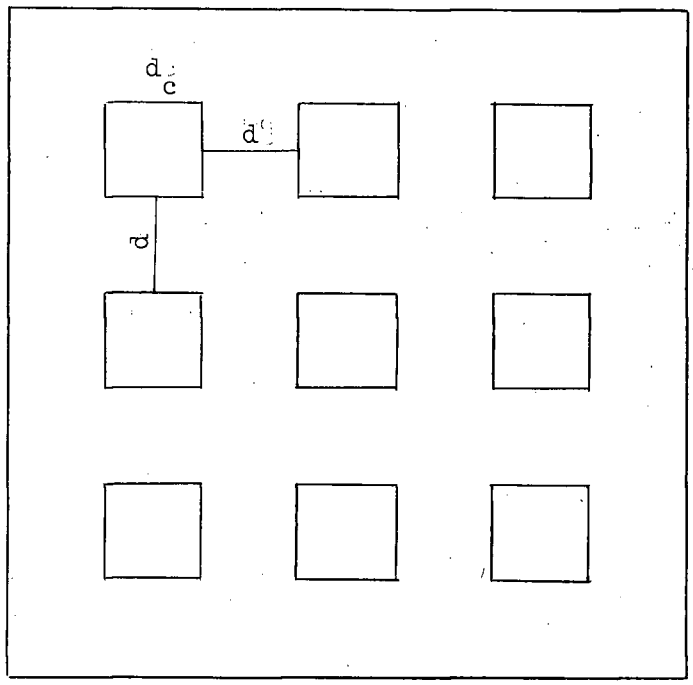

Figure 41. Model for Estimating the Maxiumu Number of Loop Sites.

value is $d = d_c/4$. This results in a site density of about 10^{12} sites/cm^2.

It should be remembered however, that the actual number of loops of critical size will be less than 10^{12} loops/cm^2 since it is highly unlikely that every possible site for creating a loop will produce one of critical

size. Assuming a success factor of about 10^{-2}, the actual density of the loops will be about 10^{10} loops/cm^2.

In view of the above, it would seem that the critical shear stress would be inversely proportional to d^2. However, it has been found in this investigation that the primary shear stress is inversely proportional to $d^{1.6}$. In order to explain this dependence, the interactions between the loops will have to be taken into account.

Consider a whisker of diameter d containing many loops of critical size as shown in Fig. 42. The loops in the circle of diameter d_o will interact

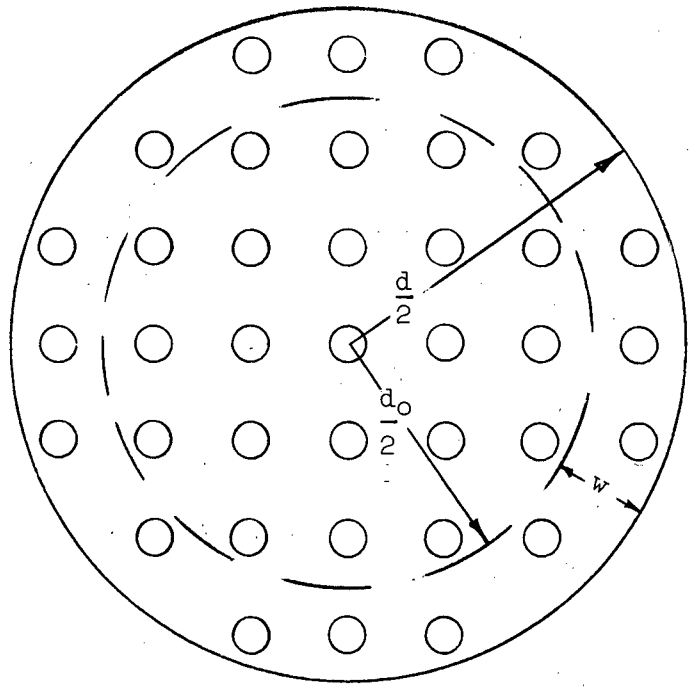

Figure 42. Diagram of a Whisker Containing Dislocation Loops.

with each other and so they will not be free to contribute to the deformation. Only those loops contained in the annular ring of width w, will take part in the deformation. The width of this annular ring must be small, probably of the order of 1000 A^{o} which corresponds to the possibility of having one or two loops in this width.

For the general case of an inverse dependence of shear stress on d^n, this means that the area A of the annular ring that contributes to the deformation must vary as d^n. This implies that $d_o = f(d)$ such that $A = Kd^n$. The area of the annular ring is given by

$$A = \frac{\pi}{4}\left[d^2 - d_o^2\right]$$

This gives that

$$\frac{\pi}{4}\left[d^2 - d_o^2\right] = Kd^n$$

or

$$d^2 - d_o^2 = kd^n$$

From this

$$d_o = d\sqrt{1 - kd^{n-2}} \qquad (7)$$

and therefore

$$k < \frac{1}{d^{n-2}} \qquad (8)$$

This means that for a whisker of diameter d, a range of values of d_o corresponding to values of k that satisfy equation (8) can be calculated. Figs. 43, 44 and 45 are plots of d_o against k for d equal to 2, 10, and 20 μ respectively with n = 1.6. These values of diameter were chosen since they cover the range tested and the one used as a standard in previous calculations.

Besides the restrictions placed on the value of k by equation (8), two other restrictions must be considered. The first one is that since $\sigma \propto d^{-n}$ and therefore $\frac{\sigma_1}{\sigma_2} = \left[\frac{d_2}{d_1}\right]^n$, then obviously the ratios of the

areas of the annular rings $\frac{A_2}{A_1} = \left[\frac{d_2}{d_1}\right]^n$. This is true only if $k_1 = k_2$ and hence once k is set for a particular diameter, it must be the same for any other diameter. The other restriction on k is imposed by the necessity of the width of the annular ring being small.

For the case being considered where n = 1.6 and taking $k = 0.05\ \mu^{.4}$, the comparisons of d_o and w for various diameters are given below.

d	2 μ	10 μ	20 μ
d_o	1.96 μ	9.92 μ	19.85 μ
w	200 A^o	400 A^o	750 A^o

During the primary test on the whisker, nucleation of loops will occur on many slip planes along the length of the whisker. Probably because of some localized condition, slip occurs in a small region. This region is then eliminated from the whisker and the whisker is retested. The whisker will now contain a residual dislocation network because of the interactions of the loops formed during the primary test on the other slip planes. This dislocation network can be considered equivalent to a region of "dislocation pressure". Under the action of an applied stress a similar process will occur as before, except that this dislocation pressure will now aid the applied stress by helping to promote the action of loops that otherwise would not contribute to the deformation. This means that the width of the annular ring in which loops can act to produce deformation is now increased.

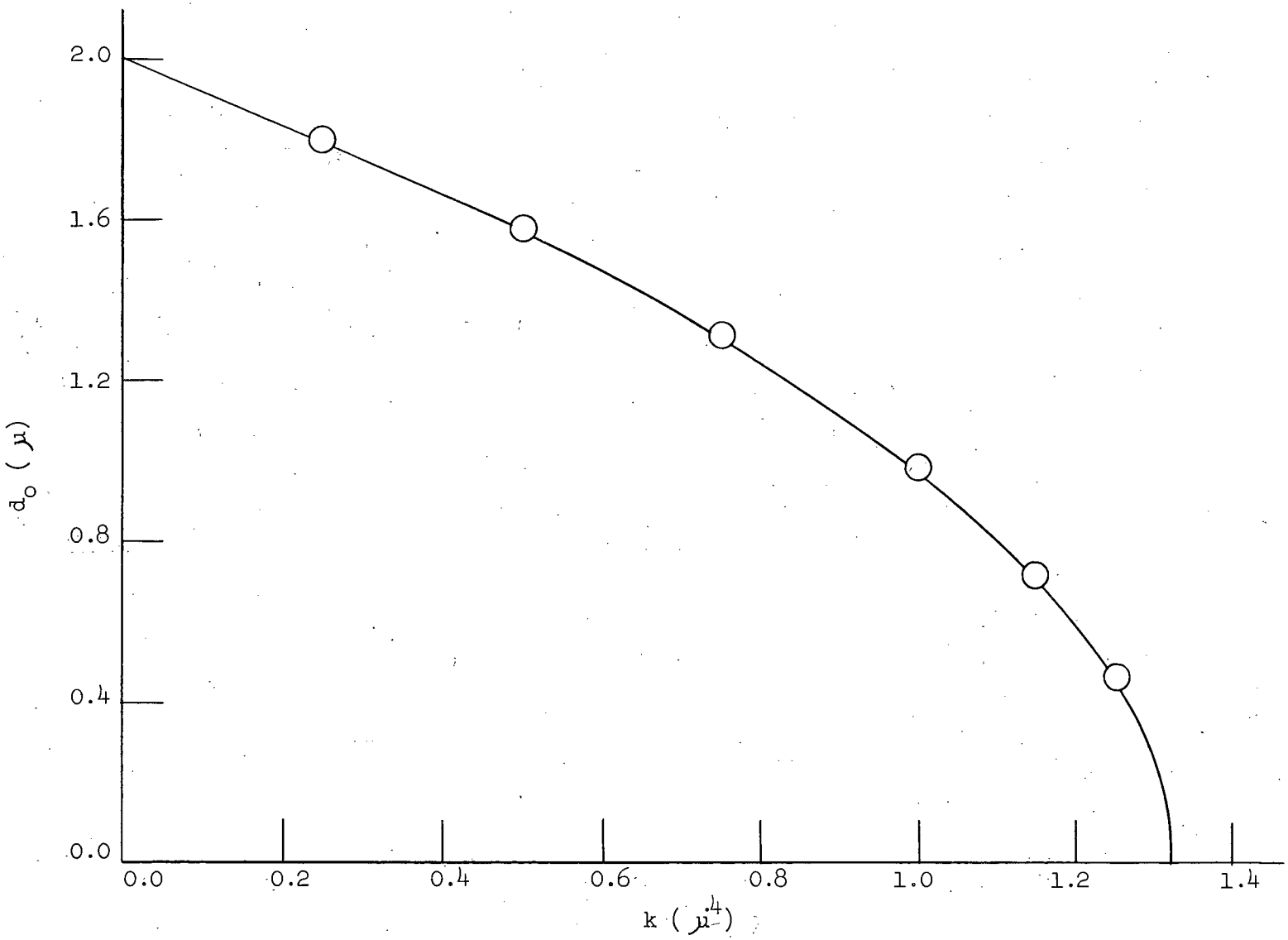

Figure 43. Diameter d_o of Annular Ring Against k for d = 2 μ. $A = kd^{1.6}$

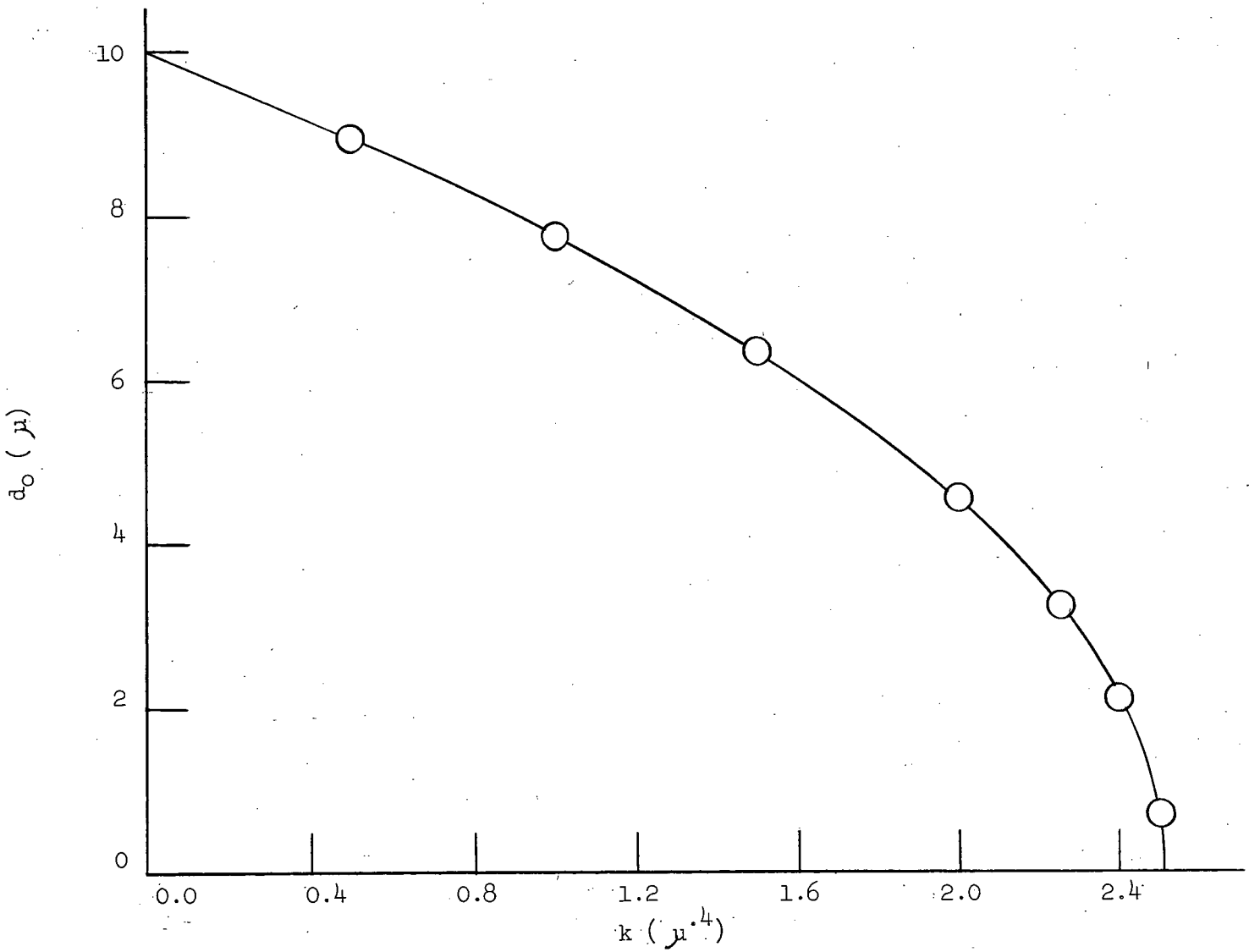

Figure 44. Diameter d_o of Annular Ring Against k for d = 10 μ. $A = kd^{1.6}$.

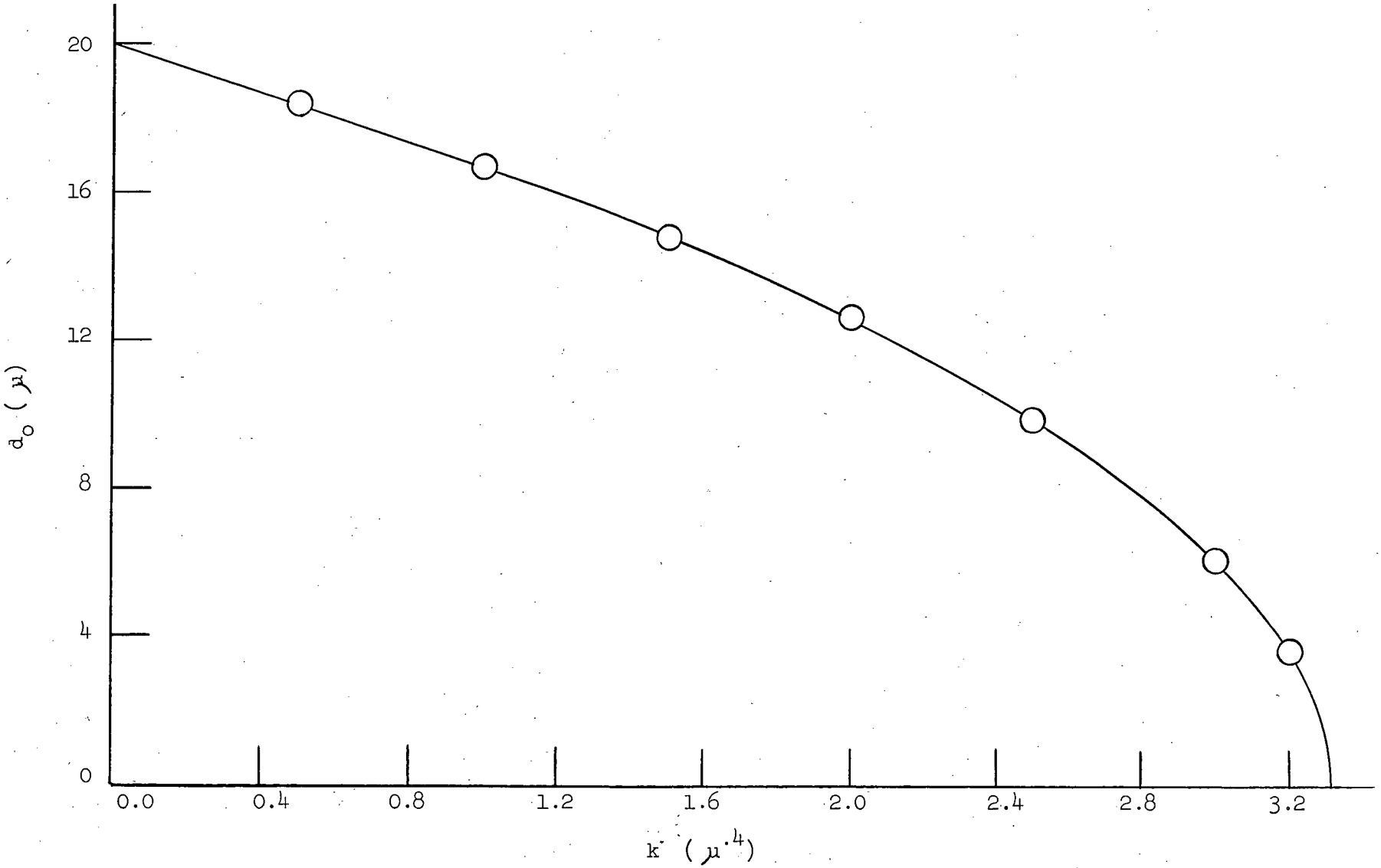

Figure 45. Diameter d_o of Annular Ring Against k for d = 20 μ. $A = kd^{1.6}$.

Experimentally it was found that the secondary yield stress varied inversely as $d^{2.5}$. Figs. 46, 47 and 48 are plots of d_o against k for n = 2.5 for whiskers of diameter 2, 10 and 20 μ respectively. These values for d_o and k were found from equations (7) and (8). As before, the restriction that k must be the same for whiskers of various diameters still holds, but the restriction concerning the width of the annular ring is no longer valid. In order to make an estimation of the new width, it is necessary to assume that for whiskers of small diameter, w does not vary greatly. This assumption is reasonable as the difference between values of stress for n = 1.6 and n = 2.5 for a whisker of small diameter is small compared to the difference in stress for whiskers of large diameter. For the actual case under consideration, for a whisker of 2 μ in diameter, w remains about the same, ie. 200 A^o. Therefore d_o is the same as before and hence the value of k corresponding to this value can be calculated from equation (7). Using this value of k which is 0.028 $\mu^{-.5}$, the following results were obtained.

d	2 μ	10 μ	20 μ
d_o	1.96 μ	9.55 μ	18.72 μ
w	200 A^o	2250 A^o	6400 A^o

For a whisker with d = 10 μ, the width of the annular ring was increased by about 5 1/2 times while for a whisker with d = 20 μ, by about 8 1/2 times.

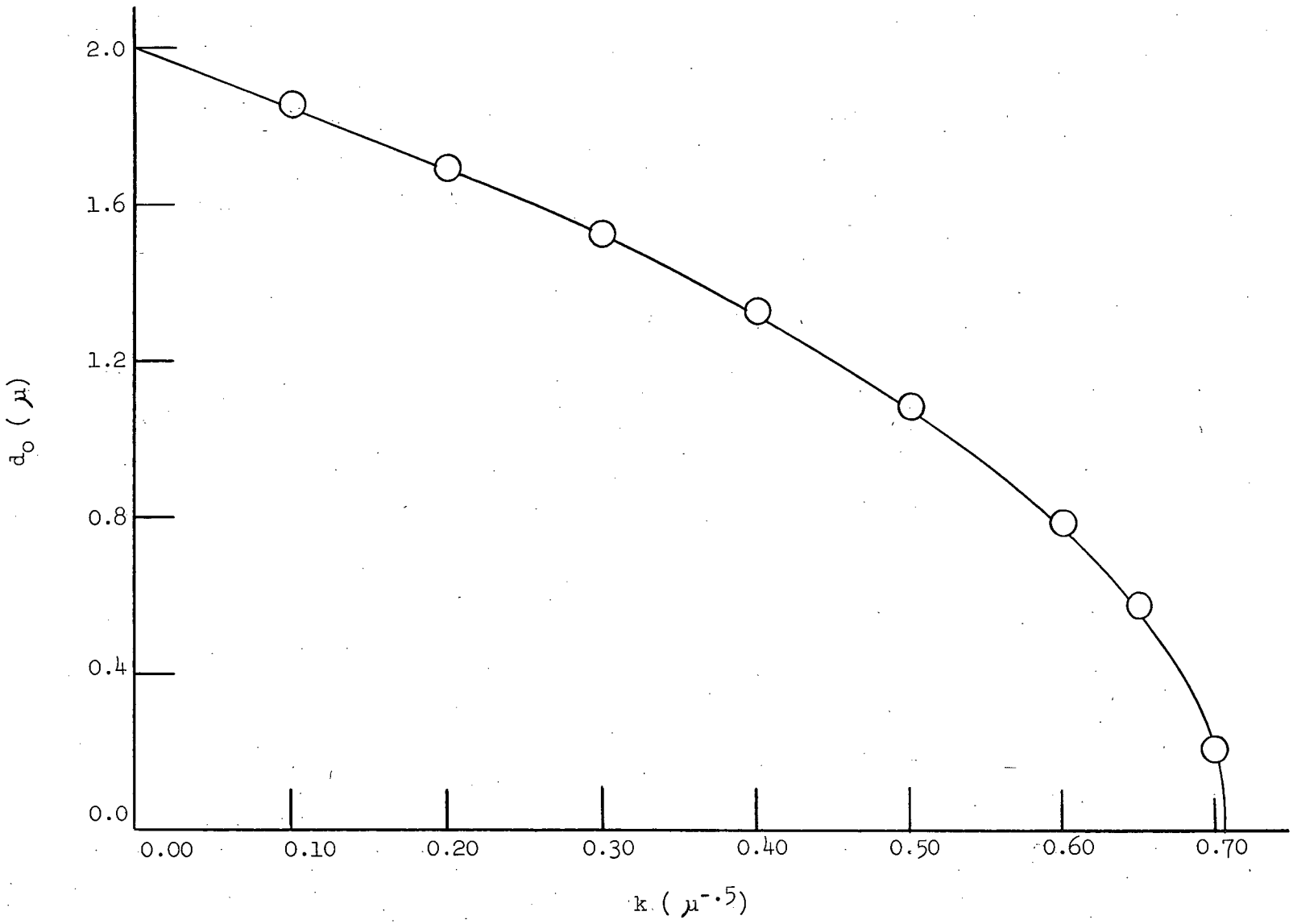

Figure 46. Diameter d_o of Annular Ring Against k for d = 2 μ. $A = kd^{2.5}$.

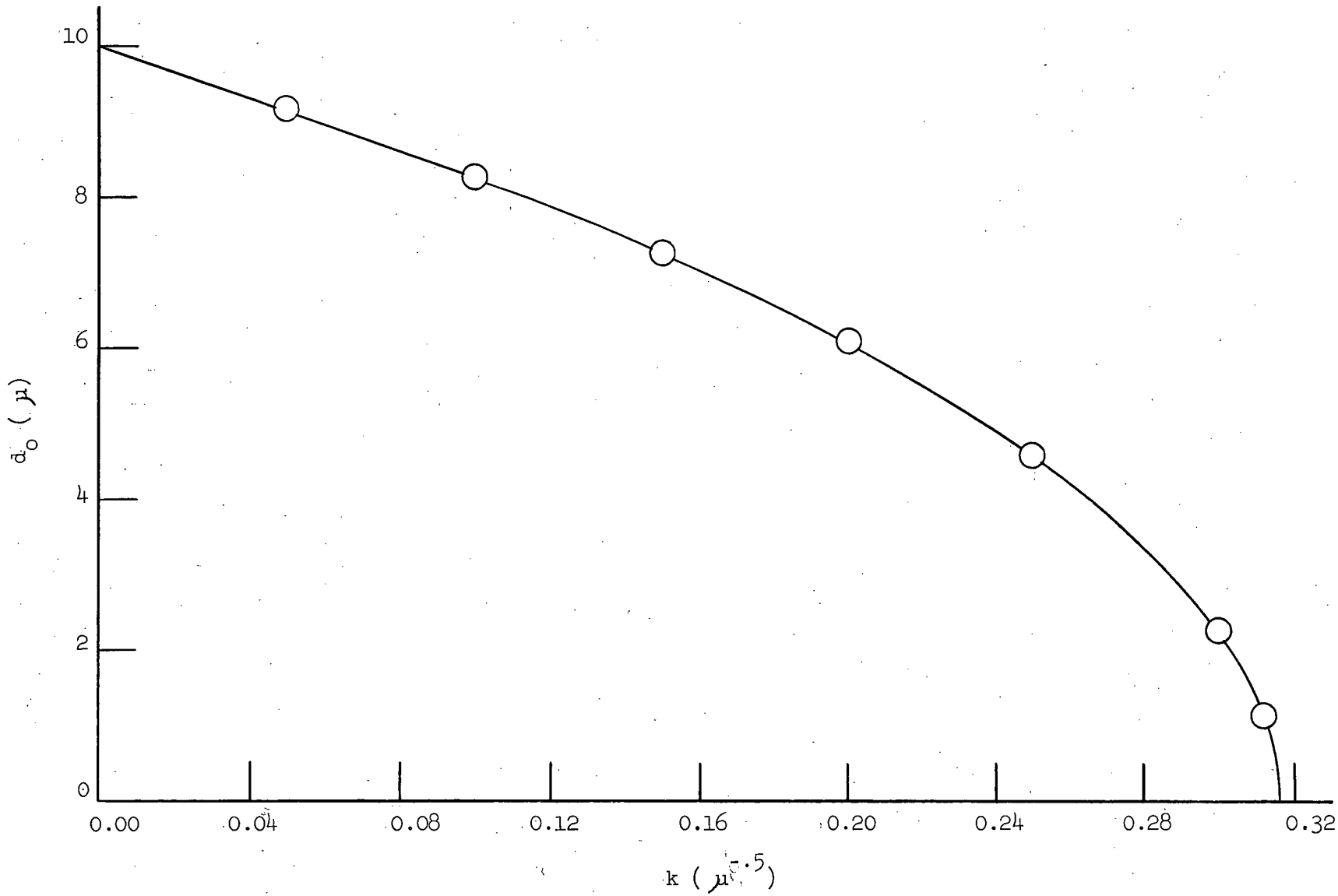

Figure 47. Diameter d_o of Annular Ring Against k for d = 10 μ. $A = kd^{2.5}$.

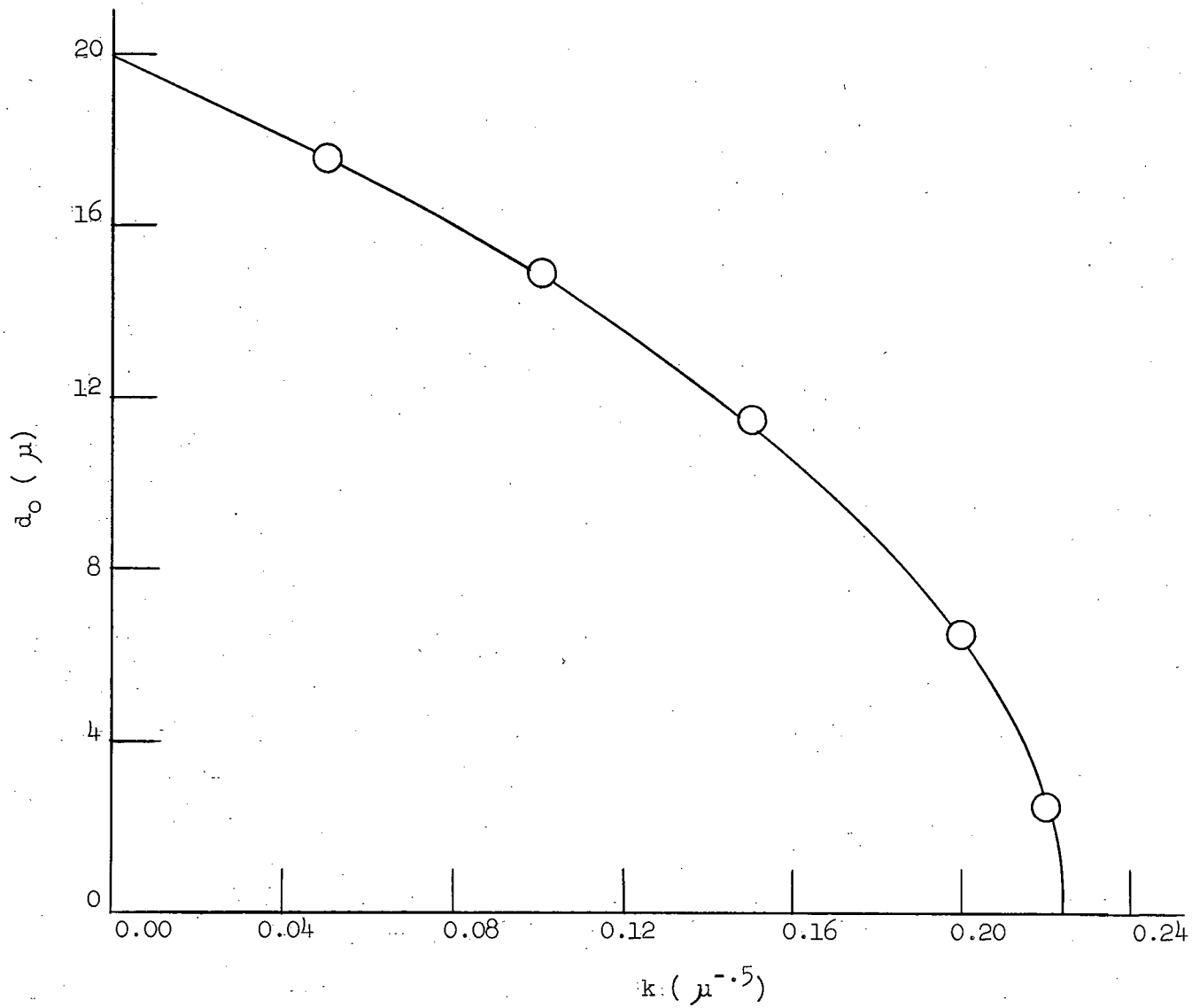

Figure 48. Diameter d_o of Annular Ring Against k for d = 20 μ. $A = kd^{2.5}$.

It should be recalled that the whole of the above discussion was based on the assumption that the whiskers were initially free of dislocations. If the assumption is now made that whiskers are not dislocation free, a different dislocation mechanism will have to be postulated to explain the observed diameter dependence of stress. However, at the present time, no adequate theories have been devised to explain this dependence.

4. Variations of Young's Modulus.

Aside from an apparent decrease in the Young's Moduli of about 30% for whiskers subjected to a secondary test, as was observed in this investigation, a significant change in the values of Young's Moduli from the accepted values has been observed by several other investigators.

Risebrough[40] performed tensile tests on zone refined aluminium which was alloyed with 0.02, 0.1 and 0.2 percent magnesium. He found that the slope of the stress-strain curve for these alloys increased as the amount of magnesium present in the aluminium increased. The average value of the Young's Modulus increased by a factor of about 2.

Investigations into the mechanical properties of thin gold films have been performed by Catlin and Walker[41] and by Neugebauer[42]. Catlin and Walker performed bend tests on single-crystal films varying in thickness between 1000 and 3000 A^{o}. These films were grown by vacuum deposition on heated (375°C) rocksalt substrates which had been cleaved to expose $\{100\}$ planes. The orientations of the films produced were completely $\{100\}$. Fig. 49 shows the variation of Young's Modulus with film thickness. The dashed line is their calculated value $\left[0.785(10^{12})\text{dynes/cm}^2\right]$ of Young's Modulus. For the thicker films there was close agreement between the calculated and measured values. However, as the thickness of the films decreased, the value of Young's Modulus increased by as much as 50%.

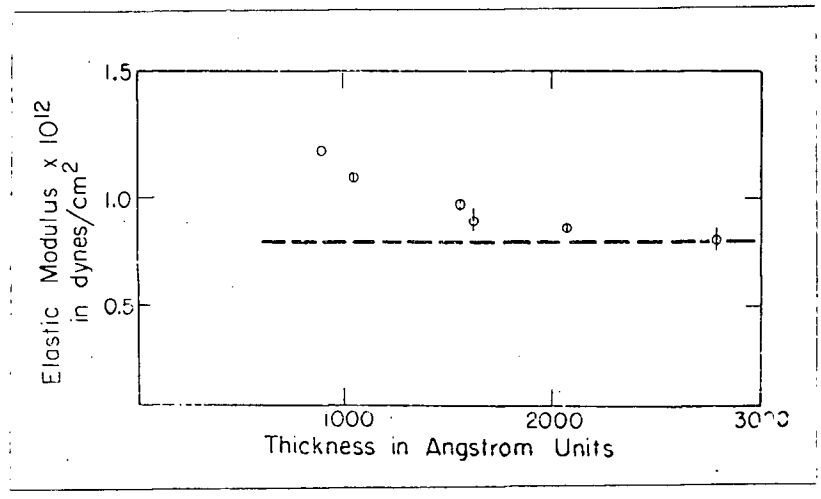

Figure 49. Variation of Young's Modulus With Film Thickness. Reproduced from Reference 41.

Tensile tests were performed on gold films by Neugebauer. He prepared the films in approximately the same manner as Catlin and Walker. Completely, partially and randomly oriented films with respect to the {100} planes of the rocksalt were produced. The type of orientation depended on the temperature of the substrate. In contradiction to Catlin and Walker, Neugebauer found no variation of Young's Modulus with film thickness.

Coleman et al[10] have reported that the Young's Moduli for zinc and cadmium whiskers were consistently lower than the accepted values by about 30%.

So far, no explanations for any of the various results mentioned above have been made.

SUMMARY AND CONCLUSIONS

1. Since the important results have been summarized in a previous section, they will not be repeated here.

2. The growth of whiskers by the hydrogen reduction of cupric chloride is greatly inhibited by the presence of any water in the cupric chloride. This is probably due to the poisoning of potential growth sites by the dipole action of the water molecules.

3. The results of tensile tests performed on copper whiskers by the author, Brenner and Saimoto are reasonably consistent. However, the results obtained by Eder and Meyers indicate that either their whiskers are abnormally weak or else their method of testing gives an apparent yield stress that is much lower than the true yield stress.

4. To explain the dependence of yield stress on diameter and the change in dependence between primary and secondary tests, a dislocation mechanism which assumed that the whiskers were initially free of dislocations was postulated.

RECOMMENDATIONS FOR FURTHER WORK

The type of tensometer used in this investigation is very limited in its uses for these reasons:

(i) the load is applied in steps,

(ii) high temperature tests are impossible because of the low melting point of the gripping compound,

(iii) whiskers of large diameter ($>$ 20 u) cannot be tested.

Therefore it would be interesting to perform tensile tests of large diameter whiskers on the Instron Testing Machine. The effect of strain rate and temperature changes could be observed. Also, it would be of interest to compare the type of stress-strain curve obtained for the whiskers of large diameter to that obtained for whiskers of small diameter.

BIBLIOGRAPHY

1. Cottrell, A.H., "Dislocations and Plastic Flow in Crystals," Claredon Press, Oxford 1953.

2. Mackenzie, J. K., Thesis, University of Bristol, 1949.

3. Bragg, W. L and Lomer, W. M., Proc. Roy. Soc. (London), A196, 171(1949).

4. Herring, C. and Galt, J., Phys. Rev. 85, 1060 (1952).

5. Gyulai, Z., Z.f. Physik, 138, 317 (1954).

6. Eisner, R. L., Acta Met., 3, 414 (1955).

7. Brenner, S. S., J. Appl. Phys. 27, No. 12, 1484 (1936).

8. Fahrenhorst, W., and Schmid, E., Z. f. Physik, 78, 383 (1932).

9. Schmid, E., and Boas, W., "Plasticity of Crystals," F. A. Hughes and Company, Ltd., London.

10. Coleman, R. V., Price, P. B., and Cabrera, N. J., J. Appl. Phys. 28, 1360 (1957).

11. Evans, C. C., Marsh, D. M., and Gordon, J. E., Cambridge Conference on Strength of Whiskers and Thin Films (1958).

12. Pearson, G. L., Read, W. T., and Feldman, W. L., Acta Met., 5, 181 (1957).

13. Cabrera, N., and Price, P.B., "Growth and Perfection of Crystals" edited by Doremus et al, John Wiley and Sons, Inc., New York (1958).

14. Brenner, S. S., Ibid, p 170.

15. Brenner, S. S., J. Appl. Phys., 28, 1023 (1957).

16. Price, P. B., Phil. Mag., 5, No. 57, Sept.(1960).

17. Taylor, G. F., Phys. Rev., 23, (1924).

18. ASM Metals Handbook 1198, (1961).

19. Eder, F. X., and Meyer, V., Naturwissenschaffen 47, 352 (1960).

20. Evans, C. C., and Marsh, D. M., "Growth and Perfection of Crystals", edited by Doremus et al, John Wiley and Sons, Inc., New York (1958).

21. Eisner, R. S., Acta Met. 3 419 (1955).

22. Gorsuch, P.D., J. Appl. Phys. 30, No. 6, 837 (1959).

23. Costanzo, R. A., Private Communication.

24. Shlichta, P. J., "Growth and Perfection of Crystals," ed. by Doremus et al, John Wiley and Sons, Inc., New York (1958).

25. Fleischer, R. L., and Chalmers, B., J. Mech. and Phys of Solids, 6, 307 (1958).

26. Roscoe, R., Phil. Mag., 21 (7), 399 (1936).

27. Cottrell, A. H., and Gibbons, D. F., Nature, 162, 488 (1948).

28. Saimoto, S., MASc. Thesis, University of British Columbia, 1960.

29. Brenner, S. S., Acta Met., 4, 62 (1956).

30. Overton, W. C. and Gaffney, J., Phys. Rev., 98, 969 (1955).

31. Frank, F. C., Discussions Faraday Soc., No. 5, 67 (1949).

32. Sears, G. W., Acta Met., 1, 458 (1953).

33. Samis, C. S., Private Communication.

34. Brenner, S. S., Thesis, Rensselaer Polytechnic Inst., 1957.

35. Gorsuch, P., G. E. Research Reprint #57-RL1840 (1955).

36. Shetty, N., Private Communication.

37. Sarakhov, A. I., Proc. Acad. Sci. USSR, Phys. Chem. Sect., 112 (1957).

38. Allan, W. J., and Webb, W. W., Acta Met. 7, 646 (1959).

39. Becker, R., Phys. Zeit., 26, 919 (1925).

40. Risebrough, N., MASc. Thesis, University of Toronto, 1961.

41. Catlin, A., and Walker, P., J. Appl. Phys., 31, No. 12, 2135 (1960).

42. Neugebauer, C. A., J. Appl. Phys., 31, No. 6, 1096 (1960).

43. Freund, J., and Williams, F., Modern Business Statistics, Prentice Hall, New Jersey.

44. Simon, L. E., "An Engineer's Manual of Statistical Methods", John Wiley and Sons, Inc., New York.

APPENDIX I

A. Procedure for Calibrating the Tensomenter

1. Two helical springs were calibrated, giving a force-extension curve.
2. The restoring force was then measured by glueing one of the springs onto the grips of the tensometer and then positioning grip B at various distances from null. This gave a distance-from-null-extension relations from which a distance-from-null-restoring force relation was determined.
3. The solenoid was calibrated with both springs mounted as above. The current-extension relations was determined by increasing the current by increments of either 1.0ma or 0.5ma. After compensating for the restoring force of the suspended rod, the current-force relationship was determined.

B. Calibration Curves and Tables

TABLE IX

Calibration of Impedance Transducer

Null at 9.345 mm

Micrometer Reading	Bridge Reading	
	30μ Scale	10μ Scale
9.20	-	-
9.22	9.65	9.55
9.24	9.60	9.50
9.26	9.60	9.60
9.28	9.80	9.20
9.30	9.50	9.40
9.32	10.75	9.50
9.34	10.45	9.20
9.36	9.55	9.20
9.38	9.20	9.70
9.40	9.05	8.65
9.42	9.40	9.10
9.44	8.85	8.55
9.46	9.15	8.80
9.48	9.30	9.25
9.50	8.95	9.05
9.52	9.40	9.00
9.54	9.05	9.75
9.56	9.40	8.40
9.58	9.10	9.35
9.60	9.70	9.20
9.62	9.45	9.40
9.64	9.45	9.25
9.66	9.25	8.90
9.68	9.75	9.35
9.70	8.50	9.25
9.72	10.20	9.25
9.74	9.30	9.35
9.76	9.75	9.20
9.78	9.90	9.45
9.80	9.30	9.10
9.82	9.50	9.35
9.84	9.75	9.75
9.86	9.30	8.65
9.88	9.10	9.80
9.90	8.90	9.20
	0.1 - one small division Sensitivity-: 2.12μ/div.	0.2 = one small division Sensitivity-: 0.432μ/div.

Calibration of Impedance Transducer

Micrometer Reading	Bridge 3 μ Scale	Micrometer Reading	Bridge 3 μ Scale
9.30	-	9.56	4.75
9.31	4.60	9.57	4.15
9.32	3.85	9.58	4.50
9.33	4.40	9.59	4.70
9.34	3.90	9.60	5.10
9.35	4.80	9.61	4.80
9.36	4.60	9.62	4.50
9.37	4.00	9.63	5.30
9.38	3.80	9.64	5.00
9.39	5.75	9.65	4.35
9.40	3.95	9.66	4.90
9.41	5.10	9.67	4.90
9.42	4.15	9.68	5.00
9.43	4.40	9.69	4.50
9.44	4.80	9.70	4.90
9.45	4.70	9.71	4.70
9.46	4.20	9.72	4.60
9.47	5.00	9.73	4.90
9.48	4.55	9.74	3.80
9.49	4.20	9.75	4.90
9.50	4.80	9.76	4.50
9.51	4.50	9.77	4.30
9.52	5.25	9.78	3.80
9.53	4.80	9.79	5.00
9.54	4.90	9.80	4.10
9.55	4.70		

0.1 = one small division

Sensitivity-: 0.219 u/div.

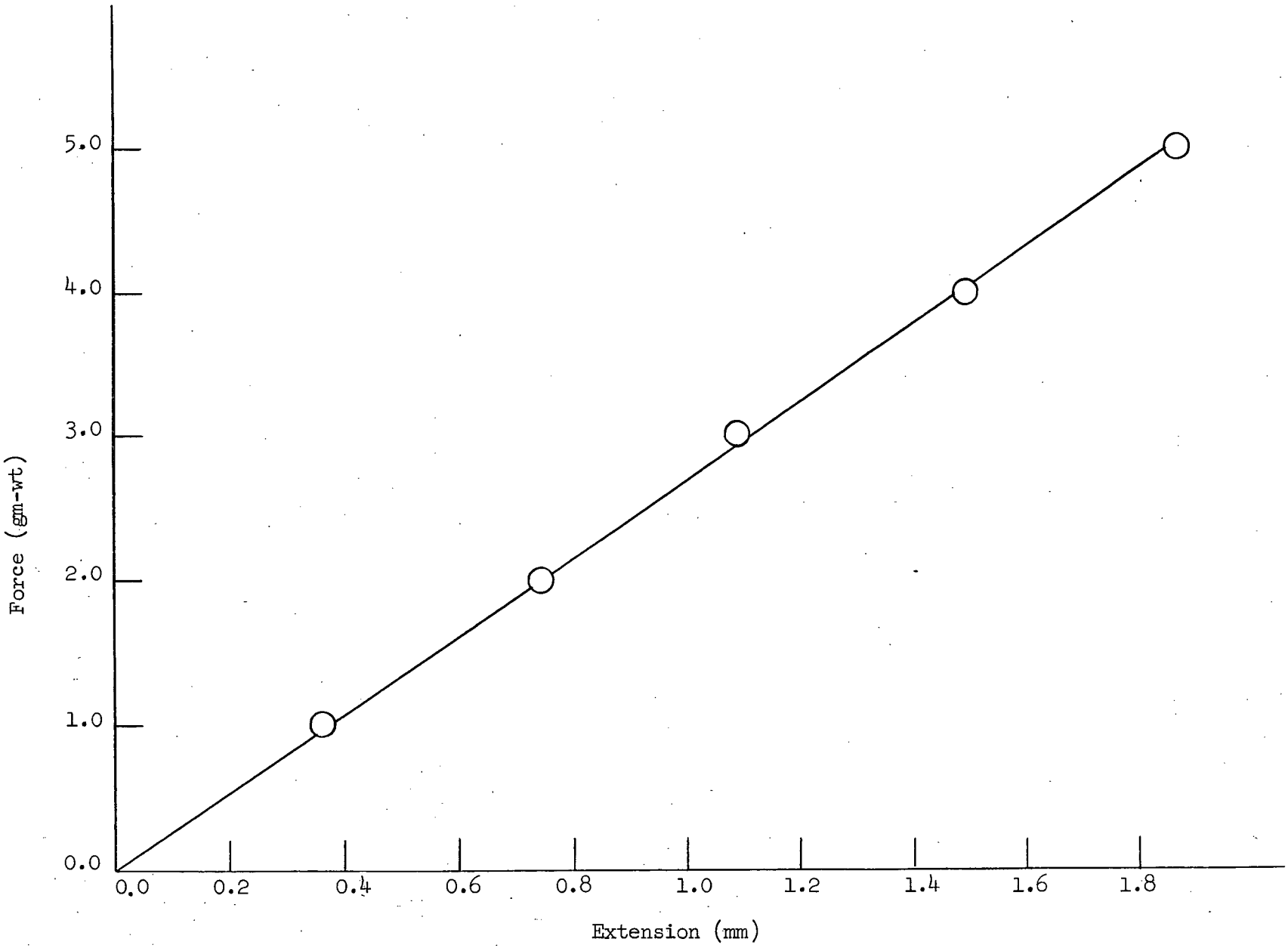

Figure 50. Calibrations of Large Helical Spring. Force-Extension Plot

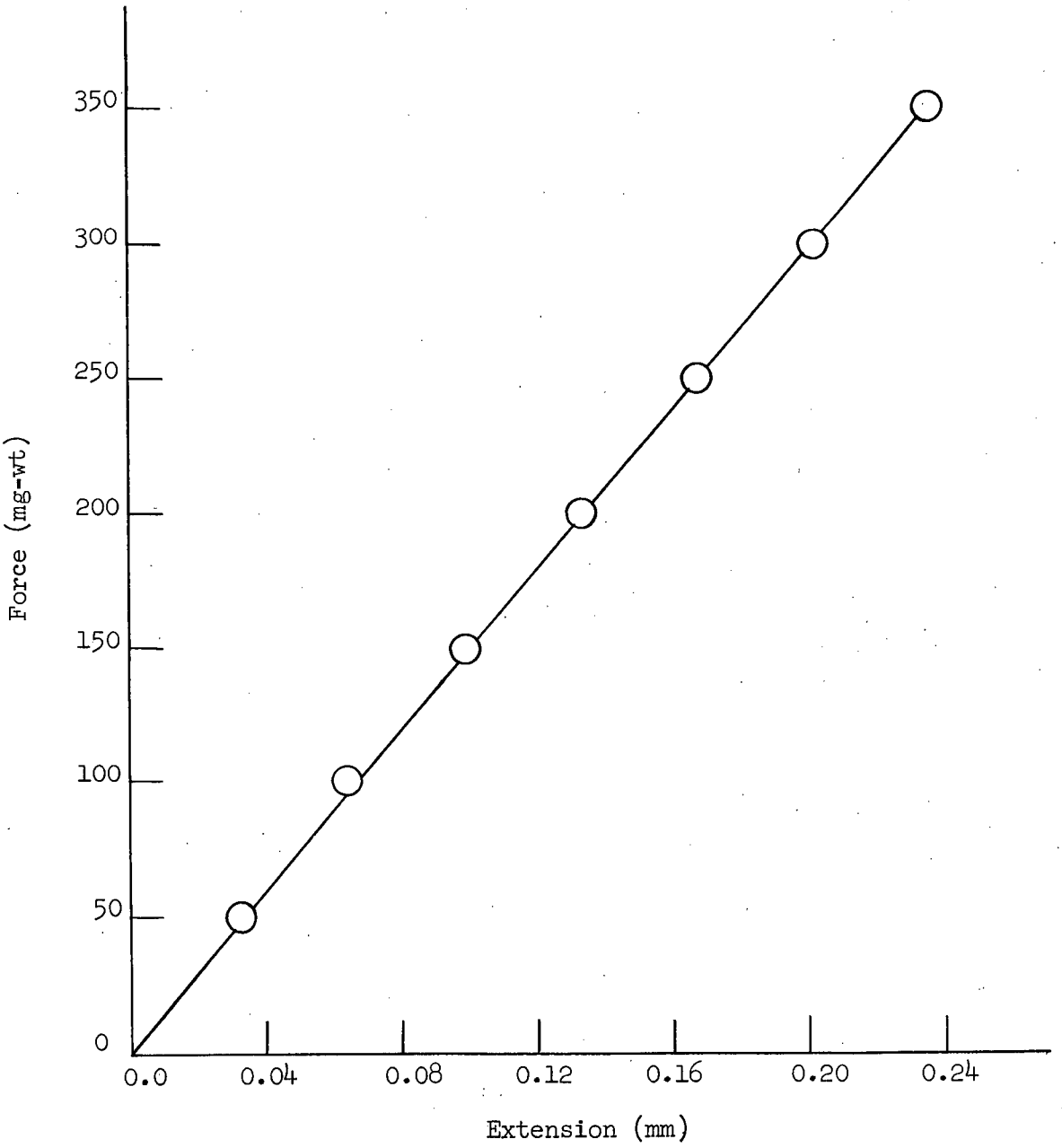

Figure 51. Calibration of Small Helical Spring.

Force - Extension Plot

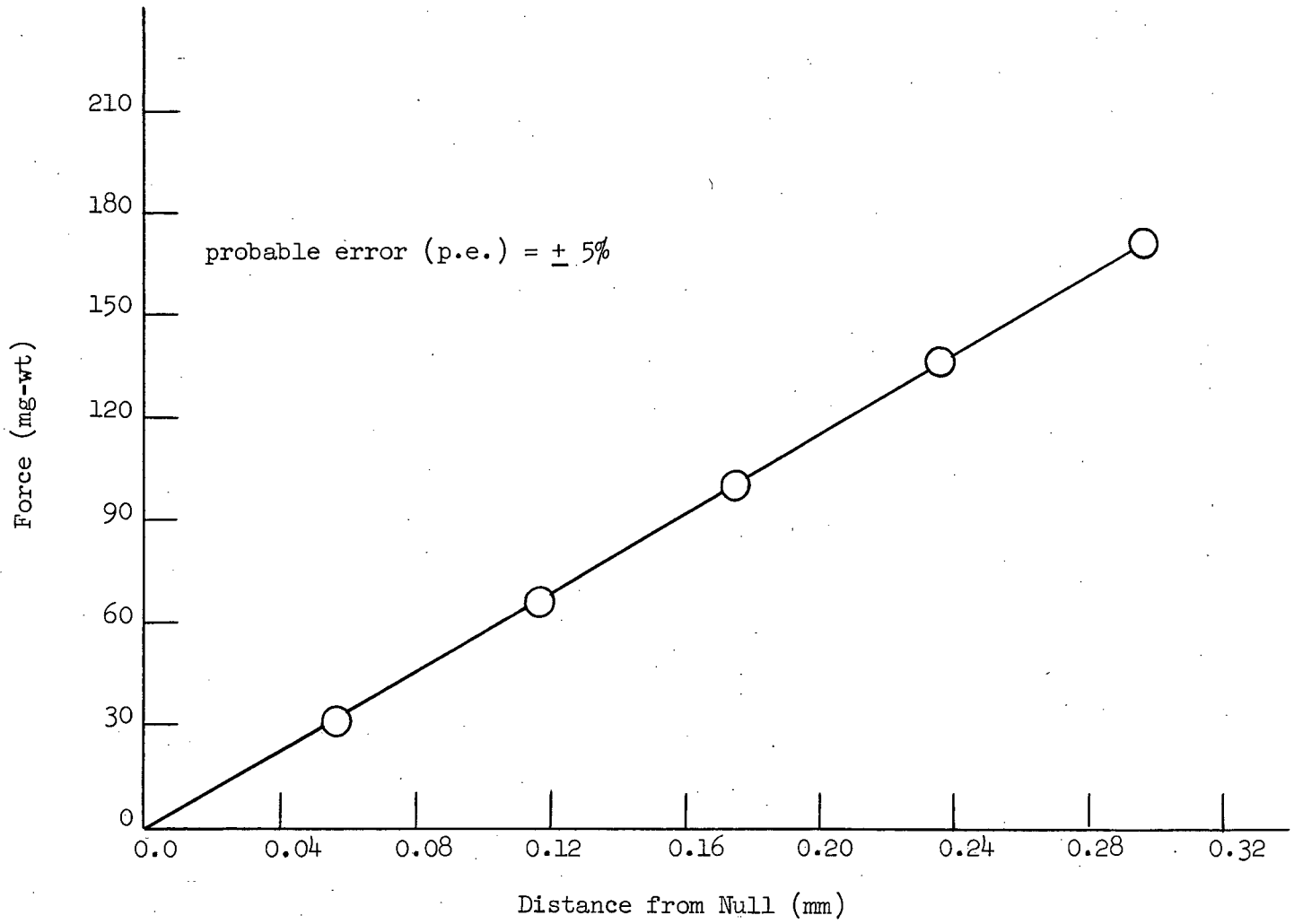

Figure 52. Calibration of the Restoring Force of the Suspended Rod. The Small Spring was Used.

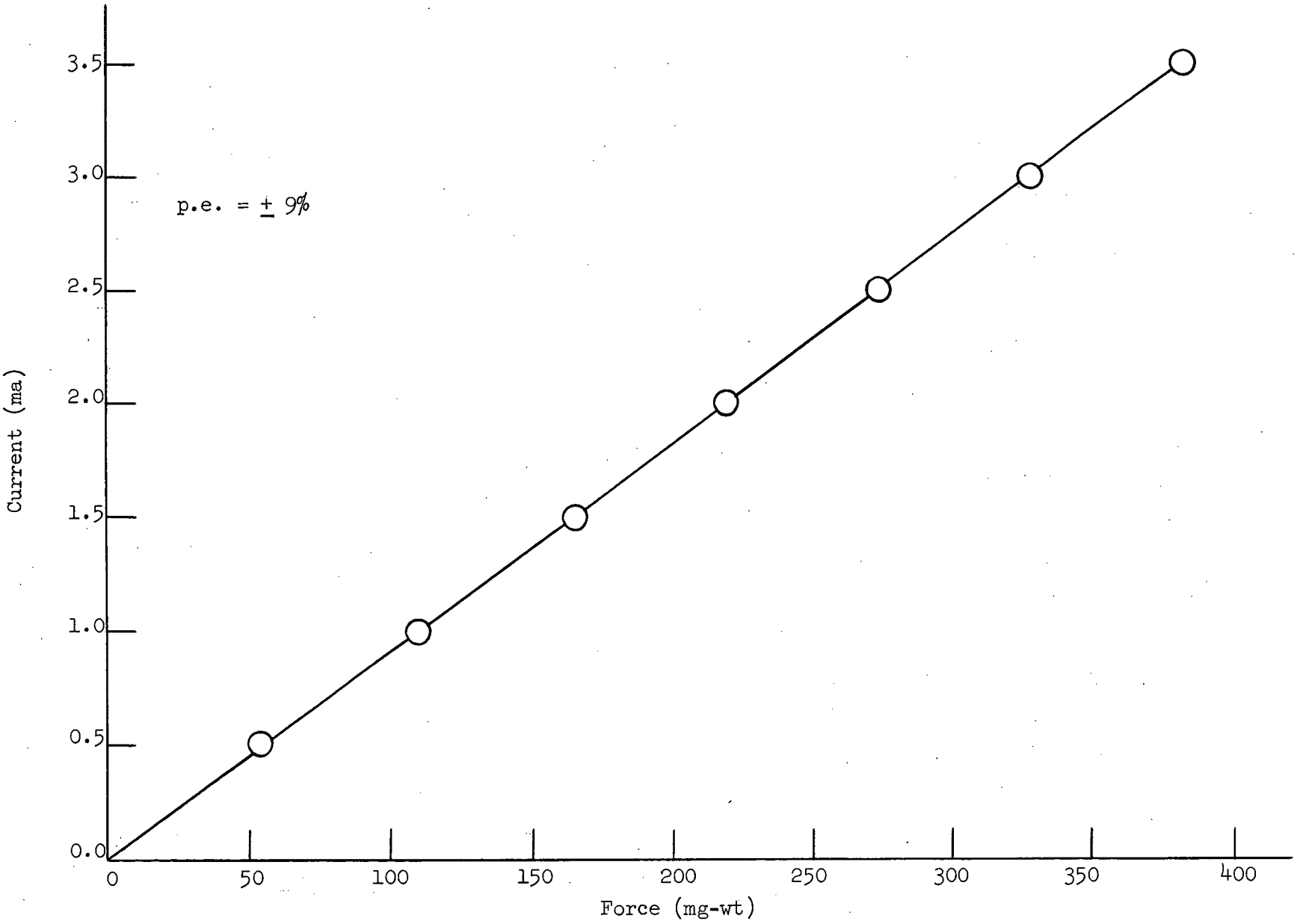

Figure 53. Current-Force Relationship at Low Current. The Small Spring was Used.

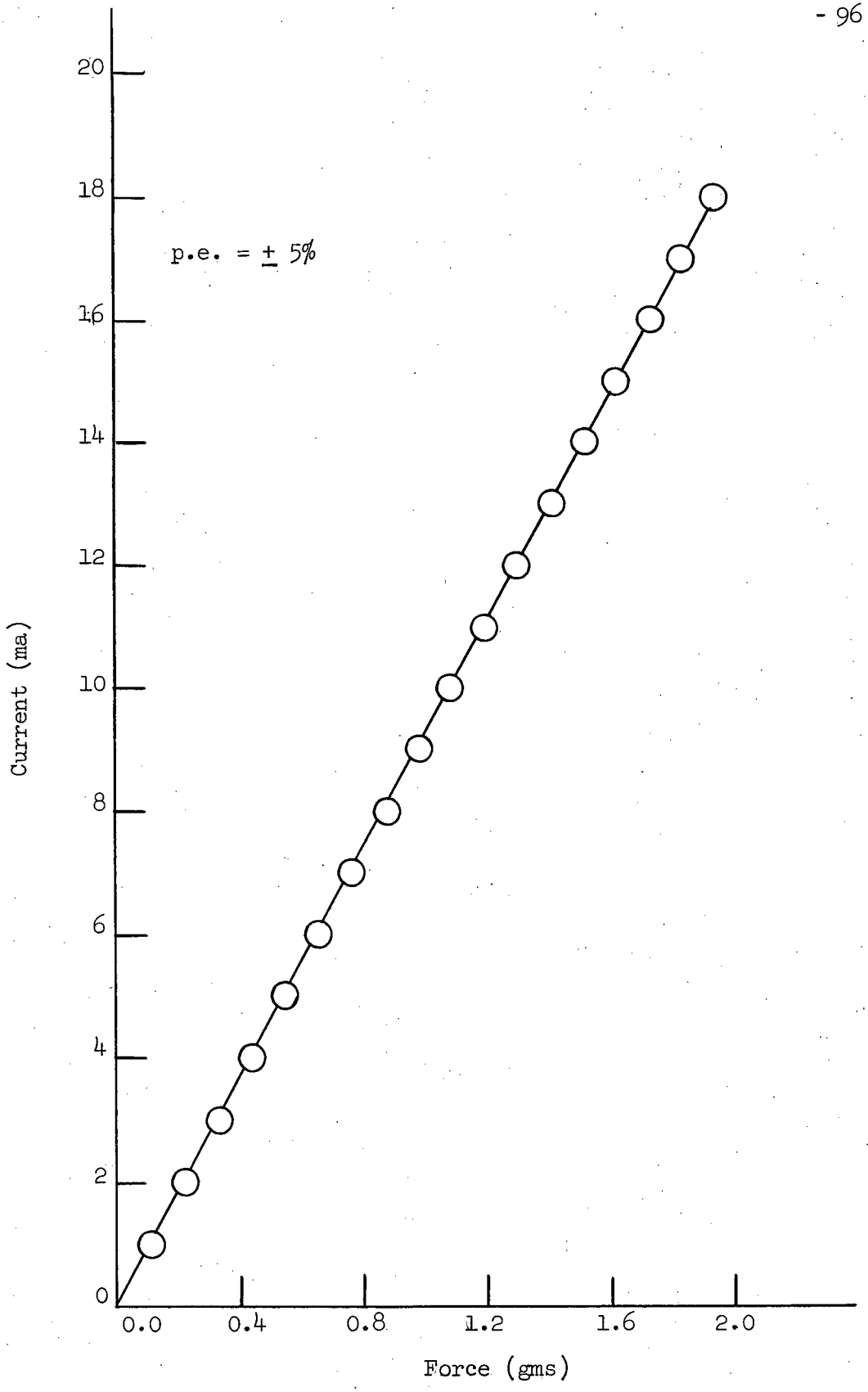

Figure 54. Current-Force Relationship. The Large Spring was Used.

APPENDIX II

TABLE IV

Comparisons Between Measured and Calculated Values of Area.

Whisker	Measured Area in u^2	
	Optical	Calculated
A	167	177
B_1	48	62
B_2	48	71
C	37	54
D_1	92	82
D_2	92	72
D_3	92	83
E	77	49
F_1	85	102
F_2	85	146
G	77	71
H	37	41
I	37	31
J	95	95
K	12	12
L	21	25
M	111	90
N	11	9
O	22	18
P	6.6	8.0
Q	11	9.6
R	18	38

TABLE IV

Comparisons Between Measured and Calculated Values of Area.

Whisker	Measured Area in u^2	
	Optical	Calculated
S_1	14	16
S_2	14	18
S_3	14	20
S_4	14	19
T_1	72	92
T_2	72	86
U	96	90
V	64	65
W	55	72
X_1	38	49
X_2	38	49
Y	62	54
Z	109	62
AA	115	102
BB	133	117
CC	102	119
DD	121	77
EE	238	227
FF	15	15
GG	50	58
HH	58	35

TABLE V

Primary Tests

Whisker	d(μ)	L(mm)	σ_m(Kg/mm^2)	% ϵ_m	E(10^4Kg/mm^2)	σ_c(Kg/mm^2)	σ_n(Kg/mm^2)
A	15.0	1.415	34.0	0.50	0.68	23.4	61.5
B_1	8.9	1.842	93.5	1.35	0.68	50.4	78.5
B_2	9.5	1.829	86.4	1.27	0.68	45.6	80.2
C	8.3	1.388	40.5	0.58	0.68	56.0	30.6
D_1	10.2	2.416	41.1	0.575	0.68	41.0	42.4
D_2	9.6	1.602	32.6	0.47	0.68	45.1	30.6
D_3	10.3	1.498	58.5	0.84	0.68	40.4	61.2
E	7.9	1.549	44.9	0.63	0.68	60.3	31.5
F_1	11.4	2.510	16.2	0.22	0.68	34.8	19.7
F_2	13.7	2.537	28.6	0.41	0.68	26.6	45.5
G	9.5	1.629	37.4	0.53	0.68	45.6	34.7
H	7.2	1.041	92.5	1.325	0.68	69.6	56.2
I	6.3	0.534	106.8	1.49	0.68	85.6	52.8
J	11.0	2.670	53.2	0.39	1.34	36.7	61.3
K	4.0	1.869	312.2	2.19	1.34	173.7	76.0
L	5.6	1.549	132.7	0.95	1.34	102.7	54.6
M	10.7	1.682	55.9	0.285	1.96	38.3	61.7

TABLE V

Primary Tests

Whisker	d(μ)	L(mm)	σ_m(Kg/mm^2)	% ϵ_m	E(10^4Kg/mm^2)	σ_c(Kg/mm^2)	σ_n(Kg/mm^2)
N	3.4	1.255	157.8	0.74	1.96	225.0	29.6
O	4.9	1.736	97.0	0.47	1.96	126.4	32.4
P	3.2	1.415	181.3	0.805	1.96	247.1	31.0
Q	3.5	1.428	110.7	0.445	1.96	214.5	21.8
R	7.0	1.362	72.5	0.35	1.96	72.6	42.3
S_1	4.5	1.922	52.9	0.22	1.96	144.5	15.5
S_2	4.8	2.830	107.8	0.505	1.96	130.6	34.9
S_3	5.0	1.922	155.8	0.74	1.96	122.4	53.8
S_4	4.9	1.041	77.4	0.36	1.96	126.4	25.9
*							
T_1	10.8	3.600	26.1	0.39	0.68	37.7	29.3
T_2	10.5	5.280	41.5	0.61	0.68	39.3	44.7
U	10.7	1.295	84.7	1.245	0.68	38.3	93.5
V	9.1	2.480	93.2	1.37	0.68	48.7	81.0
W	9.6	2.456	15.0	0.21	0.68	45.1	14.1
X_1	7.0	2.360	60.5	0.87	0.68	72.6	35.2
X_2	7.9	2.456	74.5	1.095	0.68	60.3	52.2

TABLE V

Primary Tests

Whisker	d(μ)	L(mm)	σ_m(Kg/mm^2)	% ϵ_m	E(10^4Kg/mm^2)	σ_c(Kg/mm^2)	σ_n(Kg/mm^2)
Y	8.3	2.480	67.3	0.99	0.68	56.0	50.8
Z	8.9	1.228	35.0	0.515	0.68	50.4	29.4
AA	11.4	1.642	32.3	0.475	0.68	34.8	39.2
BB	12.2	3.080	88.1	1.295	0.68	31.5	118.3
CC	12.3	5.120	12.1	0.178	0.68	31.3	55.2
DD	9.9	1.202	45.4	0.668	0.68	42.9	44.8
EE	12.4	2.460	40.2	0.30	1.34	30.8	55.2
FF	4.4	1.695	98.0	0.57	1.34	149.8	27.7
**							
GG	17.0	2.056	19.0	0.28	0.68	19.7	40.8
HH	6.7	1.896	88.4	1.30	0.68	77.7	48.1
II	8.6	4.280	79.7	0.595	1.34	53.1	63.5
JJ	7.1	2.590	89.8	0.665	1.34	71.1	53.4

* Whiskers used in Secondary tests.

** Whiskers used in annealing tests.

TABLE VI

Secondary Tests

Whisker	d(μ)	L(mm)	σ_m(Kg/mm^2)	% ϵ_m	E(10^4Kg/mm^2)	σ_c(Kg/mm^2)	σ_n(Kg/mm^2)	E/E_i
*								
CC'	12.3	5.120	12.1	0.178	0.68	-	-	-
CC''		2.123	27.3	0.637	0.35	47.3	30.6	0.51
CC'''		1.896	14.4	0.284	0.41	47.3	16.1	0.60
CC''''		1.362	33.2	0.653	0.40	47.3	37.2	0.59
*								
T_I	10.8	3.600	26.1	0.394	0.68	-	-	-
T_1'		2.270	32.0	0.484	0.65	50.6	33.5	0.96
T_1''		1.362	92.8	1.57	0.59	50.6	97.2	0.87
*								
T_2	10.5	5.280	41.5	0.61	0.68	-	-	-
T_2'		3.280	40.9	0.705	0.58	51.4	42.2	0.85
T_2''		2.189	58.8	1.062	0.56	51.4	60.6	0.82
*								
U	10.7	1.295	84.7	1.245	0.68	-	-	-
U'		0.881	60.6	1.13	0.54	50.8	63.2	0.79

TABLE VI

Secondary Tests

Whisker	d(μ)	L(mm)	σ_m (Kg/mm^2)	% ϵ_m	E(10^4Kg/mm^2)	σ_c (Kg/mm^2)	σ_n (Kg/mm^2)	E/E_i
*								
EE	12.4	2.560	40.2	0.30	1.34	-	-	-
EE'		0.961	30.6	0.55	0.57	47.2	34.3	0.42
*								
V	9.1	2.480	93.2	1.37	0.68	-	-	-
V'		0.828	63.5	1.41	0.44	56.7	59.4	0.65
*								
W	9.6	2.456	15.0	0.21	0.68	-	-	-
W'		1.028	33.7	0.495	0.62	54.5	32.8	0.91
*								
L	5.6	1.549	132.7	0.99	1.34	-	-	-
L'		0.748	130.2	0.13	1.07	98.7	69.9	0.80
*								
X_1	7.0	2.360	60.5	0.87	0.68	-	-	-
X_1'		0.908	84.3	1.29	0.65	73.4	61.1	0.96

TABLE VI

Secondary Tests

Whisker	d(μ)	L(mm)	σ_m(Kg/mm^2)	% ϵ_m	E(10^4Kg/mm^2)	σ_c(Kg/mm^2)	σ_n(Kg/mm^2)	E/E_i
*								
X_2	7.9	2.456	74.5	1.095	0.68	-	-	-
X_2'		0.721	40.9	0.93	0.65	64.0	33.9	0.96
*								
Y	8.3	2.480	67.3	0.99	0.68	-	-	-
Y'		1.121	149.6	3.32	0.45	61.0	130.0	0.66
*								
DD	9.9	1.202	45.4	0.668	0.68	-	-	-
DD'		0.935	45.9	1.16	0.40	53.3	45.6	0.59
DD''		0.721	55.6	1.335	0.43	53.3	55.3	0.63
*								
Z	8.9	1.228	35.0	0.515	0.68	-	-	-
Z'		0.301	34.3	1.17	0.30	57.7	31.5	0.44
*								
AA	11.4	1.642	32.3	0.475	0.68	-	-	-
AA'		1.068	34.6	0.565	0.58	49.1	37.3	0.85

TABLE VI

Secondary Tests

Whisker	d(μ)	L(mm)	σ_m(Kg/mm^2)	% ϵ_m	E(10^4Kg/mm^2)	σ_c(Kg/mm^2)	σ_n(Kg/mm^2)	E/E_i
*								
FF	4.4	1.695	75.0	0.57	1.34	-	-	-
FF'		1.081	143.4	1.12	1.31	148.3	51.2	0.98
*								
BB	12.2	3.080	88.1	1.295	0.68	-	-	-
BB'		1.282	100.6	1.88	0.53	47.5	112.3	0.78
**								
GG	17.0	2.056	19.0	0.28	0.68	-	-	-
GG'		0.587	15.9	0.95	0.17	47.5	19.7	0.25
**								
HH	6.7	1.896	88.4	1.30	0.68	-	-	-
HH'		0.656	50.5	1.76	0.28	77.1	34.7	0.41
**								
II	8.6	4.280	79.7	0.595	1.34	-	-	-
II'		1.469	65.1	0.73	0.90	59.5	58.0	0.67

TABLE VI

Secondary Tests

Whisker	d(μ)	L(mm)	σ_m(Kg/mm^2)	% ϵ_m	E(10^4Kg/mm^2)	σ_c(Kg/mm^2)	σ_n(Kg/mm^2)	E/E_i
**								
JJ	7.1	2.590	89.8	0.665	1.34	-	-	-
JJ'		0.908	75.2	0.505	1.46	72.0	55.4	1.09

* Ordinary Whiskers.

** Annealed Whiskers.

APPENDIX III

Sample Calculation of Young's Modulus for a Whisker With the Axis 15° Off [100]

Young's Modulus is given by

$$\frac{1}{E} = S_{11} - 2(S_{11} - S_{12} - S_{44}/2)(\gamma_1^2 \gamma_2^2 + \gamma_2^2 \gamma_3^2 + \gamma_1^2 \gamma_3^2)$$

where S_{ij} = elastic compliances

and $\gamma_{1,2,3}$ = cosines of the angles formed by the axis of the specimen with the three edges of the unit cube.

The elastic compliances for copper[30] are:

$$S_{11} = 1.49\ (10^{-4}) mm^2/Kg$$

$$S_{12} = -0.63\ (10^{-4}) mm^2/Kg$$

$$S_{44} = 1.33\ (10^{-4}) mm^2/Kg$$

For a whisker with a [100] axis,

$$(\gamma_1^2 \gamma_2^2 + \gamma_2^2 \gamma_3^2 + \gamma_1^2 \gamma_3^2) = 0$$

and $$E = \frac{1}{S_{11}} = 0.68\ (10^4)\ Kg/mm^2$$

Consider a whisker whose axis lies 15° off the [100] axis. The values $\gamma_{1,2,3}$ can be found using a stereographic projection.

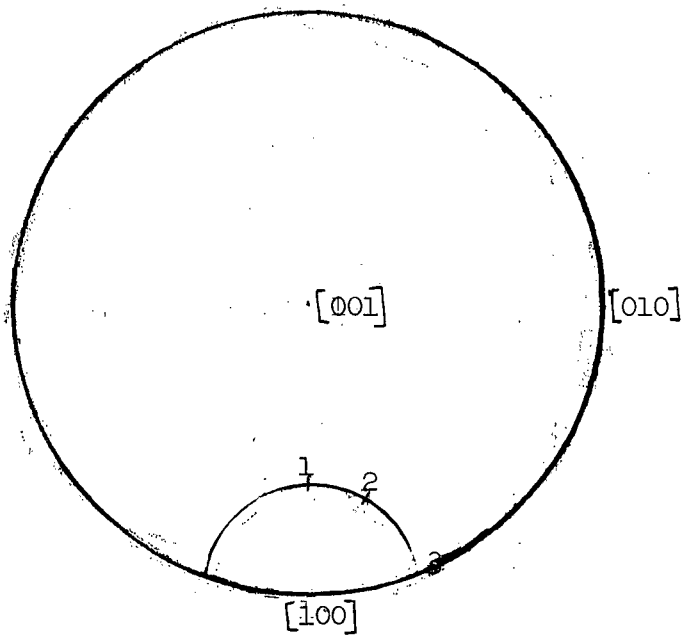

Case 1. $\gamma_1 = \cos 15^\circ \qquad \gamma_2 = \cos 90^\circ \qquad \gamma_3 = \cos 75^\circ$

then $(\gamma_1^2\gamma_2^2 + \gamma_2^2\gamma_3^2 + \gamma_1^2\gamma_3^2) = 0.062$

and $E = 0.76\ (10^4)\ \text{Kg/mm}^2$

Case 2. $\gamma_1 = \cos 15^\circ \qquad \gamma_2 = \cos 79^\circ \qquad \gamma_3 = \cos 80^\circ$

then $(\gamma_1^2\gamma_2^2 + \gamma_2^2\gamma_3^2 + \gamma_1^2\gamma_3^2) \simeq 0.062$

and $E = 0.76\ (10^4)\ \text{Kg/mm}^2$

Case 3. Equivalent to Case 1.

Therefore the error in assuming that a whisker has a $[100]$ orientation when, in fact, it is off by 15° is

$$\% \text{ error} = \left[\frac{0.76 - 0.68}{0.68}\right] 100 = 11.7\ \%$$

Similar results are obtained for whiskers assumed to have orientations of $[110]$ or $[111]$.

APPENDIX IV

A. The Method of Least Squares

The curves in Figures 17, 19, 24 and 25 were obtained by the method of least squares[43,44]. For a straight line $y = a + bx$ where a and b can be determined by the following normal equations:

$$\sum_{i=1}^{n} y_i = na + b \sum_{i=1}^{n} x_i$$

$$\sum_{i=1}^{n} x_i y_i = a \sum_{i=1}^{n} x_i + b \sum_{i=1}^{n} x_i^2$$

For results with a high scatter, it is advisable to consider x as a function of y, ie. $x = a^1 + b^1 y$ where a^1 and b^1 are found by similar normal equations as above.

These two regression lines will coincide if, and only if, the correlation factor r equals ± 1. The best line lies between these two regression lines and all three lines will pass through the point $\bar{x}_i$ and $\bar{y}_i$.

The correlation factor r is a measure of the "goodnes of fit" and is given by

$$r = \frac{\overline{x_i y_i} - \bar{x}_i \bar{y}_i}{\sigma_{x_i} \sigma_{y_i}}$$

where $\overline{x_i y_i}$ = the average of the products of the pairs.

$\bar{x}_i \bar{y}_i$ = the average of the x_i's times the average of the y_i's.

σ_{x_i} = the standard deviation of the x_i's.

σ_{y_i} = the standard deviation of the y_i's.

where $\sigma_{x_i} = \sqrt{\sum_{i=1}^{n} \frac{x_i^2}{n} - \bar{x}_i^2}$

$$y_i = \sqrt{\sum_{i=1}^{n} \frac{y_i^2}{n} - \bar{y}_i^2}$$

If the fit is poor, r will be close to 0. However, if the fit is good, r will be close to $\pm$ 1, and there is a strong correlation. It can be shown that the correlation between x and y is significant if

$$r > \frac{1.96}{\sqrt{n-1}}$$

$$-r < \frac{-1.96}{\sqrt{n-1}}$$

B. Application

1. Primary Tests

For the plot of $\log \sigma_m$ against log d, r = -0.84.

The value of $\frac{-1.96}{\sqrt{n-1}} = \frac{-1.97}{\sqrt{41}} = -0.31$

Therefore the correlation is significant.

2. Secondary Tests

For the plot of $\log \sigma_m$ against $\log d$, $r = -0.88$.

The value of $\frac{-1.96}{\sqrt{n-1}} = \frac{-1.96}{\sqrt{24}} = -0.50$

Therefore the correlation is significant.

APPENDIX V

A. Calculation of Theoretical Curves for the Volume and Surface Dependence of Stress for Constant Diameter.

1. Volume Dependence of Stress

Assume that the yield stress σ is some function f(V) of the volume where

$$V = \frac{\pi}{4} d^2 L \qquad (1)$$

It has been found that

$$\sigma = \frac{A}{d^n} + B \qquad (2)$$

However, this equation is only an approximation since it does not take into account the effect of the length L on σ.

For $L = L_1$ = constant, equation (1) can be written as

$$d = \left[\frac{4V}{\pi L_1}\right]^{1/2}$$

and

$$d^n = \left[\frac{4V}{\pi L_1}\right]^{n/2} \qquad (3)$$

Replacing d^n in equation (2) gives

$$\sigma = \frac{A}{\left[\frac{4V}{\pi L_1}\right]^{n/2}} + B$$

and using equation (1), this can be written as

$$\sigma = \frac{A}{d^n} \left[\frac{L_1}{L}\right]^{n/2} + B \qquad (4)$$

The value of L_1 is chosen to be about the average length of the whiskers tested.

a. Primary Tests

For primary tests on whiskers normalized to d = 10 μ, equation (4) becomes

$$\sigma = 39.1\left[\frac{L_1}{L}\right]^{0.8} + 2.8 \qquad (5)$$

where $L_1 = 2000\ \mu$

b. Secondary Tests

For secondary tests on whiskers normalized to d = 10 μ equation (4) becomes

$$\sigma = 34.1\left[\frac{L_1}{L}\right]^{1.25} + 39.0 \qquad (6)$$

where $L_1 = 1500\ \mu$

The curves drawn in Figs. 22 and 27 were calculated from equations (5) and (6) respectively.

2. Surface Dependence of Stress

Assume that the yield stress σ is some function f(S) of the surface area where

$$S = \pi d L \qquad (7)$$

It can be shown by similar arguments as in the above case that

$$\sigma = \frac{A}{d^n}\left[\frac{L_1}{L}\right]^n + B \qquad (8)$$

a. Primary Tests

As before the whisker were normalized to d = 10 μ and equation (8) becomes

$$\sigma = 39.1\left[\frac{L_1}{L}\right]^{1.6} + 2.8 \qquad (9)$$

where $L_1 = 2000\,\mu$

b. Secondary Tests

Similarly for d = 10 μ, equation (8) becomes

$$\sigma = 34.1\left[\frac{L_1}{L}\right]^{2.5} + 39.0 \qquad (10)$$

where $L_1 = 1500\,\mu$

The curves drawn in Figs. 22 and 27 were caluclated from equations (9) and (10) respectively.

B. Comparison of Expected Variation in Stresses Between Whiskers of Constant Length L2 and L3 for Various Diameters.

1. Volume Dependence of Stress

From the previous section A, it has been shown that

$$\sigma = \frac{A}{d^n}\left[\frac{L_1}{L}\right]^{n/2} + B \qquad (4)$$

Consider two lengths $L_2 = L_{min}$ and $L_3 = L_{max}$. It would be interesting to know what variation the the ratio $\frac{\sigma_{L_2}}{\sigma_{L_3}}$ could be expected. for whiskers normalized to various diameters. The ratio between σ_{L_2} and σ_{L_3} is given by

$$\frac{\sigma_{L_2}}{\sigma_{L_3}} = \left[\frac{A(L_1)^{n/2} + B(L_2)^{n/2}\, d^n}{A(L_1)^{n/2} + B(L_3)^{n/2}\, d^n}\right] \left[\frac{L_3}{L_2}\right]^{n/2} \qquad (11)$$

a. Primary Tests

For primary tests on whiskers,

$$L_1 = 2000\ \mu$$

$$L_2 = 1000\ \mu$$

$$L_3 = 5000\ \mu$$

and equation (11) becomes

$$\frac{\sigma_{1000}}{\sigma_{5000}} = \left[\frac{6865 + 7.03d^{1.6}}{6865 + 25.48d^{1.6}}\right] 3.62 \qquad (12)$$

Fig. 55 (a) shows a plot of this ratio for several values of d.

b. Secondary Tests

For secondary tests on whiskers,

$$L_1 = 1500\ \mu$$

$$L_2 = 500\ \mu$$

$$L_3 = 3500\ \mu$$

and equation (11) becomes

$$\frac{\sigma_{500}}{\sigma_{3500}} = \left[\frac{413 + 0.922\, d^{2.5}}{413 + 10.5\, d^{2.5}}\right] 11.4 \qquad (13)$$

Fig. 56 (a) shows a plot of this ratio for several values of d.

2. Surface Dependence of Stress

From the previous section A, it has been shown that

$$\sigma = \frac{A}{d^n}\left[\frac{L_1}{L}\right]^n + B \qquad (8)$$

In a similar manner as before, the ratio between L_2 and L_3 is given by

$$\frac{\sigma_{L_2}}{L_3} = \left[\frac{A(L_1)^n + B(L_2)^n d^n}{A(L_1)^n + B(L_3)^n d^n}\right]\left[\frac{L_3}{L_2}\right] \qquad (14)$$

a. Primary Tests

For same values of L_1, L_2, and L_3 as in B - 1(a), equation (14) becomes

$$\frac{\sigma_{1000}}{\sigma_{5000}} = \left[\frac{3004 + 1.77\ d^{1.6}}{3004 + 23.2\ d^{1.6}}\right] 13.1 \qquad (15)$$

Fig. 55 (b) shows a plot of this ratio for several values of d.

b. Secondary Tests

For the same values of L_1, L_2, and L_3 as in B - 1(b), equation (14) becomes

$$\frac{\sigma_{500}}{\sigma_{3500}} = \left[\frac{3854 + 2.18\ d^{2.5}}{3854 + 283\ d^{2.5}}\right] 129.6 \qquad (16)$$

Fig. 56 (b) shows a plot of this ratio for several values of d.

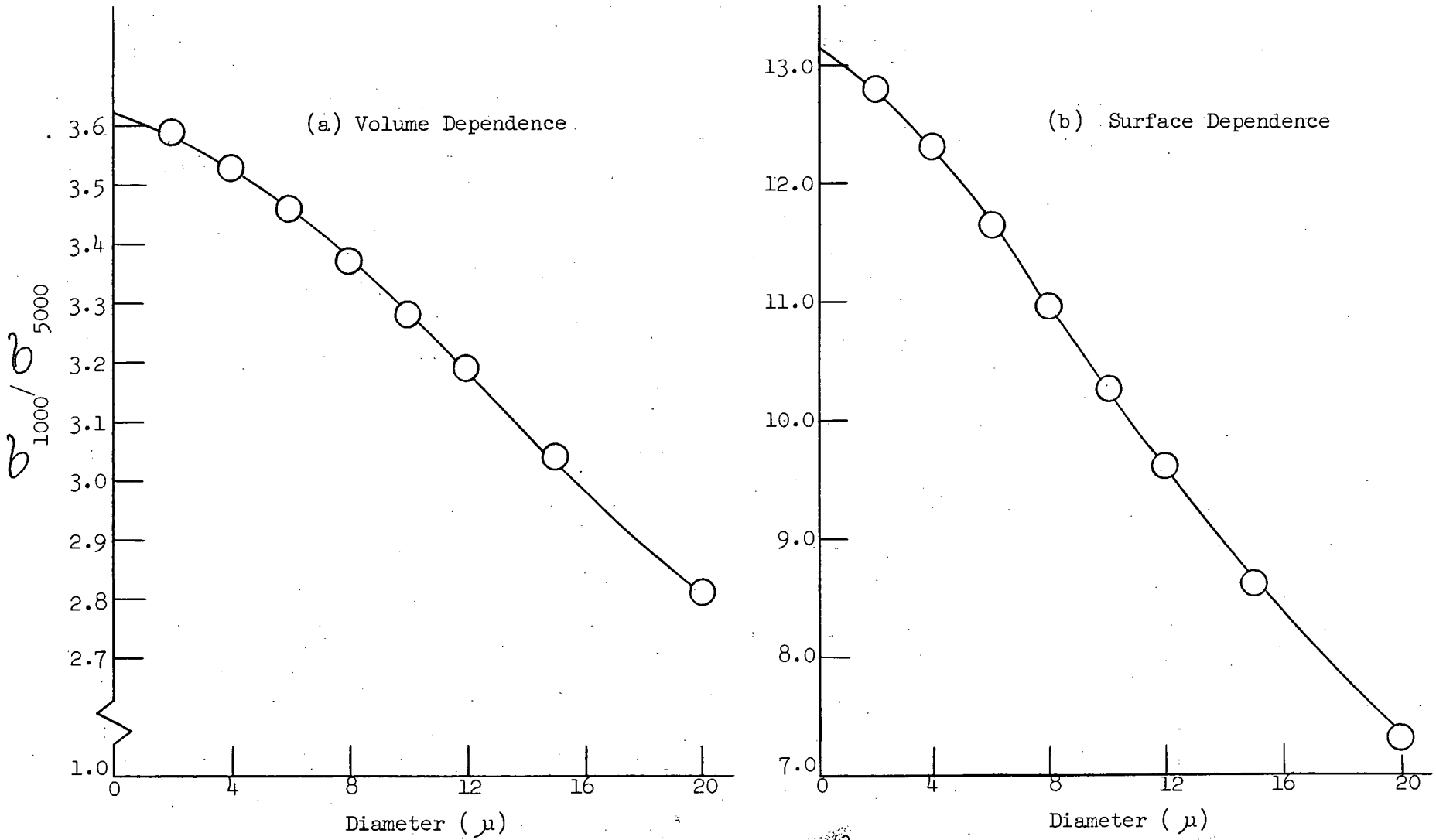

Figure 55. Ratio of Primary Yield Stresses $\frac{\sigma_{L_2}}{\sigma_{L_3}}$ Against Diameter for L_2=1000 μ and L_3=5000 μ.

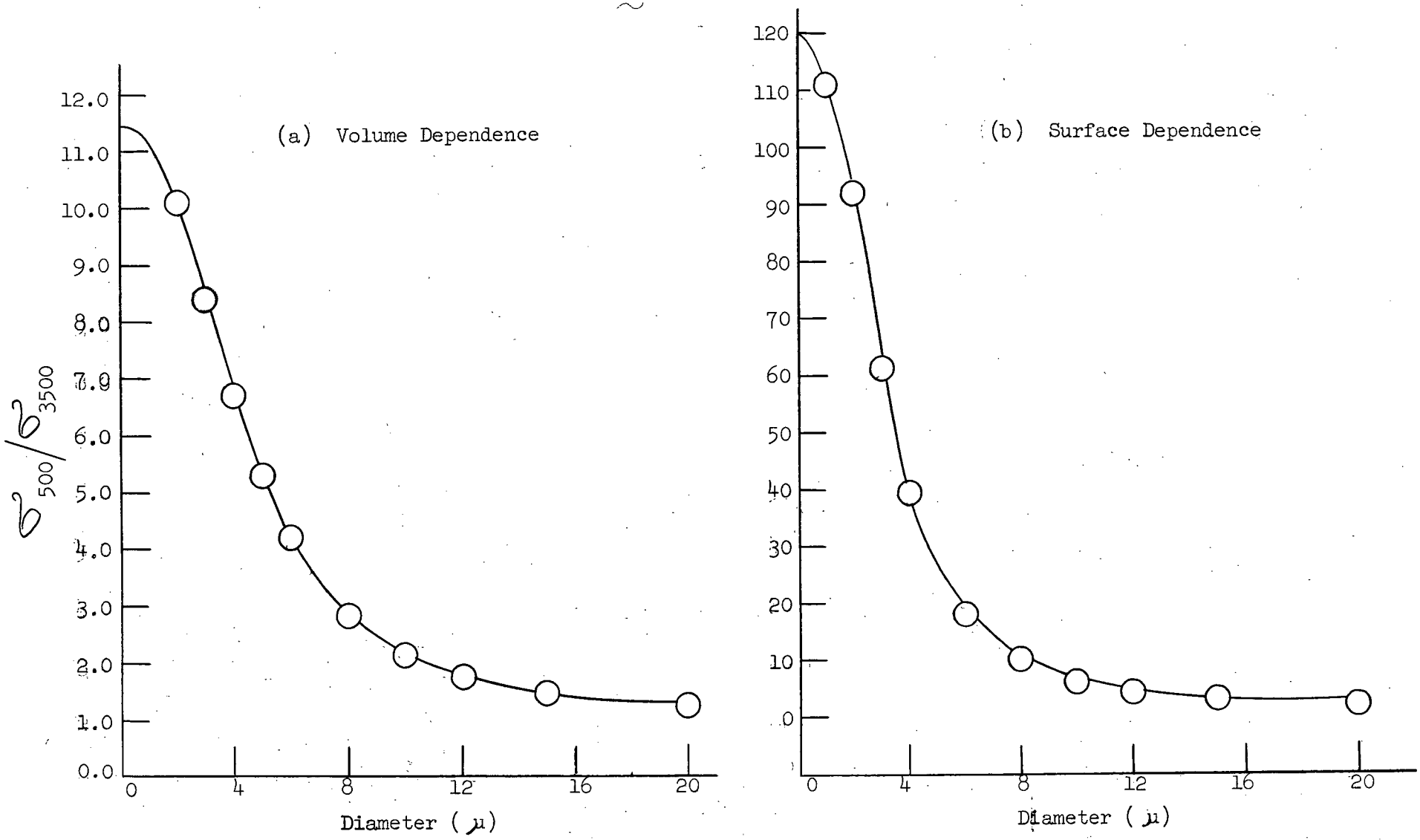

Figure 56. Ratio of Secondary Yield Stresses $\sigma_{L_2}/\sigma_{L_3}$ Against Diameter for L_2=500 μ and L_3=3500 μ.

APPENDIX VI

TABLE VII

Saimoto's Results

Whisker	Orientation	d(μ)	τ_{cr}(Kg/mm^2)	τ_{fl}(Kg/mm^2)	τ_{cr}/τ_{fl}
B1	[100]	3.3	50.0	5.15	9.7
B2	[100]	2.6	47.0	-	-
B3	[100]	6.7	45.0	2.40	18.8
B10	[100]	6.6	27.0	-	-
B11	[100]	3.8	35.8	-	-
B12	[100]	3.6	58.5	-	-
B13	[100]	7.1	34.2	2.45	13.9
B14	[100]	3.0	49.0	-	-
B20	[100]	4.5	11.5	3.00	3.9
B21	[100]	3.9	39.6	3.7	10.7
B7	[110]	9.9	16.7	1.67	10.0
B4	[111]	6.9	21.4	2.52	8.5
B5	[111]	5.5	24.0	3.02	7.9
B6	[111]	4.3	48.5	1.91	25.3
B8	[111]	3.2	19.9	2.91	6.8
B9	[111]	4.8	42.5	2.86	14.9
B15	[111]	5.0	26.0	3.16	8.2
B16	[111]	4.3	13.8	3.29	4.2

TABLE VIII

Brenner's Results

Whisker	Orientation	d(μ)	τ_{cr}(Kg/mm^2)	τ_{fl}(Kg/mm^2)	τ_{cr}/τ_{fl}
1	[100]	6.3	15.2	1.52	10.0
2	[100]	8.3	32.0	1.74	18.4
3	[100]	8.9	20.5	1.48	13.9
4	[100]	10.3	22.6	1.72	13.1
5	[100]	10.6	38.6	1.48	26.1
6	[100]	17.8	15.1	1.06	14.2
7	[100]	25.9	25.0	0.50	50.0
8	[100]	9.6	6.1	1.34	4.6
9	[100]	11.1	33.1	0.37	89.4
10	[110]	11.6	34.0	0.94	36.2
11	[110]	12.0	16.5	0.56	29.5
12	[110]	15.5	24.9	0.67	37.2
13	[110]	6.3	20.4	1.74	11.7
14	[110]	12.4	14.4	0.98	14.7
15	[111]	12.9	33.7	0.82	41.1
16	[111]	14.9	23.4	0.63	37.1
17	[111]	4.6	25.2	1.19	21.2